6-2023

Design and Analysis of Asymmetric “String-of-Pearls” Common Repeating-Ground-Track Satellite Constellations for Missions Requiring Regional Coverage

Nathaniel Choo

Design and Analysis of Asymmetric "String-of-Pearls" Common Repeating-Ground-Track Satellite Constellations for Missions Requiring Regional Coverage

DISSERTATION

Nathaniel Choo

AFIT-ENS-DS-23-J-073

DEPARTMENT OF THE AIR FORCE
AIR UNIVERSITY

AIR FORCE INSTITUTE OF TECHNOLOGY

Wright-Patterson Air Force Base, Ohio

AFIT-ENS-DS-23-J-073

Design and Analysis of Asymmetric "String-of-Pearls" Common Repeating-Ground-Track Satellite Constellations for Missions Requiring Regional Coverage

DISSERTATION

Presented to the Faculty

Graduate School of Engineering and Management

Air Force Institute of Technology

Air University

Air Education and Training Command

in Partial Fulfillment of the Requirements for the

Degree of PhD

Nathaniel Choo, MS

May 16, 2023

AFIT-ENS-DS-23-J-073

Design and Analysis of Asymmetric "String-of-Pearls" Common Repeating-Ground-Track Satellite Constellations for Missions Requiring Regional Coverage

DISSERTATION

Nathaniel Choo, MS

Committee Membership:

Darryl Ahner, Ph.D
Chair

Brian Lunday, Ph.D
Member

Nathan Gaw, Ph.D
Member

LtCol Bryan Little, Ph.D
Member

Brian McBee, Ph.D
Member

AFIT-ENS-DS-23-J-073

Abstract

Satellite constellation design must balance many factors that emerge from multiple sources, including environmental hazards and competing mission objectives. The dynamic nature of space systems makes the problem of 'optimal' satellite constellation design even more challenging. Restricting satellite constellation designs to predefined geometric frameworks can alleviate many challenges associated with the design problem; however, it raises an important question: *which geometric framework performs best for each mission set?* This research leverages simulations, metaheuristics, and mathematical programming techniques to address this question for missions focusing on Earth-observation of one or more regions.

First, this research captures the current state of satellite constellation design by presenting a novel topology approach to characterize the relationship between constellation geometry, mission sets, and design approaches commonly presented in the literature. Second, it develops a customized metaheuristic using response surface analysis for the selection of a circular repeating ground track orbit of a single satellite focused on maximizing regional coverage of a defined region(s). Third, it proposes a simple yet elegant procedure to transform non-repeating ground tracks into repeating ground tracks via geometric adjustment minimization. Fourth, it develops a design method for common repeating ground track constellations. Fifth, it develops a dynamic satellite network interdiction model to identify the worst-case degradation of satellite constellation performance resulting from a fixed number of satellite failures. Lastly, it compares two satellite constellation design frameworks according to their mission performance, robustness, and access to energy. Overall, this research expands the set of satellite constellation design methods and investigates the performance of satellite constellation designs for specific mission sets.

Acknowledgements

First and foremost, I want to thank and acknowledge my advisor, Dr. Darryl Ahner. I am deeply grateful for your mentorship and guidance throughout this process. I also want to thank the members of my committee: Dr. Brian Lunday, Lt Col Bryan Little PhD, Dr. Nathan Gaw, and Dr. Brian McBee for your patience, support, and willingness to provide your expertise.

I am very grateful for my family, who instilled in me the importance of hard work and dedication. I thank them for their unfaltering support and encouragement; I would not be here without them. I want to thank Dr. Joseph Choo MD for generously providing his technological knowledge and assistance, your help made this research possible.

I would also like to thank all of my friends here at AFIT. Our collaboration and teamwork was vital to making it through the coursework, and it made the program lighthearted and fun.

Finally, I want to express my sincere appreciation for everyone who provided me with this opportunity, most notably Dr. Darryl Ahner, Dr. Stephen Chambal, Dr. Brian McBee, and LinQuest.

Table of Contents

Page

List of Figures

List of Tables

Design and Analysis of Asymmetric "String-of-Pearls" Common Repeating-Ground-Track Satellite Constellations for Missions Requiring Regional Coverage

I. Introduction

1.1 Motivation

Satellite constellation design must consider many factors, including the technological capabilities of satellite spacecraft, environmental hazards, orbit selection, mission objectives, deployment strategy, maintenance strategy, and budgetary constraints. With so many design considerations, satellite constellation design often resorts to designing satellite constellations with 'good' properties rather than for a specific regional mission. Additionally, attempts at 'optimal' satellite constellation design usually disregard many design factors of satellite constellations by focusing on just a few select design criterion.

By focusing on only a few design criterion, methods to optimize satellite constellations often restrict the designs to predefined geometric frameworks, such as the Walker constellation [1]. Using predefined geometric frameworks for satellite constellation design allows for the exploitation of its special structure, enabling limited-parameter-optimized designs within the restricted framework. The use of predefined geometric frameworks raises an important question: *which geometric framework performs best for a specified mission?* So long as satellite constellation design processes use predefined geometric frameworks, it will remain important to monitor the merits and shortcomings of different design frameworks on emerging space missions and challenges. To overcome this limitation, this dissertation focuses on satellite constellation

design using a larger, if not the entire, parameter space for regional Earth-observation missions using the following questions.

1. What is an appropriate construct to better understand the satellite constellation literature with a focus on design frameworks and methods?

2. What orbit allows for a single satellite to best provide Earth-observation coverage to one or more distinct regions?

3. What is the best satellite constellation design for Earth-observation missions of one or more distinct regions?

Answering the first question provides an understanding of the current state of satellite constellation design in the literature. Such understanding highlights the most promising satellite constellation design methods for Earth-observation missions. Answering the second question provides direction into which orbits should be explored for Earth-observation missions of one or more distinct regions. Although the second question only considers a single satellite, its simplicity generates structure for more involved multiple-satellite constellation design. Answering the third question contributes to the process of mapping the best satellite constellations to specific mission sets.

1.2 Dissertation Overview

This dissertation uses the following organization. Chapters II-V address the three major research questions and Chapter VI provides concluding remarks and recommends for future research.

Chapter II addresses the first research question by capturing and communicating the current state of the satellite constellation design literature using a novel topology framework. The topology framework characterizes the relationship between satellite

constellation geometry, mission sets, and design approaches commonly presented in the satellite constellation design literature. The geometry aspect of the topology considers the shape of the orbits the satellites follow in the constellation, as well as the environmental challenges posed to satellites following such orbits. Different orbital geometries and environmental challenges influence the requirements of satellite spacecraft design, as well as operational planning for deploying, maintaining, and managing the finalized satellite constellation. The mission sets aspect of the topology identifies the mission of the satellite constellation, the objective metric used to quantify the quality of a particular constellation design, and the requirements governing the satellite constellation design. The consideration of alternative mission objectives and design requirements in 'optimal' satellite constellation design can result in drastically different finalized designs. Tailoring design approaches to specific mission objectives and design requirements benefit the design of satellite constellations. The design approach aspect of the topology identifies the methodologies used to design satellite constellations. In order to manage the large number of articles that exist in the satellite constellation design literature, a citation metric filters the articles to include only the top 30% of surveyed articles in the chapter's discussion. The citation metric relates the number of times an article has been cited against the number of years it has been available in the literature.

Chapter III addresses the second research question by examining the problem of finding the optimal orbit of an individual satellite for Earth-observation missions requiring regional coverage. This chapter considers circular repeating ground track orbits. The objective of the satellite is to maximize the coverage it provides to specified regions of interest. Discretized representations of one or more countries obtained through meshgrid sampling defines these regions of interest. The inherent complexities of this problem do not lend themselves to a mathematical programming approach,

as the orbital design decisions do not inform closed-form analytical equations for the objective function used to measure coverage. A simulation computes the coverage provided by a satellite to the regions of interest using a conical field of regard that remains normal to the surface of a spherical Earth. Preliminary exploration of the design space using an appropriate granular mesh demonstrates that the surface of the objective metric is non-convex, warranting the use of a metaheuristic. The customized metaheuristic uses a methodical application of designed experiments and response surface methods to guide the design of single satellite orbits to achieve improved regional observation coverage using repeating ground tracks. The performance of the metaheustic in terms of efficiency and solution quality is compared against the performances of a genetic algorithm, simulated annealing, and particle swarm optimization.

Chapter IV also addresses the second research question by examining the design of repeating ground track orbits; however, it focuses on the design of repeating ground track orbits from existing non-repeating ground track orbits. Repeating ground track orbits are of interest to Earth-observation missions focusing on regions requiring persistent and repetitive coverage. Non-repeating ground track orbits may result from orbital design methods that do not require the orbits to have repeating ground tracks or from existing orbits that become perturbed. This chapter first presents a metric to compare the similarity between two ground tracks to identify the best repeating ground track that most resembles a non-repeating ground track; however, the metric requires simulations that may be too computationally expensive for practical use. An alternative metric and design procedure is also presented to identify the repeating ground tracks most resembling the non-repeating ground tracks via geometric adjustment minimization. These ground tracks can then be shifted to provide coverage of the desired area. Several examples demonstrate that the presented method is

computationally efficient and removes the need for simulations.

Chapter V addresses the third research question by examining the satellite constellation design problem for providing coverage of one or more regions. The mission objective of the satellite constellation is to maintain continuous connectivity between the ground station and its regions of interest. Discretized representations of one or more large regions obtained through mesh grid sampling define these regions of interest. Connected satellite-terrestrial coverage is established with the headquarters location and regions of interest when they are within the conical section of the satellite's field of regard, which remains normal to the surface of a spherical Earth. Direct line-of-sight between satellites informs intersatellite connectivity. For this mission set, this chapter focuses on the design and performance of satellite constellations that have all satellites following a common repeating ground track using irregular intersatellite phasing, referred to as an asymmetric "string-of-pearls" common repeating ground track constellation design framework. Common repeating ground tracks refers to the use of only one reference single-satellite repeating ground track (vice multiple repeating ground tracks) for the design of the satellite constellation. Although a "pure" string-of-pearls approach (equally-phased satellites) simplifies constellation design, the flexibility of asymmetry enables the design of more efficient constellations. A metaheuristic leveraging designed experiments, response surface analysis, particle swarm optimization, and mathematical programming designs the asymmetric string-of-pearls constellations focusing on minimizing the number of satellites required to achieve continuous regional coverage. The metrics of connectivity, robustness, and sunlight exposure evaluate the performance of the satellite constellation design framework in several examples. The robustness of a satellite constellation is measured as its ability to maintain connectivity between the headquarters location and its regions of interest in the presence of the worst-case scenario satellite failures for in-

creasing numbers of satellite failures. A mathematical program models this satellite network interdiction problem to identify the worst-case scenario of satellite failures. The sunlight exposure experienced by the satellite constellation measures its access to energy throughout a calendar year, informing some of the design criterion for the satellite spacecraft. Illustrative examples compare the performance of the asymmetric string-of-pearls constellation design framework against the performance of the Walker constellation design framework.

Chapter VI summarizes the contributions of this dissertation research to include limitations of the research and some potential future research directions.

II. Investigating the Building Blocks of Satellite Constellations: A Survey of Orbit Design and Selection Methodologies

Abstract

Designing satellite constellations often requires consideration of many factors including mission requirements, program budget, and technological capabilities. An abundant amount of literature exists addressing satellite constellation design and it would be beneficial to have a methodology that captures and communicates its current state in the literature. This chapter presents a novel topology approach to characterize the relationship between constellation geometry, mission sets, and design approaches commonly presented in the literature with the aim at identifying the current state of satellite constellation design and the potential research opportunities that exist.

2.1 Introduction

The space environment is important for commercial, scientific, and military applications. RTI International, an independent nonprofit research institution, estimated that the Global Positioning System (GPS) has contributed about $1.4 trillion dollars (2017 dollar value) to the United States economy between 1984 and 2017 [2]. The economic benefit that space provides is expected to grow as companies continue to commercialize the space sector. For example, SpaceX's Starlink is continuing to expand its operations in space to provide broadband internet services across the globe [3, 4]. Commercial capabilities are expected to grow with the scientific research conducted in space. Research into space manufacturing is becoming an interest to many industries, including the pharmaceutical and microchip industries, since the scalable

production of certain materials, such as regenerative medicines, will require microgravity environments [5, 6]. Space is also a contested environment that has many military applications including reconnaissance, surveillance, and signal intelligence [7]. The capability of satellites to gather information and to relay data has prompted countries to design technology that can target both military and commercial satellites. The capability of SpaceX's Starlink to provide communication services to Ukraine while simultaneously thwarting off Russian efforts to disable the entire network has prompted China to consider developing anti-satellite technology specifically designed to target commercial mega-constellations [8, 9, 10].

Since space is useful to many industries and applications, one of the most fundamental satellite constellation design questions is "What mission objectives are required and what orbit(s) will be used to meet these objectives?" Satellite orbits are the building blocks of satellite constellations and some orbits are more suitable for certain missions than others. Additionally, design constraints, such as budgetary limitations, produce challenges in designing satellite constellations. The average cost of launching to low Earth orbit between 1970-2000 was $\$18,500/kg$ and with the help of recent technological advancements, the cost of launching satellites into low Earth orbit has reduced to approximately $\$2,720/kg$ [11, 12]. Meeting mission objectives while satisfying all design constraints is important for adequate satellite constellation design. This chapter presents a novel topology approach to help capture an understanding of the current state of satellite constellation design in the literature and to help identify potential research opportunities that exist. The topology characterizes the relationship between the considered geometries, mission sets, and design approaches presented in the literature.

This chapter is organized in the following order. Section 2.2 presents the topology used to characterize the literature. Section 2.3 discusses articles that are amongst

the most cited in the literature regarding satellite constellation design. Section 2.5 presents a table mapping articles to the topology.

2.2 Topology

The available literature investigating methodologies for designing and selecting orbits for space missions is extensive. The literature explores numerous methodologies addressing a wide variety of orbital geometries and mission applications. Understanding of the current state of satellite constellation design requires a framework to overcome this complexity.

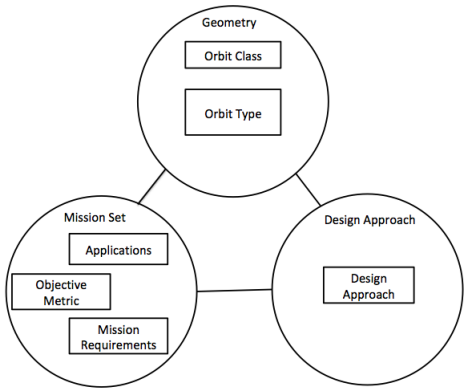

Figure 1: Topology Framework

The simple, but useful, topology presented in Figure 1 captures and relates three major aspects of any approach presented in the literature using six individual elements. The first aspect that the topology captures is the *geometry* that the authors were considering when presenting their research. The geometry is captured by the elements of Orbit Type and Orbit Class. Orbit type focuses on the shape and pattern characteristics of the orbit(s) under consideration. Some examples of orbit types include circular and elliptical orbits. Orbit class focuses on characterizing the space environment that satellites may encounter with a particular orbital geometry. The space environment is important to consider in the design of satellite constellations

because different environmental challenges exist at varying altitudes. For example, a spacecraft orbiting in low Earth orbit will experience atmospheric drag, while a spacecraft in geostationary orbit will not experience atmospheric drag. The orbit class element helps designers anticipate future design challenges in regards to the real-world implementation of a space system using a particular design. Three of the most commonly known Orbit Classes include Low Earth Orbits, Medium Earth Orbits, and Geosynchronous Orbits. Orbit type and orbit class overlap in some instances. The Molniya orbit is a highly elliptical orbit with an inclination of approximately 63.4^o that is frequently exposed to severe radiation as it passes through the Van Allen radiation belt [13]. The Molniya orbit can be used as an orbit class since it helps identify the space environment that will be encountered. The Molniya orbit can also be used as an orbit type since it has very specific orbital characteristics of being a critically-inclined highly-elliptical orbit.

The topology also captures the *mission set* under consideration. The mission set is identified by the Applications element, the Objective Metric element, and the Mission Requirements element. The Applications element identifies the general mission sets that researchers were considering when conducting their research. Although many design approaches can be applied to many different applications, authors usually focus on a particular mission set when conducting their research. For example, a method for finding an orbit that produces regional coverage for broadcasting could still be used for finding an orbit that requires regional coverage for Earth-observing missions. The Objective Metric and the Mission Requirements elements identify the specific design problem being considered. The objective metric is what researchers used to evaluate the quality of a design. The mission requirements element captures the constraints that a design must satisfy for a particular mission. A couple of examples of applications include surveillance and telecommunications. An example

of an Objective Metric is to minimize the number of satellites used in the satellite constellation. An example of a mission requirement is the requirement that the cost of deploying a satellite constellation must remain under a budgetary constraint.

Finally, the topology captures the design approach. The Design Approach provides the methodology that an article uses for designing a satellite constellation. An example of a design approach is to use simulations in conjunction with genetic algorithms to search for the best satellite constellation design for a particular mission. Capturing the general design approaches may help future researchers identify which approaches that they should investigate.

In order to manage the large number of articles that exist in the literature regarding optimal satellite constellation design, a citation metric is used to determine if an article is included in the analysis of this survey article. The citation metric accounts for both the number of citations that an article receives and the number of years since the article has been published by taking the ratio of the two values. Figure 2 shows the distribution of the citation metric values of a survey of 144 articles focusing on satellite constellation design. The citation metric threshold is set to a value of 3 citations/years available because it ensures that the top 30% of articles surveyed are included in this survey's analysis.

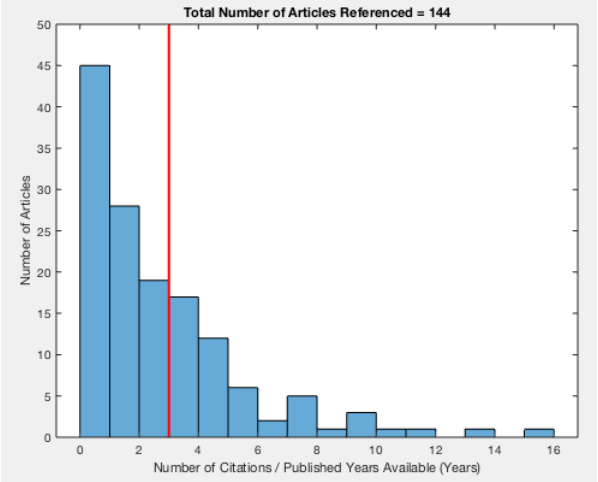

Figure 2: Histogram of the Citation Metrics Values of the Initial Survey of Articles

Expanded topology graphs are generated to help identify potential research opportunities by capturing the relative frequency of geometries, mission sets, and design approaches presented in the literature. Three expanded topology graphs were created to relate each category of the topology to one another. Figures 3 to 5 show how the expanded topology graphs will relate to each category pair.

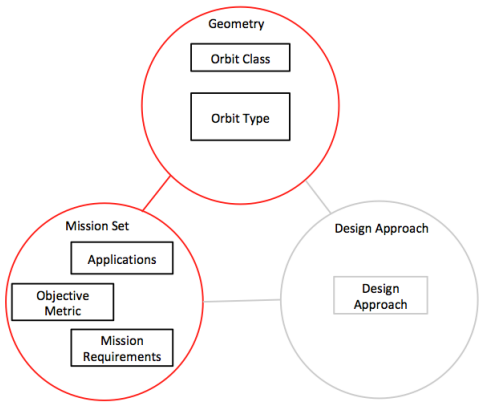

Figure 3: Expanded Topology 1 Structure: Geometry - Mission Set

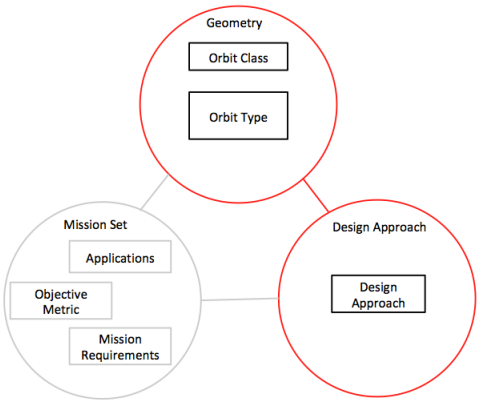

Figure 4: Expanded Topology 2 Structure: Geometry - Design Approach

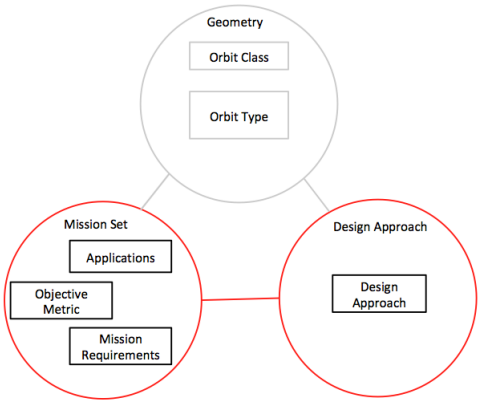

Figure 5: Expanded Topology 3 Structure: Mission Set - Design Approach

Figures 6 to 8, which relate to Figures 3 to 5, respectively, show representative expanded topology graphs. The individual sub-elements were chosen by simply identifying the terminology used in the surveyed articles. Figure 6 allows for understanding of the relationship between the geometries and mission sets and their relative frequency in the literature. Figure 7 allows for the understanding of the relationship between geometries and design approaches and their relative frequency in the literature. Finally, Figure 8 allows for the understanding of the relationship between mission sets and design approaches and their relative frequency in the literature.

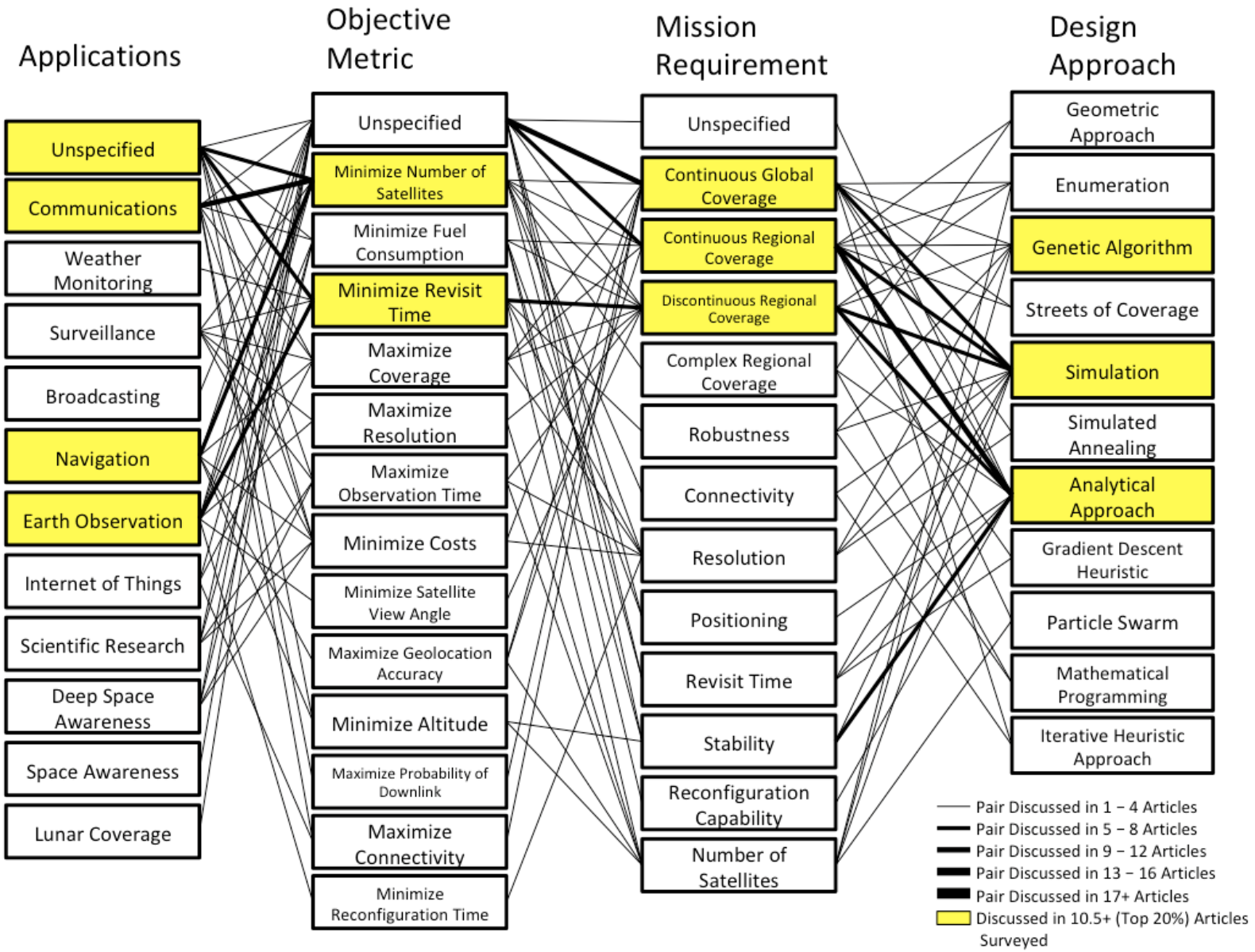

Figure 6: Expanded Topology 1: Geometry - Mission Set

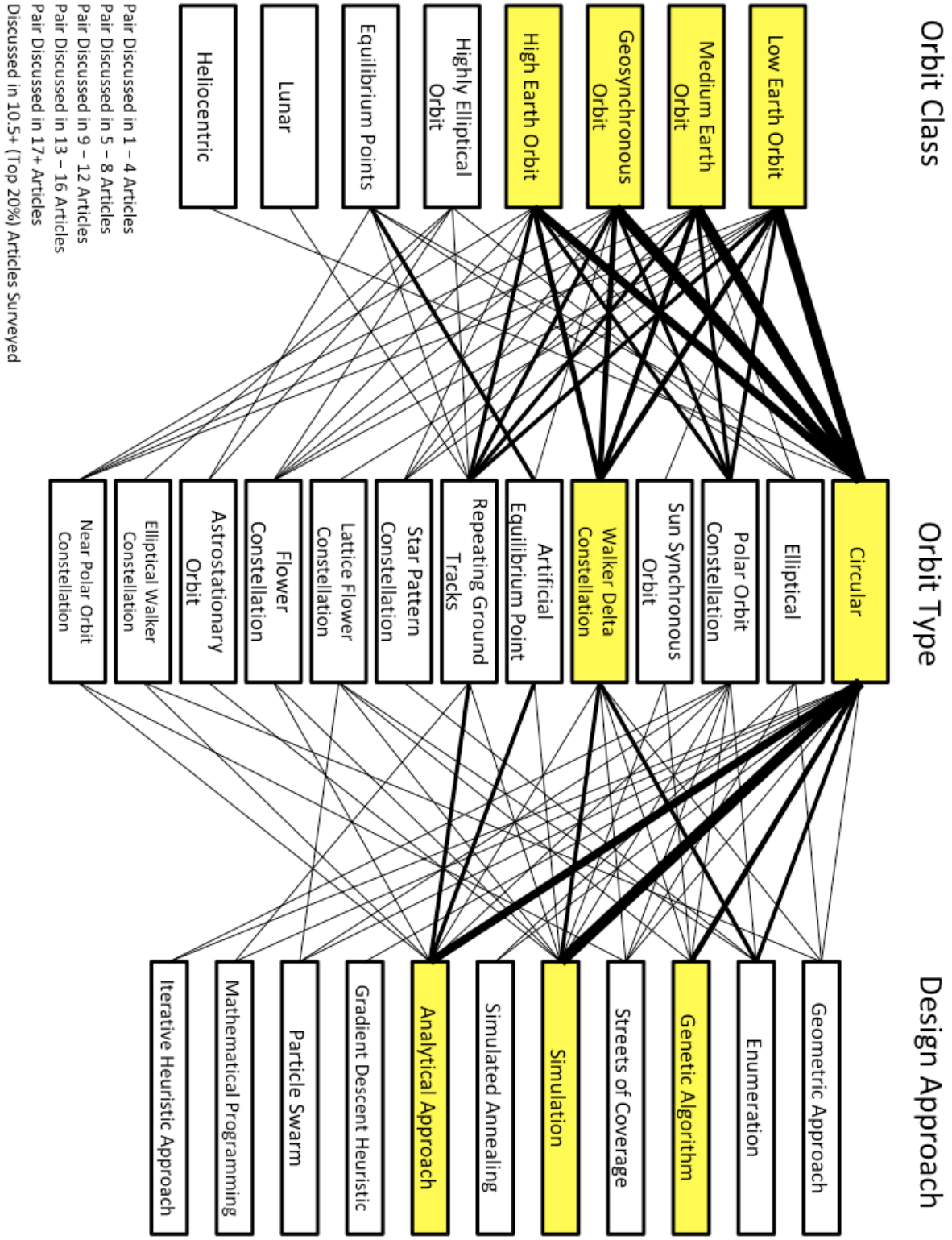

Figure 7: Expanded Topology 2: Geometry - Design Approach

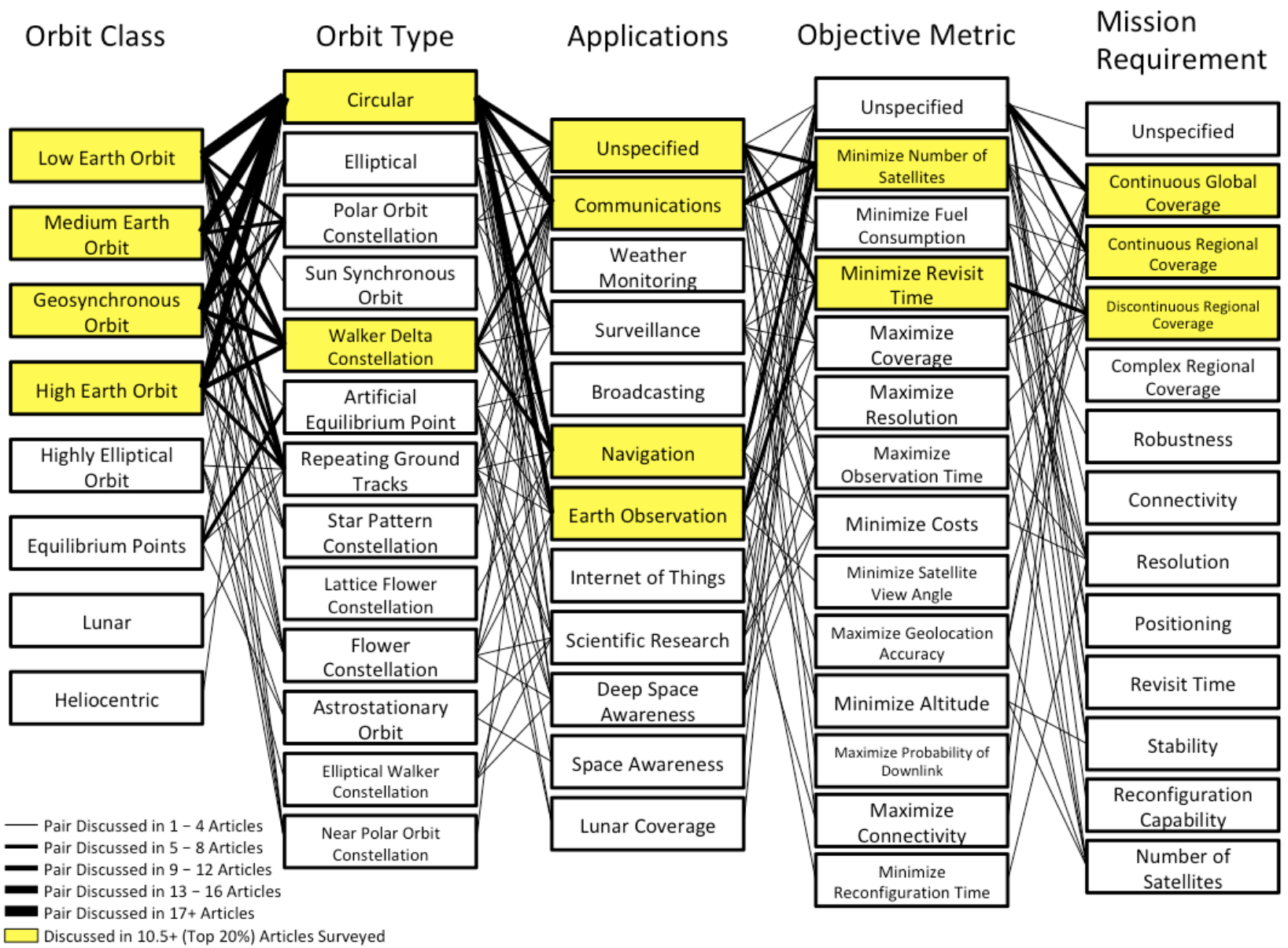

Figure 8: Expanded Topology 3: Mission Set - Design Approach

Each element of the topology is represented by a column. The sub-elements of each element are represented by labeled boxes which are placed in the column corresponding to its respective element. The sub-elements between different elements are connected with line segments. A line segment connecting two boxes indicates that there is at least one article that has been surveyed focusing on the topics identified by the two connected boxes. For example, if there is a line connecting a box labeled 'Low Earth Orbits' to another box labeled 'Repeating Ground Track Orbits', then there is at least one article addressing designing repeating ground track orbits in low Earth orbit. For visualization purposes, Figures 6 to 8 do not show the line segments between non-adjacent columns. Development of a computer program to visualize the expanded topologies using user-specified column orders would allow researchers to compare the category elements suited towards their research. Line segments in Figures 6 to 8 were obtained by identifying the sub-elements associated with each paper. For example, if a paper used a genetic algorithm to minimize the number of satellites to provide continuous global communications, then line segments would be drawn between sub-element pairs (Communications, Minimize Number of Satellites), (Minimize Number of Satellites, Continuous Global Coverage), and (Continuous Global Coverage, Genetic Algorithm) in Figure 6. An individual article can contribute to the thickness of multiple lines connecting two adjacent columns. For example, an article discussing circular orbits in both Low Earth Orbit and Medium Earth Orbit will contribute to the lines connecting both Low Earth Orbit to Circular Orbits and Medium Earth Orbit to Circular Orbits. The thickness of the line segment reflects the proportion of articles that connect the topics identified by the boxes. A thicker line segment indicates that a larger proportion of the articles focuses in a particular research area. A thin line segment indicates that there is a relatively small proportion of articles focusing on a particular research area. Several boxes are highlighted

to make the areas of research that receive more focus easier to identify.

The expanded topology graphs show that much of the research regarding optimal satellite constellation design focuses on designing circular orbit satellite constellations that have regional and global coverage properties through design methods focusing on genetic algorithms, simulations, and a variety of analytical approaches. Many of the articles focused on a geometry of circular orbits and used a Walker Delta constellation design framework, described in Section 2.3.1. The orbit classes most commonly considered included Low Earth Orbit, Medium Earth Orbit, Geosynchronous Orbit, and High Earth Orbit. Although practical applications may not focus on all of these orbit classes, most articles did not place limitations on the altitude of the orbits and consider all of these highlighted orbital classes as a result. The design approaches presented in the literature focused on genetic algorithms, simulations, and many types of analytical approaches. Genetic algorithms are popular because they are capable of exploring non-linear spaces with many local optimal solutions. Simulations are commonly used to evaluate a satellite constellation according to an objective metric that may not be able to be derived analytically. Many analytical approaches take advantage of properties of the specific design question being addressed. The most common mission sets considered in the literature include communications, navigation, and Earth-observation missions. These missions sets usually need to provide a certain level of coverage and the optimization goals are usually to minimize the number of satellites required to provide that coverage as well as minimize the duration of coverage gaps in the provided coverage.

2.3 Satellite Constellation Design Survey

This chapter will now group individual papers using the topology presented in Figure 1 according to mission sets and design approaches. Each subsection will identify

a mission set and will discuss the design approaches used to design satellite constellations for that particular mission set presented in the literature. The articles discussed in this section follow the citation metric threshold guidelines presented in Figure 2. Additional information relative to the following sections can be found in the tables in the Appendix. These tables map the set of surveyed articles to the topology discussed in Section 2.2.

2.3.1 Satellite Constellation Design Geometry Frameworks

There are an infinite number of satellite constellation designs that can be made for any particular mission set. Additionally, the design space of satellite constellations often exhibit characteristics that inhibit the usefulness of conventional linear and non-linear optimization techniques that guarantee convergence to the optimal solution. For example, the design space of a satellite constellation for a particular mission set may use an objective function with many local optimal solutions. One common method that has been used to reduce this complexity in the satellite design process is to limit the design space to a specific satellite constellation geometry framework. This section will identify several satellite constellation geometry frameworks that are commonly utilized in the literature regarding optimal satellite constellation design.

The Walker Delta constellation is a kinematically regular satellite constellation composed of uniformly spaced satellites following circular orbits with a common inclination and altitude [1]. The notation that defines a Walker Delta constellation has four parameters and is written as $\delta : T/P/F$. The parameter δ represents the orbital inclination of all of the orbits. The parameters T, P, and F represent the total number of satellites that are used in the satellite constellation, the total number of orbital planes that are used in the satellite constellation, and a phasing factor used to determine the placement of satellites in adjacent orbital planes. The phasing factor,

F, is an integer ranging from 0 to $(P-1)$. A Walker Delta constellation exhibits the following properties. First, all orbits in the satellite constellation are circular orbits with equal periods. Second, the ascending nodes of each of the P orbital planes are evenly spaced about a reference plane. Third, all of the P orbital planes have a common inclination of δ relative to the reference plane. Fourth, all T satellites are divided equally into the P orbital planes. Fifth, all satellites within an orbital plane are evenly spaced. Sixth, satellites in different orbital planes are positioned relative to one another such that sequential passages of their respective ascending nodes occur at equal intervals defined by F.

Dufour [14] introduced the Elliptical Walker constellation as a method to design kinematically regular satellite constellations consisting of elliptical orbits. Elliptical Walker Constellations are an extension of Walker Delta Constellations. In an Elliptical Walker Constellation, all of the satellites follow elliptical orbits and each orbital plane contains the same number of satellites. Elliptical Walker constellations share several defining parameters with the Walker Delta constellation. The parameters δ and a again represent the common inclination and the common semi-major axis, respectively. $T/P/F$ represents the same parameters they did in the Walker Delta constellation. The Elliptical Walker constellation uses three additional parameters, W, G, and e, to define the shape of the constellation. W is a unitless integer ranging from $-P$ to P and represents the argument of perigee of the reference orbital plane. G is a unitless integer ranging from 0 to $P-1$ and it is used to identify the relative positioning of the arguments of perigee of the remaining orbital planes relative to the reference orbital plane. The final parameter e represents the common eccentricity of the orbital planes.

The Star Pattern Constellation is a satellite constellation comprised of circular orbits that intersect at two points [15]. A Star Pattern constellation is defined by

six parameters, p, n, α, β, γ, and a, which represent the number of orbital planes, the number of satellites in each orbital plane, the half angle between two adjacent co-rotating orbits, the half angle between any two adjacent counter-rotating orbits, the relative phasing of satellites in adjacent co-rotating orbits, and the semi-major axis of the orbits, respectively. The relative inclinations between any pair of adjacent co-rotating orbits is 2α, and between any pair of adjacent counter-rotating orbits is 2β. The values of α and β chosen must satisfy Equation (1) [15].

$$(p-1)\alpha + \beta = \frac{\pi}{2} \tag{1}$$

Figure 9 shows an example of a Star Pattern constellation with $p = 5$ planes. The black circle represents the Earth. The black dotted line represents the reference plane that is used to define an inclination of 0^o. The blue lines represent the orbital planes. The arrows indicate the direction that satellite travel along the orbit. The color of the arrows are used to help differentiate the adjacent co-rotating orbit pairs and the adjacent counter-rotating orbit pairs.

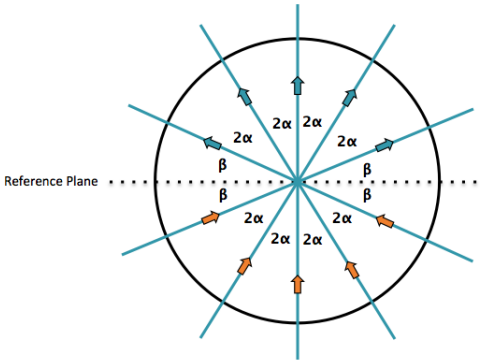

Figure 9: Example of a Star Pattern Constellation

Polar Orbit Constellations are closely related to Star Pattern Constellations. As with the Star Pattern Constellation, all of the orbital planes in the Polar Orbit Constellation intersect at two points. These points shared by the orbital planes in Polar Orbit Constellations are the North and South poles. Polar Orbit constellations are

comprised of circular orbits with a common altitude and are defined by five parameters, p, s, ω, α, and r, which represent the number of orbital planes, the number of satellites in each orbital plane, the inter-plane phasing of satellites in successive orbital planes, the angular separation of the right ascension of the ascending nodes of successive orbital planes, and the common radius of all of the circular orbits, respectively[16]. Unlike the Star Pattern constellation, the orbital spacing does not have to satisfy Equation (1). Despite these differences, some satellite constellations could be classified as both Star Pattern and Polar Orbit constellations. More specifically, the overlap of these satellite constellations occurs when the two intersection points of a Star Pattern constellation are placed at the North and South poles and when the sum of all the angular separations of the right ascension of the ascending nodes of successive orbital planes in the Polar Orbit constellation is less than or equal to π, or $(p-1)\alpha \leq \pi$.

Figure 10 shows some examples of Polar Orbit Constellations. Figures 10a and 10b can also be classified as Star Pattern Constellations. Figure 10c cannot be classified as a Star Pattern Constellation. The black circle represents the Earth. The black dot at the center of the black circle represent the North pole. Each blue line represents an orbital plane. The orbital planes are numbered according to the ordering of successive orbital planes used for inter-plane satellite spacing. The arrows represent the direction that satellites travel within an orbital plane. The orange arrows represent the ascending regions of orbits and the blue arrows represent the descending regions of orbits.

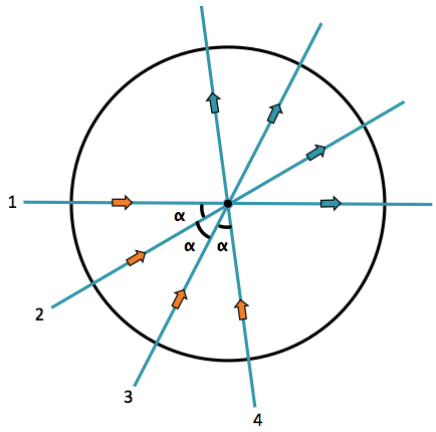

(a) Polar Orbit or Star Pattern Constellation

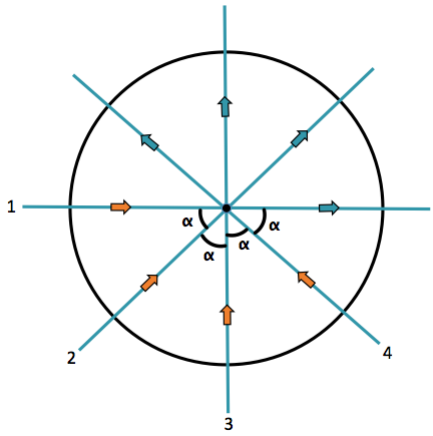

(b) Polar Orbit or Star Pattern Constellation

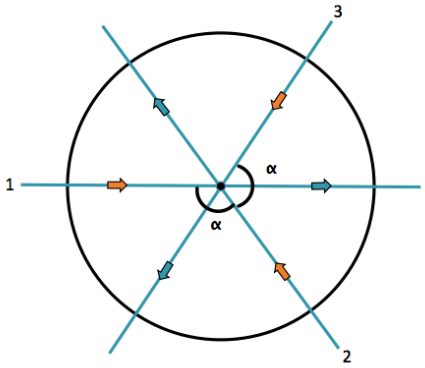

(c) Polar Orbit Constellation

Figure 10: Polar Orbit Constellation Examples

A Near Polar Orbit Constellation is a generalization of the Polar Orbit Constellation. The Near Polar Orbit constellation is defined using the same parameters as the Polar Orbit Constellation, except that the orbital planes do not have to pass through the North and South poles. However, in order to classify the satellite constellation as a Near Polar Orbit constellation, the streets of coverage of all of the orbital planes must contain the North and South poles. A street of coverage is a path of continuous coverage produced by a series of uniformly spaced satellites following a common orbit. All of the orbital planes have the same inclination, i. If C represents the common angular half-width of the streets of coverage of the orbital planes, then

$i \in [\pi/2 - C, \pi/2]$ [17]. Near Polar Orbit constellations are beneficial because there is less concern with satellite collisions at the North and South poles than there is with Polar Orbit Constellations.

The Flower constellation is a constellation of satellites that follow a common repeating ground track. Flower constellations can use either circular or elliptical orbits[18]. The term *flower* is used to describe these constellations because the relative orbital paths form the image of a flower. The image of a flower is especially apparent when elliptical orbits are used. Mortari and Wilkins [19] present the theoretical foundation of Flower Constellations relating to the repeating ground tracks and the phasing of satellites. Flower constellations are designed using a set of nine parameters, $\{N_p,\ N_d,\ F_n,\ F_d,\ F_h,\ \omega,\ i,\ \omega_{ref},\ e\}$[19]. N_p represents the number of petals in the constellation, while N_d represents the number of sidereal days it takes the orbit to complete N_p complete orbits; N_p and N_d are co-prime integers. The three parameters ω, i, and e are the standard classical orbital elements, argument of perigee, orbit inclination, and eccentricity, respectively. The ω_{ref} is the angular velocity of the reference frame. The remaining three parameters represent the phasing of satellites along the repeating ground track where F_d is the number of orbits used, F_n is the number of satellites in each orbit, and F_h is the phase step parameter used to determine the spacing of satellites. Flower Constellations adhere to the following properties. First, all satellites follow a common repeating ground track. Second, the right ascension of the ascending nodes of each orbit in the satellite constellation are evenly spaced about the reference plane. Third, although the phasing step parameter may vary for each satellite, it must be an integer less than N_d: $F_h \in \{0, 1, ..., N_d - 1\}$.

Harmonic Flower Constellations are Flower Constellations with a satellite placed in every admissible point, which are the potential satellite slots available to a given Flower Constellation [20]. Avenfdaño and Mortari [20] proved that a Flower Con-

stellation with a certain set of parameters has a limit on the number of satellites that can be in the constellation. Therefore, a Harmonic Flower Constellation is a Flower Constellation with the maximum number of satellites that can be placed in that respective Flower Constellation.

The Lattice Flower Constellation is a generalized constellation framework for designing any symmetric satellite constellation [21]. Lattice Flower Constellations were originally introduced to reduce the complexity of designing Harmonic Flower Constellations using the Flower constellation framework[22]. There are Two Dimensional Lattice Flower Constellations, three Dimensional Lattice Flower Constellations, and Four Dimensional Lattice Flower Constellations. A lattice matrix, L, is used to determine the configuration of any Lattice Flower Constellation with a variable number of parameters depending on the type of Lattice Flower Constellation used; the lattice matrix is an integer 2×2 matrix, a 3×3 matrix, or a 4×4 matrix, when using a Two Dimensional, Three Dimensional, or Four Dimensional Lattice Flower Constellation, respectively. The Two Dimensional Lattice Flower Constellation originally was created to generalize the Harmonic Flower Constellation and is based on circular orbits and Keplarian unperturbed orbits[22].

Lattice Flower Constellations are defined by a lattice matrix, L, and six additional parameters, a, e, i, ω, Ω_1, and M_1, which represent the semi-major axis, the eccentricity, the orbital inclination, the argument of perigee, the right ascension of the ascending node of the reference satellite, and the initial mean anomaly of the reference satellite, respectively. One of the main differences between the Two Dimensional Lattice Flower Constellation and a Flower Constellation is that the Two Dimensional Lattice Flower Constellation is not limited to a single repeating ground track[22]. Flower Constellations have all of its satellites following a single ground track orbit, but this is not the case for Lattice Flower Constellations.

The three dimensional Lattice Flower constellation expands upon the two dimensional Lattice Flower constellation by including the capability to use elliptical orbits at any inclination under J_2 perturbation effects [23]. One of the major issues with designing elliptical orbits in the presence of perturbations is that non-critically inclined elliptical orbits experience apsidal precession, which is the rotation of the argument of perigee of an orbit. The three dimensional Lattice Flower constellation addresses the apsidal precession by evenly distributing the arguments of perigees of multiple orbits that have a common inclination, eccentricity, and semi-major axis to ensure that the rate of apsidal precession is equivalent in all of the orbits[23]. Davis *et al.* [23] hints that the three dimensional Lattice Flower constellation is most suited for global coverage since the non-critically inclined elliptical orbits exhibit apsidal precession.

Arnas *et al.* [24] expand upon the three dimensional Lattice Flower Constellation and present the Four Dimensional Lattice Flower Constellation. The four dimensional Lattice Flower constellation generates symmetric and uniform satellite constellation designs capable of using elliptical orbits with varying semi-major axis values[24]. The capability of the four dimensional Lattice Flower constellation to utilize multiple semi-major axis values provides additional flexibility into the design space. The added flexibility allows for satellites with different purposes to be used in conjunction with one another. For example, a satellite constellation can be designed to have an intermediary layer of communication satellites that relay information from ground stations to observation satellites in geostationary orbits.

2.3.2 Continuous Global Coverage

Several satellite constellation design methodologies address continuous n-fold global coverage. Continuous n-fold global coverage indicates that any point on the Earth's surface will be covered by at least n satellites at any given moment. The most com-

mon mission applications that requires continuous n-fold global coverage presented in the literature include communications, navigation, Earth-observation, and surveillance missions. The three most commonly used design approaches for analyzing and designing satellite constellations for continuous global coverage include enumeration, analytical approaches, and metaheuristics. Among the most well cited of these methods are [1, 25, 18, 26, 27, 28, 29, 30, 15, 31, 17, 32], which are expanded upon henceforth.

Enumeration has been used for both analyzing and designing satellite constellations for continuous global coverage. Walker [1] proposes using an enumeration method to design Walker Delta Constellations that minimize the number of satellites used in the satellite constellation. Walker [25] identifies the number of satellites and the minimum inter-satellite distances as useful criteria that can be used when designing these constellations for continuous global coverage. Mortari, Wilkins, and Bruccoleri [18] propose using a Flower Constellation as a method for providing global and regional coverage using either circular or elliptical repeating ground track orbits. Ballard [26] uses an exhaustive search method to identify Walker Delta constellations that use the minimum number of satellites required to provide continuous 1-, 2-, 3-, and 4-fold global coverage. Beste [33] derives the relationship between the sensor angle of a sensor with a conic shape with the minimum number of satellites required for a Polar Orbit constellation to provide continuous 1- and 3-fold global coverage. Walker [15] compares the performance of star pattern constellations and Walker Delta constellations to minimize the number of satellites required to provide 1-fold continuous global coverage. The Walker Delta constellation was able to use fewer satellites than the star pattern constellation to provide the same level of desired coverage [15].

Analytical methods have been used to support both analysis and design of satellite constellations for continuous global coverage. Lang and Adams [31] analyze the

performance between Walker constellations and Polar Orbit constellations generated through streets-of-coverage methods focused on minimizing the overall system costs. The relative performance of either of the two constellation types considered depended on the number of satellites that were included in the satellite constellation and the desired level of n-fold coverage. Walker constellations are more efficient for continuous global coverage than Polar Orbit constellations for single-fold coverage using 20 or fewer satellites, and when 2-fold coverage or greater is desired. Polar orbit constellations are more efficient for single-fold coverage when more than 20 satellites are required for continuous global coverage. Walker [15] investigated the optimal phasing of satellites within a Star Pattern constellation for two objective functions. The first objective function was to minimize the maximum distance of any point of the Earth's surface to any of the satellites in the constellation. The second objective function was to maximize the minimum distance between any pair of satellites. Analyzing equations of spherical geometry, Walker created a set of rules to design optimal Star Pattern constellations with respect to these two objective functions. Ulybyshev [17] analytically derives the relationship between the angular separation of co-rotating orbits, the orbital inclination, and the sensor angle to minimize the number of satellites in Near Polar Orbit constellations required to provide 1- or 2-fold continuous global coverage. The performance of Near Polar Orbit constellations was compared to Polar Orbit constellations and Walker constellations in terms of the number of satellites used and the relative performance varied depending on the specific composition of the constellation[17].

Metaheuristics are useful for designing satellite constellations for continuous global coverage. Guan *et al.* [27] use a genetic algorithm to design highly-inclined Walker Delta constellations in Low Earth Orbit addressing a multi-objective problem focusing on maximizing geolocation accuracy and minimizing the number of satellites used in

the satellite constellation. Whittecar and Ferringer [28] investigate the optimality of using Walker Delta constellations for continuous global coverage using a genetic algorithm to design satellite constellations with a given number of satellites following circular orbits with common semi-major axis values and inclinations. The multi-objective considered is to minimize the maximum revisit time and maximize the minimum daily visibility time of any point on the globe. The best designs found by the genetic algorithm for continuous global coverage were approximately Walker Delta constellations suggesting that Walker Delta constellations may be the best satellite constellations for continuous global coverage when only satellites following orbits with a common altitude and inclination are considered.

Han *et al.* [29] use a multi-objective particle swarm algorithm to design Low Earth Orbit satellite constellations based on 2 Dimensional Lattice Flower Constellations for augmenting existing global navigation constellations in Medium Earth Orbit and Geosynchronous orbits. The multi-objective optimization problem focuses on maximizing geolocation accuracy, maximizing satellite visibility, and minimizing orbital altitude using a fixed number of satellites. Huang, Colombo, and Bernelli-Zazzera [30] present a method for multi-objective optimization of satellite constellations considering several constellation properties include coverage, robustness, collision avoidance, launch, and end-of-life strategy. A multi-agent based approach creates a Pareto-frontier of solutions focusing on maximizing performance of the satellite constellation and minimize the costs of operation. The approach focuses on Walker and Polar orbit satellite constellations in Low Earth Orbit and Medium Earth Orbit. Casanova *et al.* [32] compare three different approaches to designing two dimensional Lattice Flower Constellations for maximizing the geolocation estimation accuracy in global positioning. The three methods examined were a genetic algorithm, a particle swarm algorithm, and a brute force method. Overall, the particle swarm algorithm was

the best performing method, the genetic algorithm was the second best performing method, and the brute force method was the worst performing method[32].

2.3.3 Continuous Regional Coverage

Several satellite constellation design methods address continuous n-fold regional coverage. Continuous n-fold regional coverage is provided when every point of a region of interest is covered by at least n satellites at any given moment. Some applications that are commonly considered requiring continuous n-fold regional coverage include communications, Earth-observation, surveillance, weather monitoring, broadcasting, and navigation. The most common design approaches used to design satellite constellations for continuous regional coverage include analytical approaches and metaheuristics. Among the most cited of these methods include [34, 35, 36, 16, 37, 35, 38, 39, 40, 41, 42, 43], which are expanded upon henceforth.

Analytical methods have been used for both analyzing and designing satellite constellations for continuous regional coverage. Lang [34] compares the performance of Walker Delta constellations and Polar Orbit Constellations to provide continuous coverage between $20^o - 60^o$ latitude focused on minimizing the number of satellites. The Walker Delta constellation required fewer satellites than the Polar Orbit constellation to provide continuous coverage between these latitudes. Heiligers *et al.* Rider [35] presents an analytical method based on streets of coverage and differential equations for minimizing the total number of satellites used in a symmetric circular Polar orbit constellation providing continuous n-fold coverage above a specified latitude. Rider [36] presents a closed-form solution method using streets of coverage to design circular inclined orbit satellite constellation for providing coverage between two latitudes while focusing on minimizing the number of satellites used in the satellite constellation. Adams and Rider [16] present a method based on streets of coverage to design

circular Polar Orbit constellations to provide continuous coverage above a specified latitude focusing on minimizing the number of satellites in the constellation.

Ulybyshev [37] presents a geometric method for designing Elliptical Walker constellations with critically inclined elliptical orbits focused on minimizing the number of satellites in the constellation. Ullock and Schoen [38] present an analytical method combined with an enumeration technique to compare the performance between symmetric and asymmetric Polar Orbit constellations focusing on reducing the number of satellites in the satellite constellation. Appropriate inter-plane satellite phasing between adjacent co-rotating orbital planes improves coverage properties of Polar Orbit constellations [38]. Asymmetric Polar Orbit constellations were able to provide continuous regional coverage with fewer satellites than symmetric Polar Orbit constellations [38].

Orbital geometry impacts the amount of orbital maintenance required for a satellite to maintain a desired trajectory, an important aspect for missions requiring continuous regional coverage. Design of satellite constellations for continuous regional coverage also focus on minimizing fuel consumption because high fuel usage in orbital maintenance and maneuvering reduces the lifespan of satellites, and consequently the satellite constellation. Frozen orbits, which one or more orbital parameters remain stable in the presence of perturbations, are one option for minimizing satellite fuel requirements [39]. Other approaches investigate utilizing solar sails to reduce propellant fuel consumption. Heiligers *et al.* [40] present analysis of systems control methods using hybrid solar sails and solar electric propulsion to create displaced geostationary orbits, which is an orbit that maintains its position in geosynchronous orbit above or below the equatorial plane. The analysis focused on identifying the control method that minimized lifetime fuel consumption to maximize the life of the satellite. Ceriotti and McInnes [41] investigate the conditions needed to minimize the propellant

consumption of a spacecraft using solar electric propulsion in conjunction with a solar sail to enable a spacecraft to remain constantly above one of the Earth's poles.

Metaheuristics have also been used for designing satellite constellations for continuous regional coverage. Dai, Zheng, and Chen [42] use a genetic algorithm to design satellite constellations in circular Low Earth Orbit for multi-objective optimization focusing on maximizing the coverage of region of interest and minimizing the total number of satellites used in the constellation. Maihot and Gurfil [43] use a genetic algorithm to design Walker and 3 Dimensional Lattice Flower constellations in Low Earth orbit to maximize the accuracy of geolocation. Mailhot and Gurfil [43] compare the performance of a genetic algorihtm against an enumeration method for designing Three Dimensional Lattice Flower Constellations. The genetic algorithm performed better than the enumeration method since it was not restricted to discretized points of the design region.

2.3.4 Discontinuous Regional Coverage

Satellite constellation design methods also focus on discontinuous regional coverage. Discontinuous regional coverage is where a region of interest only receives coverage periodically. These designs are important because missions may not always require continuous coverage. Common applications for discontinuous coverage includes surveillance, weather observations, geological studies, and other scientific research applications. The most common design approaches to design satellite constellations for discontinuous regional coverage includes metaheuristics, enumeration, and analytical techniques. Amongst the most commonly cited approaches include [44, 45, 46, 47, 48, 49, 50, 51, 52, 53, 54, 55, 56], which are expanded upon henceforth.

Many design approaches utilize metaheuristics to design satellite constellations for

discontinuous regional coverage. Ferringer and Spencer [44] used a genetic algorithm to generate Pareto fronts to analyze the tradeoffs between revisit time and image quality of a satellite constellation with a fixed number of satellites in circular orbit at a common altitude. Fraire *et al.* [45] present a heuristic based on gradient descent to design circular Low Earth Orbit satellite constellations to minimize the number of satellites used in satellite constellation while ensuring that the maximum revisit time remains below a desired threshold. Ferringer, Clifton, and Thomson [46] compare the efficiencies of different parallel multi-objective evolutionary algorithm paradigms for designing circular orbit satellite constellations using a genetic algorithm to minimize the maximum and average revisit times. The goal was to identify the best method to efficiently utilize the computer hardware for parallel processing when designing circular orbit satellite constellations. Savitri *et al.* [49] use a semi-analytical technique to reduce the computational load of a genetic algorithm to generate satellite constellations with an available number of satellites in circular low Earth orbit. The method generates a Pareto frontier focusing on the objectives of maximizing the proportion of points of interest covered, maximizing the average proportion of time that the region of interest is covered, minimizing the maximum revisit time to the region of interest, and minimizing the average revisit time to the region of interest. Abdelkhalik and Mortari [50] explore the utility of genetic algorithms for finding orbits that provide coverage to a set of points of interest on the Earth's surface within a specified time frame without the need for orbital maneuvers while maximizing the resolution of the satellite images and the observation times. Abdelkhalik and Gad [51] present a genetic algorithm with a second order gradient method to find an individual orbit that provides coverage to a set of targets on the Earth's surface in the presence of J_2 orbital perturbations focused on maximizing the number of sites visited and minimizing the amount of time required to visit each of the sites.

Enumeration and analytical approaches are also used for designing satellite constellations for discontinuous regional coverage. Buzzi *et al.* [47] use an enumeration method to design a Walker Constellation focused on minimizing the mean revisit time while using three or fewer orbital planes of satellites. Nadoushan and Assadian [48] present a simple formulation based on Number Theory to generate circular repeating ground track orbits to meet the desired revisit time and satellite tilt requirements with low computational burden. Razoumny [52] presents deterministic and stochastic methods for analyzing revisit times of single satellite and N-satellite repeating ground track constellations. Ortore, Cinelli, and Circi [53] present equations relating multiple orbit parameters to identify satellite arrangements to produce either uniform ground track distances or constant revisit times. Sengupta, Vadali, and Alfriend [54] present a semi-analytical technique that can be used to evaluate coverage time of a point of interest on the Earth's surface by a satellite with a conical sensor in circular low Earth orbit. The semi-analytical approach performed similarly to numerical integration. Vtipil and Newman [55] present a simple algorithm based on epicycle motion to compute the semi-major axis needed for an elliptical orbit to meet the criterion to be a repeating ground track orbit. An efficient method for determining repeating ground track orbits is beneficial for orbit optimization design methodologies. Lee [56] presents a closed-form solution for designing a constellation of satellites following a common circular ground track orbit to minimize the revisit time provided to a single point of interest on the Earth's surface by identifying intersection points along the ground track.

2.3.5 Reconfigurable Satellite Constellations

Satellite constellation design methods also focus on reconfigurable satellite constellations. Reconfigurable satellite constellations are satellite constellations designed

with the intent to regularly toggle between two or more different configurations. This allows different missions to be accomplished using the same set of satellites. Design approaches rely on metaheuristics to design reconfigurable satellite constellations. A common application under consideration is Earth-observation missions for searching and monitoring disasters. One configuration can be used to search the globe for disasters, then the configuration can be adjusted to improve the coverage properties to the disaster location.

Paek *et al.* [57] compare the effectiveness of simulated annealing and genetic algorithms to optimize satellite constellations capable of reconfiguring to meet both global coverage and regional coverage requirements focused on minimizing revisit time, maximizing coverage area, minimizing reconfiguration times, and minimizing the total mass (number of satellites used in the constellation $\times$ satellite mass) while meeting image resolution requirements. The satellite mass includes the mass of the propellant required to meet the delta-V for satellite maneuvers. Circi, Ortore, and Bunkheila [58] introduce the concept of sliding ground track patterns as a method to meet the coverage requirements of a variety of missions requiring periodic coverage. The concept of sliding ground track patterns is the utilization of low-cost maneuvers to change the repeating ground track pattern of a satellite constellation to obtain different coverage properties needed for the particular mission at hand. The method focuses on satellites that are uniformly distributed about a common circular repeating ground track.

2.3.6 Complex Regional Coverage

Satellite constellation design methods sometimes focus on complex regional coverage. Complex regional coverage is irregular, but deliberate, coverage to a region of interest. For example, a region of interest requiring 1-fold coverage between times

0000-0500 and 4-fold coverage between 0500-2400 is a region requiring complex regional coverage. Applications requiring such coverage are more associated with demand that varies at regular intervals. For example, the demand for communication services or broadcasting services in a particular region may be significantly greater during the day than at night. The capability to design satellite constellations that provide complex regional coverage adds flexibility to the types of missions addressed in satellite constellation design. Two well-cited approaches include [59, 60]. Ulybyshev [59] presents a geometric method for designing Walker Delta constellations for complex regional coverage focused on minimizing the number of satellites within the constellation. Lee and Ho [60] present a binary integer linear programming approach to design satellite constellations for complex regional coverage using a set of arbitrary repeating ground track orbits focused on minimizing the number of satellites used for the satellite constellation.

2.3.7 Large-Scale Mega Satellite Constellations

Satellite constellations design methods have begun to address optimal large-scale mega-satellite constellations. Many of the optimization techniques used for optimal satellite constellation design struggle when designing satellite constellations with a large number of satellites. A common application for these mega constellations is continuous global coverage relating to broadband internet. Amongst these approaches regarding optimal mega satellite constellations include [61, 62, 63, 64].

Kak and Akyildiz [61] present an optimization framework for large-scale satellite constellation design focused on a uniform distribution of satellites following circular orbits. The objective is to maximize coverage and connectivity and minimize the number of satellites using a simulated annealing approach. Deng *et al.* [62] present an optimization approach that designs ultra-dense circular Low Earth orbit satellite

constellations focused on minimizing the number of satellites used in the constellations while satisfying each terrestrial-satellite terminal backhaul requirement. The method first generates a polar orbit constellation that satisfies the desired coverage requirements and then iteratively removes redundant satellites. Al-Hourani [63] uses stochastic geometry as an analytical method to find the optimal altitude of dense satellite networks using circular Low Earth orbits aimed at maximizing the probability of downlink coverage in communications between randomly generated users across the globe. Wagner and Black [64] present a method using genetic algorithms to design disaggregated heterogenous satellite constellations, which are satellite constellations composed of satellites with different sensor capabilities and purposes, for regional and global coverage focused on minimizing revisit times. Additionally, a method to evaluate the robustness of the satellite constellation using mixed integer linear programming is presented.

2.3.8 Space Coverage

Several papers also address space coverage in satellite constellation design methods [65, 66, 67, 68, 69]. Common applications include deep space observations for scientific research as well as lunar coverage for surveillance and communications. Although the topology still works for these design methods and applications, the individual approaches will not be expanded upon in this chapter since the discussion of this chapter focuses on Earth focused missions.

2.3.9 Potential Research Areas

Orbital debris and space congestion are, and will continue to be, a major concern in satellite constellation design as the density of debris and the number of satellites in orbit increases. Wertz *et al.* [13] present a thorough discussion of the environmental

hazards posed by orbital debris, the difficulty in tracking and modeling orbital debris, as well as the implications of orbital debris on orbit design. The risk of collisions increases with the amount of orbital debris and number of satellites orbiting in space. Collisions with satellites not only increase the density of debris in space, but also degrade the mission performance of the remaining satellite constellation. Appropriate end-of-life strategies for disposing satellites helps limit the amount of orbital debris; however, end-of-life strategies may also require extensive planning to avoid collisions during disposal [13]. As a result, methods addressing orbital debris and end-of-life strategies in satellite constellation design will remain a fruitful and beneficial area of research in the near-future.

2.4 Conclusion

This chapter presents a novel topology approach to analyze the current state of the literature as it relates to optimal satellite constellation design. The developed topology implements a 6-tuple classification scheme that is useful in organizing the articles in the literature regarding optimal satellite constellation design. The topology provides a construct to identify potential research opportunities that exist by characterizing the relationships between the geometries, the mission sets, and the design approaches commonly used in the literature as well as a reference of current methodologies for satellite constellation design. Figures 6 to 8 illustrate the focus of past research while also identifying the areas which may be ripe for future research. The most referenced literature uses genetic algorithms, simulations, and a variety of analytical approaches to design circular orbit satellite constellations addressing global and regional coverage for the application of communication, navigation, and Earth observing missions.

2.5 Appendix: Mapping Articles to the Topology

This appendix contains tables used to map specific articles to the topology presented in this paper. Table 7 maps each article in the set of surveyed articles to the topology. Table 7 can be used to help identify potential research opportunities and to direct readers towards specific papers that might be beneficial to their research. The numbers in Table 7 are identifications corresponding to the specific sub-elements of the categories used in the topology. The identification numbers for Orbit Class, Orbit Type, Applications, Design Approach, Objective Metric, and Mission Requirements identified in Table 1, Table 2, Table 3, Table 4, Table 5, and Table 6, respectively. Articles included in Table 7 do not have to meet the citation metric used to determine which articles are included in the analysis of this paper.

Table 1: Orbit Class ID

ID	Orbit Class
1	Low Earth Orbit
2	Medium Earth Orbit
3	Geosynchronous Orbit
4	High Earth Orbit
5	Highly Elliptical Orbit
6	Equilibrium Points
7	Lunar
8	Heliocentric
9	Mars Centered Orbit

Table 2: Orbit Type IDs

ID	Orbit Type
1	Circular
2	Elliptical
3	Geostationary
4	Polar Orbit Constellation
5	Sun Synchronous Orbit
6	Walker Delta Constellation
7	Artificial Equilibrium Point
8	Repeating Ground Track Orbits
9	Star Pattern Constellation
10	Lattice Flower Constellation
11	Flower Constellation
12	Astrostationary Orbit
13	Elliptical Walker Constellation
14	Near Polar Orbit Constellation
15	Revisit Orbit
16	Apogee at Constant Time of Day Equatorial Orbit (ACE)

Table 3: Application IDs

ID	Application
1	Unspecified
2	Communications
3	Weather Monitoring
4	Surveillance
5	Broadcasting
6	Navigation
7	Earth-Observation
8	Earth Resources
9	Disaster Monitoring
10	Internet of Things
11	Scientific Research
12	Deep Space Awareness
13	Space Awareness
14	Reconnaissance
15	Lunar Coverage

Table 4: Design Approach IDs

ID	Design Approach
1	Unspecified
2	Geometric Approach
3	Enumeration
4	Genetic Algorithm
5	Streets of Coverage
6	Simulations
7	Simulated Annealing
8	Analytical Approach
9	Gradient Descent
10	Particle Swarm
11	Mathematical Programming
12	Iterative Heuristic Approach
13	Differential Evolution

Table 5: Objective Metric IDs

ID	Objective Metric
1	Unspecified
2	Minimize Number of Satellites
3	Minimize Fuel Consumption
4	Minimize Revisit Times
5	Maximize Coverage
6	Maximize Resolution
7	Maximize Observation Time
8	Minimize Costs
9	Minimize Satellite View Angle
10	Maximize Geolocation Accuracy
11	Minimize Altitude
12	Maximize Probability of Downlink
13	Maximize Connectivity
14	Minimize Reconfiguration Time
15	Maximize Quality of Service (QoS)
16	Minimize System Response Time
17	Maximize Stability
18	Maximize Angular Spacing of Orbits
19	Maximize Inter-satellite Spacing

Table 6: Mission Requirement IDs

ID	Mission Requirement
1	Unspecified
2	Continuous Global Coverage
3	Continuous Regional Coverage
4	Discontinuous Regional Coverage
5	Complex Regional Coverage
6	Robustness
7	Demand
8	Resilience
9	Connectivity
10	Budget
11	Altitude
12	Resolution
13	Positioning
14	Collision Avoidance
15	Revisit Time
16	Stability
17	Reconfiguration
18	Number of Satellites
19	Space Situational Awareness Coverage

Table 7: Literature Directory

Article	Orbit Class	Orbit Type	Application	Design Approach	Objective Metric	Mission Requirement	Number Citations	Citation Metric (#citations /Years)
[70]	[1,2,3,4]	[1,6]	1	3	2	[2,3]	18	1.1
[71]	[1,2,3,4,5]	[1,2]	2	[4,5,8]	[2,11]	3	52	2.2
[37]	5	[2,13]	7	[2,8]	2	3	25	1.9
[72]	[1,2,3,5]	[1,2]	2	6	[2,11]	2	2	0.1
[73]	[1,2,3,4]	1	[2,6,7]	[3,8]	11	[2,3]	10	0.6
[74]	[1,2,3,4]	1	6	[3,8]	2	2	17	0.4
[26]	[1,2,3,4]	[1,6]	[2,6]	3	2	2	317	7.5
[75]	5	2	2	2	13	[3,9]	1	0.1
[76]	[1,2,3,4]	[1,6]	1	[3,6]	4	4	54	1.4
[77]	[1,2,3,4]	[1,6]	1	6	9	2	13	0.5
[78]	2	[2,5]	2	6	1	[2,16]	24	0.9
[79]	1	[1,6]	1	3	2	2	59	2.1
[80]	[1,2,3,4]	[1,6]	1	[3,6]	2	2	69	2.0
[16]	[1,2,3,4]	[1,4]	[2,4,6]	[6,10]	2	3	190	5.4
[81]	3	[1,2,3,6,8]	7	[3,6]	5	[2,3]	14	0.4

Table 7 continued from previous page

Article	Orbit Class	Orbit Type	Application	Design Approach	Objective Metric	Mission Requirement	Number Citations	Citation Metric (#citations /Years)
[36]	[1,2,3,4]	1	[2,4,6]	[5,8]	2	3	132	3.7
[35]	[1,2,3,4]	[1,4]	4	[5,8]	2	3	130	3.5
[82]	[1,2,3,4]	1	[6,7]	5	2	[2,3]	32	0.5
[25]	[1,2,3,4]	[1,6]	1	3	[2,7]	2	341	9.0
[15]	[1,2,3,4]	[1,6,9]	2	3	2	2	171	3.3
[18]	[1,2,3,4,5]	[1,2,8,11]	[2,6,7,11,12]	6	1	[2,3,4]	134	7.4
[83]	5	2	2	8	5	3	4	0.2
[84]	1	[1,8,14]	2	[5,8]	2	2	1	0.0
[85]	[2,5]	[2,5]	2	1	[2,8]	2	32	1.5
[33]	[1,2,3,4]	[1,4]	1	8	2	2	194	4.4
[86]	[1,2,3,4]	1	[2,6]	2	2	2	24	0.5
[87]	[1,2,3,4]	[1,4]	4	[3,8]	2	3	162	2.7
[88]	1	[1,6]	2	3	[9,11]	9	2	0.2
[89]	[2,5]	2	2	[2,8]	8	3	0	0.0
[14]	5	[2,13]	1	[3,6]	2	[2,3]	23	1.2
[90]	[1,2,3]	[1,2,4,6]	2	6	[8,13]	2	11	0.6
[91]	5	[2,16]	2	1	1	[5,7]	3	0.2
[92]	[1,2,3]	1	2	[4,6]	[2,9]	[2,3]	23	1.2
[93]	1	1	[2,6,7]	[5,6]	2	3	2	0.1
[94]	3	[1,6]	1	[4,6]	[2,5]	2	60	2.5
[95]	[1,2,3,4]	1	7	[4,6]	4	4	64	2.5
[34]	[1,2,3,4]	[1,4,6]	1	[3,6]	2	3	27	3.0
[96]	5	2	2	[2,5]	2	3	14	0.5
[97]	5	2	2	6	2	3	8	0.3
[98]	1	1	2	6	2	3	3	0.1
[99]	1	[1,6]	2	8	13	2	4	0.1
[100]	5	2	[2,3,4,6]	[2,8]	2	2	44	1.4
[101]	1	1	1	[5,8]	2	2	26	0.8
[102]	5	2	[2,3,6]	[3,6]	9	2	99	2.8
[103]	5	2	1	[2,6]	2	[2,3]	90	2.4
[38]	[1,2]	[1,4]	1	[3,8]	2	3	40	0.7
[104]	1	1	2	[2,8]	5	[2,3,4]	26	1.2
[17]	[1,2,3,4]	[1,14]	2	[5,8]	2	2	37	1.6
[105]	5	2	5	3	7	[3,16]	2	0.1
[106]	[1,2,3,4]	1	5	3	9	2	65	1.3
[107]	[1,2,3,4]	[1,6]	[2,6]	[4,6]	2	[2,3,6]	52	2.2
[108]	5	2	2	2	1	[2,13]	6	0.4
[59]	[1,2,3,4]	[1,6]	[2,6,7]	[2,8]	2	5	95	6.8
[57]	[1,2,3,4]	1	7	[4,6,7]	[2,4,5,14]	12	34	11.3
[27]	1	[1,6]	6	[4,6]	[2,10]	2	20	10.0
[109]	1	[1,6]	6	[5,6]	10	[2,11,18]	1	0.5
[110]	[1,2,3,4]	[1,2]	[2,6]	[4,6]	8	3	5	1.3
[111]	1	[5,8,11]	7	[4,6]	17	4	14	0.8
[112]	1	[1,6]	[8,11]	[3,6]	[4,8]	4	0	0.0
[113]	[1,2,3,4]	1	1	[4,6]	4	4	15	0.9
[61]	[1,2]	1	[2,10]	[6,7]	[2,5,13]	2	13	4.3
[114]	9	[1,6]	[2,6]	[4,6]	[4,8]	[2,9]	5	1.0

Table 7 continued from previous page

Article	Orbit Class	Orbit Type	Application	Design Approach	Objective Metric	Mission Requirement	Number Citations	Citation Metric (#citations /Years)
[115]	1	1	2	11	2	[2,9]	1	1.0
[44]	[1,2,3,4]	1	7	[4,6]	[4,6]	18	89	5.6
[64]	[1,2,3,4]	1	1	[4,6,11]	4	6	6	3.0
[116]	1	[1,5,8]	[4,9,14]	[4,6]	2	[3,4,12,15]	1	0.5
[117]	1	1	6	[4,6,7]	5	[3,4]	9	0.9
[118]	[1,2,3]	[1,6]	6	[4,6]	[8,10]	2	2	0.3
[42]	1	1	2	[4,6]	[2,5]	3	19	4.8
[119]	[1,2,3,4]	[1,6]	7	[4,6]	[4,6,8]	[3,4]	0	0.0
[120]	[1,2,3,4]	[1,6]	[4,7,9,14]	[4,6,7]	[2,4,14]	[2,3,4,10,17]	23	2.3
[121]	[1,2,3]	[1,6]	6	[4,6]	[8,10]	2	4	0.6
[122]	1	[1,4]	2	7	2	[2,7,17]	22	1.3
[62]	1	[1,4]	2	[6,12]	2	[2,9]	7	3.5
[63]	1	1	2	8	12	2	13	13.0
[123]	1	[1,6]	2	[4,6]	15	[2,3,16]	6	2.0
[124]	2	[1,5]	[7,9]	[3,6]	16	2	8	2.7
[65]	8	1	[11,12]	[6,7]	[7,8]	12	78	4.3
[125]	[1,2,3,4]	[1,8]	[7,9]	[4,11]	[3,14]	[3,17]	5	2.5
[126]	1	[1,6]	2	[4,6]	2	[3,7]	9	2.3
[19]	[1,2,3,4,5]	11	1	8	1	1	82	5.9
[55]	5	[2,8]	1	8	11	16	35	3.5
[45]	1	1	10	[6,9]	2	[4,15]	14	7.0
[66]	[5,6]	[2,7,12]	[11,12]	6	1	16	2	INF
[127]	[1,2,3,4]	[1,8]	9	11	3	[4,17]	8	1.6
[128]	5	2	[11,13]	6	5	[6,10]	26	1.9
[46]	[1,2,3,4]	1	1	[4,6]	4	4	54	3.6
[129]	[1,2,3]	1	13	[2,3,6,8]	11	19	13	1.2
[67]	5	13	[11,12]	8	3	[4,13]	7	7.0
[28]	[1,2,3,4]	[1,6]	1	[4,6]	[4,7]	18	32	4.0
[130]	[1,2,3,4]	1	13	[3,6,8]	2	3	14	1.8
[131]	1	[1,4,6]	2	[4,6]	4	[2,3]	6	2.0
[132]	2	[1,6]	2	[4,6]	2	[2,3]	6	1.0
[29]	1	[1,10]	6	[6,10]	[6,10,11]	18	15	15.0
[40]	[3,6]	[1,7]	[2,7]	8	3	[3,16]	59	5.4
[133]	1	[1,6]	7	[4,6]	[4,5,8,16]	3	3	1.5
[134]	1	[5,8]	7	[4,6]	[4,6,17]	16	15	1.9
[43]	1	[6,10]	6	[4,6]	10	3	3	INF
[135]	1	[1,5]	7	3	4	4	14	1.0
[136]	[1,2]	1	2	[4,6]	[2,9,18,19]	2	18	0.9
[47]	[1,2,3,4]	[1,6]	3	[3,6]	4	4	28	9.3
[137]	3	1	[2,3,4]	1	8	[6,8]	5	0.4
[1]	[1,2,3,4]	[1,6]	[2,4,6]	[3,6]	2	2	198	4.4
[138]	1	[1,6]	1	[2,4,6]	[2,4,5]	[3,4]	0	0.0
[139]	[6,7]	[1,2,7]	[13,15]	6	1	16	5	2.5
[58]	[1,2,3,4]	[1,8]	1	8	3	[4,17]	39	4.9
[140]	5	[2,8]	7	[4,6]	6	[5,15]	8	0.7
[30]	[1,2]	[1,4,6]	[2,4,6]	[4,6]	[5,8]	2	6	6.0
[141]	[1,2,3,4,5]	11	1	8	1	13	14	0.8

Table 7 continued from previous page

Article	Orbit Class	Orbit Type	Application	Design Approach	Objective Metric	Mission Requirement	Number Citations	Citation Metric (#citations /Years)
[142]	[1,2,3,4]	[1,8]	[2,4]	8	1	4	43	1.9
[48]	[1,2,3,4]	[1,8]	7	8	[4,9]	4	34	4.9
[143]	[1,2,3,4,5]	[1,2]	2	6	[7,13,15]	2	12	0.7
[31]	[1,2,3,4]	[4,6]	1	5	8	2	72	3.0
[49]	1	1	1	[4,6,8]	[4,5,7]	4	43	8.6
[144]	[1,2,3,4,5]	[1,2,8]	1	8	9	[4,15]	13	1.1
[50]	[1,2,3,4]	1	4	[4,6]	[6,7]	4	60	3.8
[145]	[1,2,3]	[1,8,15]	[7,9]	8	4	4	17	2.8
[146]	[1,2,3,4]	[1,8]	7	[6,8]	3	16	1	0.3
[54]	1	1	7	8	4	4	36	3.0
[147]	[1,2,3]	[1,5,8]	9	6	6	[3,4]	3	0.3
[148]	[1,2,3,4]	[1,8]	[2,7]	8	17	16	18	1.3
[149]	1	[1,5]	7	13	[7,9]	[4,15]	14	2.0
[68]	7	8	15	8	1	16	55	3.7
[150]	5	2	2	[2,8]	1	4	14	0.8
[151]	[1,2,3,4]	1	[4,7]	[2,6,8]	1	4	1	1.0
[51]	1	5	7	[4,6]	[4,5]	4	39	3.5
[60]	[1,2,3,4,5,6]	8	1	11	2	5	11	5.5
[52]	[1,2,3,4]	[1,8]	1	8	4	4	30	5.0
[53]	[1,2,3,4]	[1,8]	[2,6,7,11]	8	1	[13,15]	19	3.8
[152]	6	7	5	8	1	3	108	3.5
[153]	6	7	[11,12]	8	1	16	6	1.2
[154]	6	[1,7]	1	8	1	16	33	3.0
[155]	6	[2,7]	1	8	1	16	22	2.2
[156]	6	7	[11,12]	8	17	16	3	0.8
[69]	6	7	[2,15]	8	1	[3,16]	55	4.2
[157]	6	7	[12,13]	8	1	[3,16]	40	4.4
[158]	6	7	1	[6,8]	1	16	9	1.3
[41]	6	7	[2,7]	8	3	3	42	3.8
[159]	5	2	[2,5]	[3,6]	1	2	15	0.8
[22]	[1,2,3,4]	[1,10]	[2,4,6,7]	1	1	1	68	7.6
[23]	[1,2,3,4,5]	[1,2,10]	[2,4,6,7]	1	1	1	41	4.6
[24]	[1,2,3,4,5]	[1,2,10]	[2,4,6,7]	1	1	1	9	9.0
[32]	1	[1,10]	6	[3,4,6,10]	10	18	5	0.5
[56]	[1,2,3,4]	[1,8]	[4,7]	8	4	4	4	4.0

III. Orbital Parameter Determination of Single Satellite Circular Orbits for Regional Coverage Using a Response Surface Methodology

Abstract

Enhanced terrestrial regional coverage compels the development of a customized metaheuristic for the selection of a circular repeating ground track orbit for a single satellite. A methodical application of designed experiments and response surface methods guides the design of single satellite orbits to achieve improved regional observation coverage using repeating ground tracks. Testing compares the performance of the metaheuristic against the performance of a genetic algorithm approach, a simulated annealing approach, and a particle swarm algorithm approach. The metaheuristic is more computationally efficient than both the genetic algorithm and simulated annealing approaches, and obtains comparable solution results to the genetic algorithm, simulated annealing, and particle swarm approaches.

3.1 Introduction

Satellite constellations using circular orbits are popular for Earth-focused missions (e.g., communications, observation). Myriad of satellite constellation design literature presents approaches to design circular orbit satellite constellations that rely on predefined geometry frameworks, such as Walker and Polar Orbit constellations [1, 17, 26, 28, 31]. Choo *et al.* [160] present a comprehensive survey of satellite constellation design methodologies. Although satellite constellations may be necessary for certain missions, a single satellite may suffice where the region of interest is small, continuous coverage is not required, or geosynchronous orbits are used. This yields the question: "*What is the best circular orbit for regional coverage if only a*

single satellite is available?"

Related Literature

The satellite constellation design literature presents iterative algorithms and analytical methods to select and evaluate single-satellite, repeating ground track orbits for a single point of interest on the Earth's surface [145, 48, 56]. Lee [56] presents an iterative algorithm to design single-satellite, circular repeating ground track orbits for discontinuous regional coverage to minimize revisit time to a single point on the Earth's surface by identifying self-intersection points of the ground tracks. However, most missions require regions of interest spanning a surface area greater than a single point or more than one region on the Earth's surface (e.g., Global Positioning System, surveillance, navigation).

Satellite constellation design literature frequently uses metaheuristics capable of exploring nonlinear objective functions with many local optimal solutions for satellite constellation design. Paek *et al.* [57] use a simulated annealing algorithm to design Walker constellations suitable for altering coverage between regional and global discontinuous coverage for agile Earth observations. Chen *et al.* [161] use a differential evolution algorithm to reconfigure an existing satellite constellation for a new mission purpose. Wang *et al.* [162] design satellite constellations using a hybrid-resampling particle swarm algorithm that overcomes the drawbacks of the premature convergence and the long computation times commonly observed of standard particle swarm algorithms. Genetic algorithms [163] commonly select circular satellite orbits for both discontinuous and continuous regional coverage in both single and multiobjective optimization design problems [44, 46, 49, 50, 51].

Although response surface methodology optimizes design performance in many industries, including engine performance [164], munitions use [165], aircraft wing design [166], and waste water processing [167], it does not receive much focus in

satellite constellation design or orbit selection [160]. Response surface methodology guides optimization using the predicted response information obtained through the application of design of experiments and regression analysis [168]. Response surface analysis uses fitted surface information to predict the response of an objective near the sampled points of the designed experiment, which could benefit satellite orbit selection processes.

Contributions

This chapter makes the two specific contributions. The first presents a custom metaheuristic based on sequential linear regression and response surface analysis to design single-satellite, circular orbits with repeating ground tracks for regional coverage. Next, an example scenario compares the performance of the metaheuristic against baseline genetic algorithm, simulated annealing, and particle swarm approaches.

In the remainder of the chapter, Section 3.2 describes the orbital design problem, its unknown parameters, and the methodology to identify them. Section 3.3 reports the results of computational testing to compare the proposed metaheuristic with baseline solution methods. Section 3.4 summarizes insights and identifies extensions to this research.

3.2 Problem Definition and Solution Methodology

The problem of single-satellite, circular repeating ground track orbit design focused on maximizing the average observational coverage provided to a region of interest on the Earth's surface, which is a nonlinear objective function, benefits from an efficient exploration of the orbital design space.

3.2.1 *Orbital Design Space*

A four-tuple, $(L, M, i, \lambda_{init})$, represents the design space of single-satellite, circular repeating ground track orbits. L and M represent the repeating parameters of a repeating ground track. The repeating parameters L and M indicate that a satellite uses L orbits to repeat a ground track once every M sidereal days. Often referred to as an $L : M$ resonance pair, the L and M must be co-prime integers, i.e., their greatest common factor is 1 [1]. The parameter i represents the orbital inclination and λ_{init} represents the longitude of the initial ascension across the equatorial plane.

The inherent complexities of such a problem do not lend themselves to a mathematical programming approach; the orbital design decisions do not inform a closed-form analytic equation for the objective function. However, a simulation can evaluate any design, so it is necessary to design a solution method that effectively and efficiently explores the design space.

In a computationally exhaustive approach, one could sample the design space with an appropriate granular mesh. Exploring an instance of the (i, λ_{init})-space for an $L : M$ pair, testing to simulate the satellite at a granularity of considering 0.1-degree increments for $i \in (0^o, 180^o)$ and $\lambda_{init} \in [0^o, 72^o]$ requires evaluation of 1,298,521 design points for a single replication. Stochastic simulations would require simulating for an adequate number of replications to attain appropriate variance reduction and confidence in the estimated coverage.

Figure 11 depicts the results of applying this approach for a single-satellite, circular repeating ground track orbit for $(L, M) = (5, 1)$ at an elevation angle of 35^o with the objective of maximizing the coverage provided to a discretized represenation of South Korea. The contours depict the expected average coverage time relative to the repeat period of the ground track (termed the average proportion of coverage) of the discretized region.

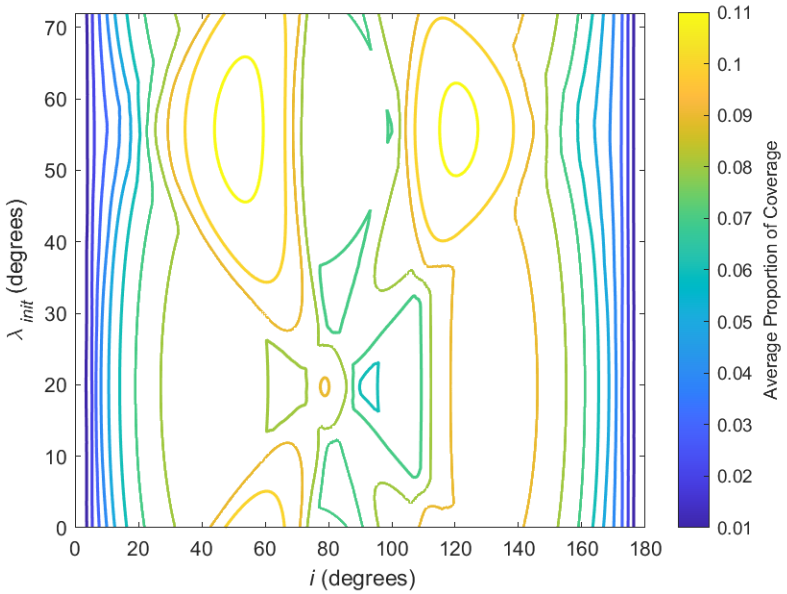

Figure 11: Average Proportion of Coverage Provided to a South Korea using a Single Satellite

The initial testing reveals two insights. First, the response surface is non-convex. As such, deliberate techniques are necessary to cleverly search the space for locally optimal design points, and, in turn, identify global optimal design points. Second, this exhaustive testing approach is not computationally practical. The approximation of this surface required approximately 18 hours of computational effort on a computer using an Intel(R) Core(TM) i3-4160 CPU with 16 GB of RAM. Moreover, it may not be sufficiently granular to identify a global optimal solution. For both of these reasons, a customized metaheuristic approach may be well-suited to address instances of this problem.

3.2.2 *Customized Metaheuristic*

Among the most commonly embraced metaheuristics in the literature are genetic algorithms [163], simulated annealing [169], and particle swarm optimization [170]. Testing in Section 3.3 will compare these approaches, but the anticipated nature of

the design performance surface (e.g., see Figure 11) compels the development of a customized metaheuristic. This section details its motivation, structure, and procedural aspects.

The proposed metaheuristic, termed the *Iterative $L : M$ Pair Method*, explores the single-satellite, circular repeating ground track orbit design space by iteratively considering a pre-defined set of $L : M$ resonance pairs. The metaheuristic iteratively considers $L : M$ pairs to ensure they remain co-prime integers. For each considered $L : M$ resonance pair, a methodical application of a designed experiment and response surface analysis explores the design ranges of factors i and λ_{init}. Algorithm 1 outlines the Iterative $L : M$ Pair Method.

Algorithm 1 Iterative $L : M$ Pair Method

```
1: Initialize the set of L : M pairs to explore
2: for Each L : M pair do
3:     Define the design space
4:     Initialize the design regions
5:     while Design regions exist do
6:         for Each design region do
7:             Create a designed experiment
8:             Evaluate the design points
9:             Fit and analyze regression models
10:            Identify design regions for subsequent iterations
11: Update the best solution found
```

Line 1 in Algorithm 1 initializes the set of $L : M$ pairs to consider. In Line 3, it defines the design space, which is a hyperrectangle defined by the upper and lower bounds for each design factor. Line 4 initializes the design regions, which are subspaces of the design space, within each of which the procedure will exploit the objective response surface to independently explore the design space. Line 7 uses designed experiments to sample each design region. This research applies nearly-orthogonal Latin hypercube designs to sample each design region because they have good space-filling properties [171]. Additionally, orthogonal designs exhibit less multi-

collinearity in regression models than non-orthogonal designs, making them favorable for regression analysis [168]. Line 8 uses simulations to evaluate the objective metric associated with each of the sampled design points. Lines 9 and 10 respectively analyze the responses in each of the design regions and, leveraging those derived insights, creates new design regions to further explore the design space. This process continues until termination, after which outputs the design point corresponding to the best objective metric value found in the search process. The processes for initializing and analyzing the design regions merits elaboration.

Initialize the Design Regions (Line 4, Algorithm 1)

Initialization creates the first set of design regions used to explore the design space. The particular initialization approach used in this chapter applies the following steps. First, the procedure creates a temporary design region, $\mathscr{R}_{Temp}$, equal to the design space, $\mathscr{D}$, and samples design points from the region using an appropriate space covering design. If none of the design points correspond to an objective function value greater than a specified initialization threshold, δ, the procedure divides $\mathscr{R}_{Temp}$ into 2^N equally-sized temporary design regions, where N represents the number of design factors, and the process repeats.

Lemma 1: For a single-satellite, circular repeating ground track orbit with a given $L : M$ pair, a feasible region $\mathscr{D} \equiv \{(i, \lambda_{init}) : i^{LB} \leq i \leq i^{UB}, \lambda_{init}^{LB} \leq \lambda_{init} \leq \lambda_{init}^{UB}\}$, and a response function $f : (i, \lambda_{init}) \to \mathbb{R}$, if $\exists(\bar{i}, \bar{\lambda}_{init}) \in \mathscr{D} : f((\bar{i}, \bar{\lambda}_{init}) > \delta$ for some user-defined $\delta \in \mathbb{R}$, the aforementioned, iterative partition and (sub)region sampling procedure will identify $(\bar{i}, \bar{\lambda}_{init})$.

Proof: Let $\mathscr{D} \equiv \{(i, \lambda_{init}) : i^{LB} \leq i \leq i^{UB}, \lambda_{init}^{LB} \leq \lambda_{init} \leq \lambda_{init}^{UB}\}$, $f : (i, \lambda_{init}) \to \mathbb{R}$, and $\delta \in \mathbb{R}$. Clearly, $\mathscr{D}$ is a closed convex set. Let $(\mathscr{D}, d)$ define a metric space, with $d : \mathscr{D} \times \mathscr{D} \to \mathbb{R}$. Suppose $\exists(\bar{i}, \bar{\lambda}_{init}) \in \mathscr{D} \ni f((\bar{i}, \bar{\lambda}_{init})) > \delta$.

If $i^{LB} = i^{UB} = \bar{i}$ and $\lambda_{init}^{LB} = \lambda_{init}^{UB} = \bar{\lambda}_{init}$, then $\mathscr{D} \equiv \{(i, \lambda_{init}) : \bar{i} \leq i \leq \bar{i}, \bar{\lambda}_{init} \leq$

$\lambda_{init} \leq \bar{\lambda}_{init}\}$. Therefore, $\mathscr{D} = \{(\bar{i}, \bar{\lambda}_{init})\}$ and $(i_s, \lambda_s) = (\bar{i}, \bar{\lambda}_{init})$ for any sampled $(i_s, \lambda_s) \in \mathscr{D}$.

Suppose $i^{LB} < i^{UB}$ or $\lambda_{init}^{LB} < \lambda_{init}^{UB}$ (i.e., $\mathscr{D}$ is not a singleton). Let $\{Q_1, Q_2, ...\}$ be a countably infinite set of closed and convex subsets of $\mathscr{D}$ such that $Q_1 = \mathscr{D}$, $Q_{k+1} \subset Q_k \ \ \forall k \in \mathbb{N}$, and $(\bar{i}, \bar{\lambda}_{init}) \in Q_k \ \ \forall k \in \mathbb{N}$. Let $V^k_{(\bar{i}, \bar{\lambda}_{init})} \equiv \{d((i, \lambda), (\bar{i}, \bar{\lambda}_{init})) : (i, \lambda) \in Q_k\}$. Since $Q_{k+1} \subset Q_k \ \ \forall k \in \mathbb{N}$, then $V^{k+1}_{(\bar{i}, \bar{\lambda}_{init})} \subset V^k_{(\bar{i}, \bar{\lambda}_{init})} \ \ \forall k \in \mathbb{N}$, thus, $\sup(V^{k+1}_{(\bar{i}, \bar{\lambda}_{init})}) \leq \sup(V^k_{(\bar{i}, \bar{\lambda}_{init})}) \ \ \forall k \in \mathbb{N}$. Let $\{(i_k, \lambda_k)\}$ be a sequence of samples in $(\mathscr{D}, d)$ where $(i_k, \lambda_k) \in Q_k \ \ \forall k \in \mathbb{N}$ and $d((i_k, \lambda_k), (\bar{i}, \bar{\lambda}_{init})) \in V^k_{(\bar{i}, \bar{\lambda}_{init})} \ \ \forall k \in \mathbb{N}$. Therefore, since $\{Q_1, Q_2, ...\}$ is a set of closed and convex subsets of $\mathscr{D}$ with $Q_{k+1} \subset Q_k \ \ \forall k \in \mathbb{N}$ and $(\bar{i}, \bar{\lambda}_{init}) \in Q_k \ \ \forall k \in \mathbb{N}$, and $\sup(V^{k+1}_{(\bar{i}, \bar{\lambda}_{init})}) \leq \sup(V^k_{(\bar{i}, \bar{\lambda}_{init})}) \ \ \forall k \in \mathbb{N}$, then $\exists N \in \mathbb{Z}$ and $\varepsilon > 0$ such that $d((i_n, \lambda_n), (\bar{i}, \bar{\lambda}_{init})) < \varepsilon \ \ \forall n \geq N$. Therefore, $\{(i_k, \lambda_k)\}$ converges towards $(\bar{i}, \bar{\lambda}_{init})$. $\square$

Given the result of Lemma 1 and the need to bound the computational effort for Algorithm 1, the iterative evaluation and subdivision within the initialization procedure is subject to two termination criteria for initialization: (1) at least one design point in any of the design regions within an iteration corresponds to an objective function value greater than a specified initialization threshold, or (2) the number of initialization iterations exceeds a user defined number. In the former case, all temporary design (sub)regions containing at least one design point corresponding to an objective function value greater than the specified initialization threshold become the initial design region(s) used to explore the design space.

Design and Conduct an Experiment (Lines 7 & 8, Algorithm 1)

Analyzing each design region separately obtains new design regions for sequential iterations. The following steps obtain the data necessary to analyze each region. First, nearly-orthogonal Latin hypercube designs sufficient for fitting second-order response surface models sample design points from each design region. Deterministic

simulations that model the orbit of a satellite throughout the period of its repeating ground track evaluate the sampled design points according to an objective function of coverage provided by a satellite to a region of interest.

Fit and Analyze Regression Models (Line 9, Algorithm 1)

Next, linear regression generates a response surface on response data transformed using a Box-Cox [172] transformation. A Box-Cox transformation addresses violations to the assumption of normality in the response variable required for linear regression. Analysis yields two regression models: a main effects model and a second order response surface model. The main effects model captures information about the general improving direction of the design region. A second order response surface model captures important information about the improving directions of design regions within the eigenvalues and eigenvectors associated with the fitted surface. Equation (2) shows a representation of the second order response surface model [168]. The variables $\hat{y}$, x, b_0, and b represent the predicted response, the vector of factors, the intercept, and the regression coefficients of the model, respectively. Equation (3) defines B [168].

$$\hat{y} = b_0 + x'b + x'Bx \tag{2}$$

$$B = \begin{bmatrix} b_{11} & b_{12}/2 & \dots & b_{1N}/2 \\ b_{12}/2 & b_{22} & \dots & b_{2N}/2 \\ \vdots & & \ddots & \vdots \\ sym. & & & b_{NN} \end{bmatrix} \tag{3}$$

The stationary point, eigenvectors, and eigenvalues of the fitted second order response surface determine the approach used to select new design regions for subsequent iterations. Equation (4) calculates the stationary point, x_s, and solving Equation (5) finds the normalized eigenvectors, V, and the corresponding eigenvalues, Λ, of the fitted second order response surface model [168].

$$x_s = -\frac{1}{2}B^{-1}b \tag{4}$$

$$V'BV = \Lambda \tag{5}$$

The eigenvectors (i.e., the columns of V) identify the characteristic directions of the response surface, and the eigenvalues (i.e., the diagonal entries of Λ) identify the increasing or decreasing behavior along their corresponding eigenvectors [168]. If all of the eigenvalues are positive, the stationary point is the minimum point of the fitted response surface. If all of the eigenvalues are negative, the stationary point is the maximum point of the fitted surface. Finally, if the eigenvalues are of mixed signs, the stationary point is a saddle point [168]. The following sections address the applications of these cases to creating new design regions.

Identify Design Regions for Subsequent Iterations (Line 10, Algorithm 1)

Anytime the incumbent solution updates (i.e., a new best solution is found), a new design region explores in the surrounding subregion of this new incumbent solution in the subsequent iteration. Regardless of the updates to the incumbent solution, response surface analysis conducted on each design region informs the creation of new design regions for subsequent iterations.

Figure 12 shows a flowchart of creating new design regions for subsequent iterations using the fitted response surface information of a current design region $\mathscr{D}_{current}$. The specific method that creates new design regions depends on the location of the stationary point, x_s, the respective positive and negative signs of the diagonal elements of the eigenvalue matrix, Λ, and the moveability of the current design region. Let a design region be termed *moveable* if all of the boundary lengths of the current design region are smaller than a proportion, $r_{max} \in [0, 1]$, of their respective overall design space boundary lengths and *unmoveable* if any of the boundary lengths of the current design region are greater than a proportion, r_{max}, of its respective overall

design space boundary length. For example, suppose that a design region has two boundary lengths a and b. Let A and B be the boundary lengths of the design space being explored that correspond to the factors associated with a and b, respectively. Then if either $a > Ar_{max}$ or $b > Br_{max}$, then at least one of the boundary lengths of the design region is greater than a proportion, r_{max}, of their respective design space boundary length. The following paragraphs elaborate on the several methods used to create new design regions for subsequent iterations.

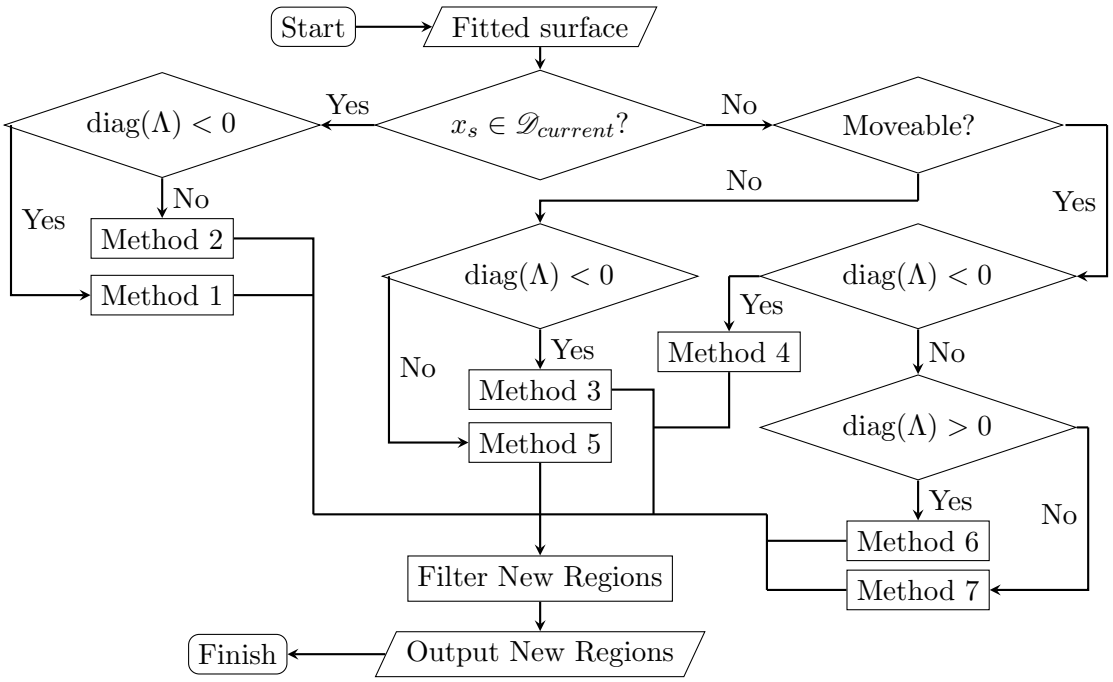

Figure 12: Flowchart of Identify Design Regions for Subsequent Iterations (Line 10, Algorithm 1)

Method 1: When the stationary point indicates a local maximum within the current design region, a new region explores near the predicted maximum by creating a scaled version of the current design region centered about the stationary point. A shrink proportion parameter, $\gamma_{scale} \in (0, 1)$, scales each edge of the design region to obtain the edge lengths of the new design region. Note that the new region can include areas outside of the current analyzed design region.

Method 2: The current design region divides into new design regions when the stationary point is either a saddle point or a local minimum within the design region. New design regions are selected by partitioning the current design region into potentially new design subregions and then selecting the potentially new design subregions corresponding to improving directions of the fitted response surface. The stationary point determines where the design region will be divided; the stationary point becomes a corner of each potentially new design region. A tunable parameter, θ_{max}, determines which of the potentially new design regions become new design regions for the following iteration. Let $u_{region} \in \{-1, 1\}^N$ represent a vector identifying each potentially new design region. These vectors correspond to the direction from the stationary point into the respective potentially new design region such that the minimum angle between any of the closest boundaries is maximized. Let $v_{pos} \in V_{pos}$ represent an eigenvector of the fitted surface corresponding to a positive eigenvalue and u_{region} represents the vector corresponding to a potentially new design region. The next iteration of design regions include any of the potentially new design regions that satisfy either of the following conditions for any of the eigenvectors associated with positive eigenvalues.

$$\cos^{-1}\left(\frac{u_{region} \cdot v_{pos}}{||u_{region}||||v_{pos}||}\right) \leq \theta_{max} \quad \text{or} \quad \cos^{-1}\left(\frac{u_{region} \cdot -v_{pos}}{||u_{region}|||| - v_{pos}||}\right) \leq \theta_{max}$$

Multiple methods use a single direction vector, g, to produce a new design region when the stationary point of the fitted second order response surface model lies outside of the design region. The specific approach and direction vector used depends on the characteristics of the fitted second order surface as well as the size of the current design region. However, all of the approaches using a single direction vector to create a new design region rely on two actions termed *directional compression* and *directional shifting*.

Directional compression shrinks a current design region into a new smaller design region along a single direction vector, g. Directional compression occurs in the following steps. First, the procedure determines the center point of the new design region. Equation (6) defines the range of potential values for the i^{th} factor of the new center point. C_i represents the value of the i^{th} factor of the center point of the current design region. R_i represents the center point values of factor i in the new region and g_i represents the direction vector value corresponding to factor i. H_i represents the half-length of the boundary corresponding to the i^{th} factor in the current design region. The scaling parameter, $\gamma_{scale} \in (0, 1)$, shrinks the size of the design region.

$$C_i - (1 - \gamma_{scale})\frac{g_i}{||g||}H_i \leq R_i \leq C_i + (1 - \gamma_{scale})\frac{g_i}{||g||}H_i \tag{6}$$

The center point of the new design region becomes the intersection of the artificial boundary formed by the union of all the factor ranges defined by Equation (6) and the direction vector, g, anchored at the center of the current design region. The new design region becomes the largest design region that remains both a subset of the current design region and is symmetric about the newly identified center point. Figure 13 show an example of producing a new design region from a current design region using directional compression.

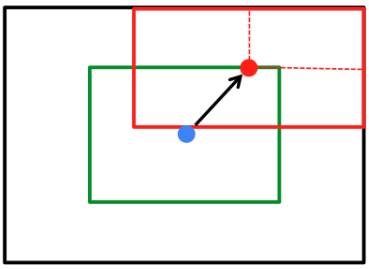

Figure 13: Compression of a Design Region

The outer black box represents the current design region. The center blue dot represents the center of the current design region. The inner-center green box repre-

sents the set of possible locations at which the center of the new design region can exist. The black arrow represents the direction vector. The upper red dot represents the center of the new design region. The red dashed lines represent the half-widths used to define the size of the new design region, and the upper red box represents the new design region.

Directional shifting creates a new design region from a current design region by simply shifting the current design region into a new position in the design space along a direction vector, g. The size of the new design region matches the current design region. Equation (7) determines the new position of the center point of the new design region.

$$C_{new} = C_{current} + d_{border} v + \alpha_{step} \frac{H_f}{v_f} v \tag{7}$$

The parameter f represents the factor corresponding to the border of the current design region that the direction vector stemming from the center of the current design region would first intersect. C_{new} represents the center of the new design region. $C_{current}$ represents the center of the current design region. H_f represents the half-width of the design region corresponding to factor f. The vector v is the unit vector along the direction vector and v_f is the element of v corresponding to factor f. The parameter d_{border} represents the distance of the center point of the current design region along the direction vector to the border of the design region. The step size parameter, $\alpha_{step} \in (-1, 1]$, determines the distance that the region shifts.

Method 3: If the stationary point of the fitted second order response surface indicates a local maximum exists outside of an unmoveable design region, then direction compression creates the new design region using a direction vector defined by Equation (8). $C_{current}$ represents the center point of the current design region.

$$g = x_s - C_{current} \tag{8}$$

Method 4: If the stationary point indicates a local maximum existing outside of a moveable design region, then directional shifting creates the new design region also using a direction vector defined by Equation (8).

Method 5: If the stationary point indicates either a local minimum or a saddle point existing outside of an unmoveable design region, then directional compression creates the new design region using a direction vector defined by the gradient of a fitted main effects model.

Method 6: If the stationary point indicates a local minimum exists outside of a moveable design region, then directional shifting creates the new design region using a direction vector defined by the gradient of a fitted main effects model.

Method 7: If the stationary point indicates that a saddle point exists outside of a moveable design region, then the following steps obtain the new design region. First, the procedure identifies the eigenvector, v_{mp}, corresponding to the most positive eigenvalue. Then, Equation (9) identifies the point, x_{temp}, along the direction of this eigenvector anchored about the stationary point that is a minimum distance from the current design region's center point, x_c.

$$x_{temp} = x_s + \frac{v'_{mp}x_c - v'_{mp}x_s}{v'_{mp}v_{mp}}v_{mp} \tag{9}$$

If x_{temp} lies outside of the design region, directional shifting uses the gradient of the main effects model to shift the design region. However, if x_{temp} lies within the current design region, then the current design region compresses along the direction $x_{temp} - x_c$ and re-centers around x_{temp}. Direction shifting then shifts this compressed region along the direction vector defined by Equation (10).

$$g = \frac{\frac{v'_{mp}x_c - v'_{mp}x_s}{v'_{mp}v_{mp}}v_{mp}}{||\frac{v'_{mp}x_c - v'_{mp}x_s}{v'_{mp}v_{mp}}v_{mp}||} \tag{10}$$

Finally, the edge lengths of the design region expand to match the original edge lengths of the design region. This process allows the design region to shift about the increasing direction of a ridge that passes through the current design region.

Filter New Regions: Design regions may terminate prior to beginning the next iteration. Termination of design regions can occur under several scenarios. A design region terminates when it appears to be converging to a local maximum, when the movement of the design region and size of the design regions are below specified thresholds. Termination of a design region also occurs when the best objective function value associated with its sampled design points is less than a proportion of the lowest objective function values associated with the design points of any other design region in the current iteration. A design region also terminates if the largest objective function value associated with its sampled design points is less than a proportion of the best objective function value found from a sample design point found in any iteration of the search method. A design region also terminates if it samples the same location of the design space as a smaller design region being considered in the same iteration.

3.3 Computational Results

The following example uses Algorithm 1, a genetic algorithm, a simulated annealing approach, and a particle swarm algorithm approach to find circular repeating ground track orbits for a single satellite to provide coverage to a region of interest. This example randomly selects a discretized representation of New Zealand as the region of interest. The goal is to find an orbit that maximizes the average proportion of coverage provided by a single satellite to the region of interest over the repeat period of the ground track. Simulations use Equation (11) to determine the average proportion of coverage provided to the region of interest, where C_{Avg}, P, $t_p^{covered}$, and

t_{period} is the average proportion of coverage, the number of discretized points representing the region of interest, the total duration of coverage provided to point p of the discretized region of interest, and the period length of the repeating ground track, respectively.

$$C_{Avg} = \frac{\sum_{p=1}^{P} t_p^{covered}}{t_{period} P} \tag{11}$$

A satellite covers a point of interest when the satellite is above a specified elevation angle above the horizon tangent to the point of interest on a spherical Earth. The elevation angle is set to 35^o. The set of considered $L : M$ resonance pairs restricts repeating ground tracks to a maximum repetition period of $M = 5$ sidereal days and orbits to semi-major axis values between 6,500 km - 7,500 km to investigate low Earth orbit. The inclination ranges from $i \in (0^o, 180^o)$ and the longitude of the initial ascension across the equatorial plane ranges from $\lambda_{init} \in [0^o, 360^o/L)$ for each considered $L : M$ resonance pair.

A nearly-orthogonal Latin hypercube design [171] used 17-design points and 33-design points to sample the design regions of Algorithm 1. Algorithm 1 uses random combinations of search parameters within the ranges identified in Table 8. Section 3.2 discusses each of the search parameters. With regard to initialization of design regions in Line 4 of Algorithm 1, the maximum number of initialization iterations is 3; however, Algorithm 1 managed to initialize design regions for each design space explored prior to reaching this iteration limit.

Table 8: Ranges of Search Method Parameters Explored - Implemenation 1 and 2

Parameter	**Symbol**	**Range**
Shrink Proportion	γ_{scale}	[0.5, 0.975]
Step Size	α_{step}	[-0.75, 1]
Step Size Criterion	r_{max}	[0.1, 0.5]
Minimum Size	d_{min}	[0.07, 0.25]
Convergence Threshold	ε	[0, 0.01]
Convergence Criterion Size	r_{conv}	[0, 0.25]
Maximum Angle	θ_{max}	[45^o, 90^o]
Dominated Region Buffer	ψ_d	[0, 0.5]
Dominated Region Size Criterion	s_ψ	[0, 0.65]
Top Buffer	ψ_{top}	[0, 0.5]
Top Size Criterion	s_{top}	[0, 0.65]
Redundancy Proportion	s_{red}	[0, 1]

This example compares the computational performance of the Iterative $L : M$ Pair method (RSM) in searching the design space for a single-satellite circular repeating ground track against a genetic algorithm (GA) approach, a simulated annealing (SA) approach, and a particle swarm (PSO) algorithm approach. MATLAB [173] provided the genetic algorithm, simulated annealing, and particle swarm algorithms. The metaheuristics used the parameter settings recommended in the MATLAB documentation (see [173]), except for reducing the maximum number of iterations without improvement prior to termination to 10 iterations for both the genetic algorithm and particle swarm, and limiting the maximum number of samples to 5000 for the simulated annealing algorithm for each design space explored. These user-defined metaheuristic parameters were tuned to reduce the computational costs associated with each metaheuristic, while maintaining their ability to find good solutions.

Table 9 summarizes the performance results of each of the explored metaheuristics, focusing on the objective function values of the identified solutions, and the computational time required by each search method. Each metaheuristic is implemented 10 times to obtain a distribution of results; a sample size of 10 for each search method ensured the experiment completed in one week using a computer with an AMD Ryzen 9 9500X processor with 32 GB of RAM. Table 9 reports statistics of each sample, specifically the maximum values in the first row, the averages in the second row, the minimum values in the third row, and the standard deviations in the last row.

Table 9: Summary of Results, Semi-Major Axis Range = [6500 km, 7500 km], Elevation Angle = 35 deg.

	Avg. Proportion of Coverage					**Computation Time (min)**				
Method	**RSM (17 design points per region)**	**RSM (33 design points per region)**	**GA**	**SA**	**PSO**	**RSM (17 design points per region)**	**RSM (33 design points per region)**	**GA**	**SA**	**PSO**
max.	0.0180709	0.0180714	0.0180760	0.0180737	0.0180764	112.4	78.8	99.2	161.6	53.1
avg.	0.0180378	0.0180662	0.0180710	0.0180661	0.0180644	49.7	46.7	86.3	151.4	49.2
min.	0.0179397	0.0180604	0.0180545	0.0180545	0.0180242	24.1	25.1	78.9	135.6	43.0
std. dev.	0.0000366	0.0000043	0.0000085	0.0000071	0.0000196	29.7	16.1	6.8	9.1	3.0

The maximum objective function values obtained by the genetic algorithm, simulated annealing, and particle swarm algorithm of approximately 0.0180760, 0.0180737, and 0.0180764, respectively, were greater than the maximum objective function values obtained by Algorithm 1 using 17 design points and by Algorithm 1 using 33 design points of approximately 0.0180709 and 0.0180714, respectively. The genetic algorithm has the largest average objective function value of approximately 0.0180710, followed by Algorithm 1 using 33 design points, the simulated annealing algorithm, the particle swarm algorithm, and Algorithm 1 using 17 design points with average objective function values of approximately 0.0180662, 0.0180661, 0.0180644, and 0.0180378, respectively. Algorithm 1 using 17 design points also found the worst solution with an objective function value of approximately 0.0179397, followed by the particle swarm algorithm with an objective function value of approximately 0.0180242. However,

it is noteworthy to mention that this worst objective function value found of approximately 0.0179397 is within 0.76% of the best objective function value found by the particle swarm algorithm of approximately 0.0180764, suggesting only a modest practical difference between the average objective function value performance of Algorithm 1 using 17 design points and the other metaheuristics. The range of the objective function values obtained were largest in Algorithm 1 using 17 design points followed by the particle swarm algorithm, and smallest in Algorithm 1 using 33 design points.

The computation time required by Algorithm 1 using 17 design points has the largest range from approximately 24.1 minutes to approximately 112.4 minutes. Algorithm 1 using 33 design points has the second largest computational time range from approximately 25.1 minutes to approximately 78.8 minutes. Next is the simulated annealing algorithm with a computation time range of approximately 135.6 minutes to 161.6 minutes, and the genetic algorithm with a computation time range of approximately 78.9 minutes to approximately 99.2 minutes. The particle swarm algorithm has the smallest computational time range of approximately 43.0 minutes to approximately 53.1 minutes. Particle swarm optimization has the smallest standard deviation in computation time of approximately 3.0 minutes and Algorithm 1 using 17 design points has the largest standard deviation in computation time of approximately 29.7 minutes. Therefore, the particle swarm approach has more predictable computational costs than Algorithm 1. Algorithm 1 using 33 design points has the smallest average computation time of approximately 46.7 minutes, closely followed by the particle swarm algorithm and Algorithm 1 using 17 design points with averages of approximately 49.2 minutes and 49.7 minutes, respectively. The genetic algorithm and simulated annealing algorithms appear to have larger average computation times of approximately 86.3 minutes and 151.4 minutes, respectively.

Conclusions regarding the average differences between the performance of the metaheuristics require appropriate testing for significance. Tables 10 and 11 report both the test statistics and the statistical significance of the pair-wise comparisons of the average objective function values and average computation times used by each metaheuristic, respectively, using an $\alpha = 0.05$. The pair-wise comparison of the average performance of the metaheuristics are evaluated using the Tukey method [174]. This analysis uses the Tukey method since all sample sizes are equal and it controls the overall error rate [175].

Table 10: Average Proportion of Coverage - Absolute Difference in Method Averages - Tukey Multiple Comparison Test for Significance

T_{Test}	**RSM (33 design points per region)**	**GA**	**SA**	**PSO**
RSM (17 design points per region)	$0.0000283^{*}_{<}$	$0.0000331^{*}_{<}$	$0.0000282^{*}_{<}$	$0.0000266^{*}_{<}$
RSM (33 design points per region)	-	0.0000048	0.0000001	0.0000017
GA	-	-	0.0000049	0.0000065
SA	-	-	-	0.0000016

$\alpha = 0.05$.
Critical Value: $T_{crit} = 0.0000246$.
*Significance ($T_{test} > T_{crit}$)
<: Row average is less than column average
>: Row average is greater than column average

Table 11: Computation Time (min) - Absolute Difference in Method Averages, Tukey Multiple Comparison Test for Significance

T_{Test}	**RSM (33 design points per region)**	**GA**	**SA**	**PSO**
RSM (17 design points per region)	2.95	$36.65^{*}_{<}$	$101.78^{*}_{<}$	0.50
RSM (33 design points per region)	-	$39.60^{*}_{<}$	$104.73^{*}_{<}$	2.44
GA	-	-	$65.13^{*}_{<}$	$37.16^{*}_{>}$
SA	-	-	-	$102.28^{*}_{>}$

$\alpha = 0.05$.
Critical Value: $T_{crit} = 20.33$
*Significance ($T_{test} > T_{crit}$)
<: Row average is less than column average
>: Row average is greater than column average

No significant difference exists between the average objective function values obtained by Algorithm 1 using 33 design points, the genetic algorithm, the simulated annealing algorithm, and the particle swarm algorithm. The average objective function values of Algorithm 1 using 17 design points is significantly less than the averages of all of the other metaheuristics. The significant difference in the average objective function values obtained by Algorithm 1 using 17 and 33 design points demonstrates the benefit of increased sampling density when using designed experiments. Overall, Algorithm 1 using 33 design points, the genetic algorithm, the simulated annealing algorithm, and the particle swarm algorithm all performed similarly in terms of solution quality.

The differences in the average computation time between each pair of Algorithm 1 using 17 design points, Algorithm 1 using 33 design points, and particle swarm algorithm are insignificant. The average computation time associated with the genetic algorithm is significantly greater than the average computation time of the Algorithm 1 using both 17 and 33 design points, as well as the particle swarm algorithm. The average computation time associated with the simulated annealing algorithm is significantly greater than all of the other metaheuristics. Although the simulated annealing algorithm has significantly greater computation time than the other metaheuristics, its maximum computatation time of approximately 161.6 minutes is acceptable for single satellite orbit selection. Therefore, although there are significant differences in computation time between the metaheuristics, all have acceptable computation times.

Visualizing the relative performance of each metaheuristic benefits observations beyond statistical testing. Figure 14 depicts the computation time required by each metaheuristic against the corresponding objective function value associated with the solution found. The shape and color of each data point identifies the respective

metaheuristic. The dashed red line represents the best objective function value found by any of the metaheuristics.

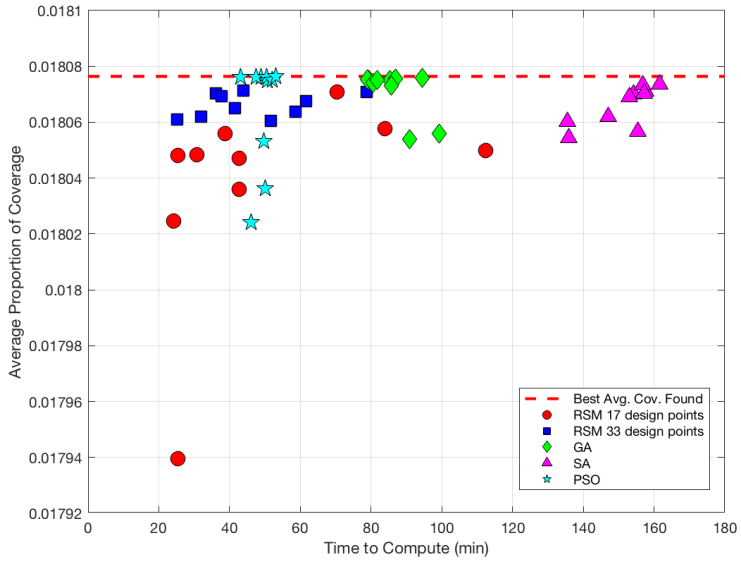

Figure 14: Average Proportion of Coverage vs Computation Time, Semi-Major Axis = [6500 km, 7500 km], Elevation Angle = 35 deg.

Despite statistical insignificance, it visually appears in Figure 14 that the Algorithm 1 implementations struggle to achieve the same solution density in the proximity of the best objective function value found as the particle swarm and genetic algorithms. This result may suggest that Algorithm 1 serves a better purpose of quickly reaching a region near a local optimal solution prior to the implementation of a second algorithm more suited for solution refinement.

Overall, both Algorithm 1 implementations have better computational efficiency than both the genetic algorithm and simulated annealing approaches and similar computational efficiency as the particle swarm approach. Similarly, Algorithm 1 using an adequate sampling density achieves comparable objective function values to the genetic algorithm, simulated annealing algorithm, and the particle swarm algorithm. Therefore, satellite constellation design methods may benefit from a response surface

methodology approach to guide the initial search through the design space prior to using other search methods.

3.4 Conclusions and Recommendations

This chapter presents a customized metaheuristic that applies designed experiments and response surface methods to design circular repeating ground track orbits for regional coverage, and compares this solution technique to a genetic algorithm, a simulated annealing algorithm, and a particle swarm algorithm, commonly used metaheuristic approaches in the literature. The objective functions associated with the performance of satellite orbits tend to be non-convex, warranting the need to develop reliable search methods. Combining information from multiple local response surface approximations of a non-convex objective function could provide promising predictions about the potential location(s) of global optimal solutions. The customized metaheuristic's use of predicted response information provides insights into the benefit of response surface methodology in the design of satellite orbits with non-convex objective functions. The customized metaheuristic is significantly more computationally efficient than the genetic algorithm and simulated annealing approaches, and achieves comparable quality solutions as each of the baseline metaheuristics on the instances examined. As a result, response surface analysis techniques can play an important role in satellite orbit design methodologies that must explore non-convex objective functions.

Future research will adjust the customized metaheuristc to expand its capability to explore both circular and elliptical orbits. Additionally, future research should examine the application of response surface analysis to satellite constellation design.

IV. Optimal Repeat Parameter Selection for Modifying Orbits from Non-Repeating into Repeating Ground Track Orbits

Abstract

Satellites following orbits with repeating ground tracks periodically have coverage that visits the same regions of the Earth's surface, a beneficial trait. The satellite constellation design literature presents many design approaches to identify suitable orbital parameters to achieve these repeating ground tracks; however, some methods search the broader, continuous parameter space yielding parameter estimates that do not yield the desired repeating ground tracks. Additionally, existing repeating ground track satellite orbits may become perturbed also yielding non-repeating ground tracks. From the perspective of observing regions of persistent and enduring interest, it is both relevant and important to identify the best repeating ground track orbit as a reference to modify an existing non-repeating ground track orbit, a problem thus far receiving scant attention within the published literature. This chapter proposes and demonstrates a simple yet elegant procedure to transform non-repeating ground tracks into repeating ground tracks via geometric adjustment minimization. The procedure is both computationally efficient and avoids the need for simulations.

4.1 Introduction

Repeating ground track orbits benefit missions requiring repetitive and consistent satellite passages over a region of interest. Choo *et al.* [160] present a thorough survey of satellite constellation design approaches, many of which consider repeating ground tracks. Such approaches frequently focus on the conditions [142, 148], the design [134, 18, 56, 48, 145], and the maintenance [146] of repeating ground track orbits.

Repeating ground track orbit design and maintenance methods focus on varying levels of perturbations caused by environmental factors. Vtipil and Newman [55] present an efficient method for determining the semi-major axis for both circular and elliptical orbits to meet repeating ground track conditions, considering perturbations due to the non-spherical shape of the Earth. Aorpimai and Palmer [176] derive an analytical solution for the conditions required to achieve a repeating ground track orbit, given higher order geopotential harmonics. Fu *et al.* [177] present design and orbital maintenance methods for repeating ground track orbits in low Earth orbit, considering perturbation forces both due to the non-spherical shape of the Earth and atmospheric drag. Low *et al.* [178] present an efficient numerical method for designing a reference trajectory for the maintenance of repeating ground track orbits with low inclinations at low Earth orbit.

It may be necessary to adjust the parameters of an orbit once its ground track no longer possess the desired repeating behavior. The literature presents such orbital adjustment methods to modify an orbit not currently meeting repeat requirements into the desired repeating ground track orbit. Pu *et al.* [179] use a genetic algorithm to minimize the fuel consumption required to adjust the trajectory of a satellite to redesign its orbit into a desired repeating ground track orbit. Ju *et al.* [180] present a method to quickly redesign an orbit into a desired repeating ground track orbit in low Earth orbit using dimensionality reduction and decoupling optimization.

Although these orbital design methods are capable of identifying the appropriate orbital parameters for repeating ground tracks, and these orbital adjustment methods are capable of correcting non-repeating ground track orbits into repeating ground track orbits, these methods require *a priori* selection of the repeat parameters of the desired repeating ground track. A method capable of identifying the best repeat parameters to modify a non-repeating ground track orbit into a repeating ground track

orbit would benefit orbital correction methods as well as orbit design methods. This chapter proposes an approach to transform non-repeating ground tracks into repeating ground tracks for design methods when the parameters of the desired repeating ground track are not selected *a priori*.

This research makes two contributions to the satellite orbit design literature. First, it presents an elegant method to identify the best parameters for modifying a non-repeating ground track into a repeating ground track. Second, it proposes a metric to compare the similarities between two ground tracks. As supporting evidence of these contributions, this work illustrates the first contribution via several example orbital transformations, and it examines the outcomes within the context of the second contribution.

The remainder of the chapter is organized as follows. Section 4.2 presents the method for determining appropriate repeat parameters for modifying an orbit and the metric for comparing two ground tracks. Section 4.3 demonstrates the utility of the methods using several examples, and Section 4.4 provides concluding remarks.

4.2 Methodology

It may be necessary to modify an existing non-repeating ground track orbit into a repeating ground track orbit. Modifying the current orbit to have an arbitrarily selected repeating ground track may be sub-optimal as its new ground track may not closely resemble its original ground track. This section presents a method to identify the repeating ground track that most resembles the ground track of the current non-repeating ground track orbit.

Comparing Ground Track Similarity

The *average angular separation* quantifies the similarity between two ground tracks. Evaluating Equation (12) finds the average angular separation, θ_{avg}, between

two ground tracks over a specified period, T. The symbols $\boldsymbol{s}_1(t)$ and $\boldsymbol{s}_2(t)$ represent the subsatellite positions in Euclidean coordinates of satellites following the two orbits being compared at time t. Note that the initial positions of the satellites should be the same to properly compare two ground tracks, (i.e., $\boldsymbol{s}_1(0) = \boldsymbol{s}_2(0)$).

$$\theta_{avg} = \frac{1}{T}\int_{t=0}^{T} \cos^{-1}\left(\frac{\boldsymbol{s}_1(t)\cdot\boldsymbol{s}_2(t)}{||\boldsymbol{s}_1(t)||||\boldsymbol{s}_2(t)||}\right) dt \tag{12}$$

Evaluating Equation (13) provides a useful approximation of the average angular separation between two ground tracks. The parameters D and t_d represent the number of discretized time points and the time associated with the d^{th} discretized time point, respectively.

$$\hat{\theta}_{avg} = \frac{1}{D}\sum_{d=1}^{D} \cos^{-1}\left(\frac{\boldsymbol{s}_1(t_d)\cdot\boldsymbol{s}_2(t_d)}{||\boldsymbol{s}_1(t_d)||||\boldsymbol{s}_2(t_d)||}\right) \tag{13}$$

The average angular separation remains in the range $[0, \pi]$. The two ground tracks being compared are identical when the average angular separation equals 0. The two ground tracks are opposite of one another (i.e., two satellites following the ground tracks would remain on opposite sides of the Earth) when the average angular separation equals π. Lastly, the two ground tracks are orthogonal on average when the average angular separation is $\pi/2$. Therefore, ground tracks with smaller average angular separation are more similar than ground tracks with larger average angular separation.

Ideally, directly minimizing Equation (12) would identify the repeating ground track most resembling the ground track of the current orbit. Unfortunately, a metaheuristic may be required to manage both the nonlinearity of Equation (12) and the requirement of a repeating ground track. Additionally, the iterative nature of the methods capable of identifying orbital parameters associated with repeating ground tracks [142, 140, 180, 39] makes direct use of Equation (12) even more challenging. Simulations can be utilized to approximate Equation (12) using Equation (13); how-

ever, such simulations may be too computationally expensive to evaluate each possible repeating ground track. An alternative metric capable of identifying the repeating ground track that most resembles the ground track of the current orbit with less computation expense than simulations would benefit the repeating ground track selection process.

Alternative Metric for the Repeating Ground Track Selection Process

The L:M resonance pair defines the repeat parameters of a repeating ground track. The L:M resonance pair identifies the number of orbits a satellite takes (L) as well as the number of sidereal days required to repeat a repeating ground track (M). A satellite following a repeating ground track having a particular L:M resonance pair will complete the track using L orbits in M sidereal days. L and M must be co-prime integers to yield a repeating ground track (i.e., the greatest common divisor of L and M is 1) [1].

Modifying an existing non-repeating ground track orbit into a repeating ground track orbit requires the selection of an L:M resonance pair. This section sets forth the process to identify such repeat parameters when the desired L:M resonance pair is unknown. The repeat parameters for a repeating ground track should yield an outcome that closely resembles the non-repeating ground track for which it substitutes. The process of identifying this optimal L:M resonance pair occurs via the following four steps. First, the process determines the draconitic period, T_d, the amount of time between two passages of the ascending node of an orbit [181]. Equations (14) to (17) identify the draconitic period for an orbit, considering perturbed motion due to a non-spherical Earth [181]. The parameters J_2, a, e, i, Ω, ω, μ, and R represent the zonal harmonic coefficient due to Earth's oblateness, the semi-major axis, the eccentricity, the inclination, the right ascension of the ascending node, argument of perigee, the gravitational constant of the Earth, and the radius of the Earth, respec-

tively. Additionally, n represents the mean motion of the orbit, Δn represents the variation in mean motion, T_o represents the orbital period in Keplarian motion, and $\dot{\omega}$ represents the apsidal precession rate.

$$T_d = \left(\frac{1 - \Delta n/n}{1 + \dot{\omega}/n}\right) T_o \tag{14}$$

$$T_o = 2\pi\sqrt{\frac{a}{\mu}} \tag{15}$$

$$\begin{aligned}\frac{\Delta n}{n} = J_2 \left(\frac{R}{a(1-e^2)}\right)^2 \sqrt{1-e^2}\frac{3}{4}(2 - 3\sin^2(i)) \left(1 + J_2 \left(\frac{R}{a(1-e^2)}\right)^2 \frac{1}{8}\right. \\ \left.\left[10 + 5e^2 + 8\sqrt{1-e^2} - \left(\frac{65}{6} - \frac{25}{12}e^2 + 12\sqrt{1-e^2}\right)\sin^2(i)\right]\right)\end{aligned} \tag{16}$$

$$\frac{\dot{\omega}}{n} = J_2 \left(\frac{R}{a(1-e^2)}\right)^2 \left(3 - \frac{15}{4}\sin^2(i)\right) \tag{17}$$

Second, the process finds the equatorial shift of the ascending node, $\Delta\lambda_E$, of the sub-satellite point after each orbit relative to the surface of the Earth. Solving Equations (18) and (19) finds the equatorial shift of the ascending node after a single orbit under J_2 perturbations [181]. The term $\dot{\Omega}_T$ represents angular rotation rate of the Earth about its poles and $\dot{\Omega}$ represents the nodal precession rate of the orbit.

$$\Delta\lambda_E = -\left(\dot{\Omega}_T - \dot{\Omega}\right) T_d \tag{18}$$

$$\dot{\Omega} = J_2 \left(\frac{R}{a(1-e^2)}\right)^2 \cos(i) \left(-\frac{3}{2}\right) \sqrt{\frac{\mu}{a^3}} \tag{19}$$

Third, Equation (20) identifies the ratio, ρ_{shift}, between the number of $\Delta\lambda_E$ and one complete rotation of 360^o. The ratio ρ_{shift} can be interpreted as the number of orbits required for the ascending node to complete one complete rotation about the equator relative to the surface of the Earth.

$$\rho_{shift} = \frac{360^o}{|\Delta\lambda_E|} \tag{20}$$

Finally, the process uses ρ_{shift} to identify an appropriate L:M resonance pair to modify the non-repeating ground track orbit into a repeating ground track orbit using the following two steps. First, the process defines the set of potential L:M resonance pairs that satisfy the following requirements: (1) the orbits associated with the L:M pairs have semi-major axis values within a specified range, $a_{range} \in [a_{min}, a_{max}]$; (2) the period remains within a desired limit, M_{max} sidereal days; and (3) L and M are co-prime integers. Let the function f(L,M) map an L:M pair to the semi-major axis value of its corresponding repeating ground track orbit, and the function $g(a, b)$ map two numbers, $a, b \in \mathbb{R}$, to their greatest common divisor. Second, the process solves the following mathematical program to identify an appropriate L:M resonance pair.

$$\begin{aligned}
\min \quad & |\mathrm{M}\rho_{shift} - \mathrm{L}| && (21)\\
\text{s.t.} \quad & \mathrm{M} \leq M_{max}, && (22)\\
& f(\mathrm{L},\mathrm{M}) \in a_{range}, && (23)\\
& g(\mathrm{L},\mathrm{M}) = 1, && (24)\\
& \mathrm{L},\mathrm{M} \in \mathbb{Z}_+ && (25)
\end{aligned}$$

In Equation (21), the mathematical program minimizes the absolute difference between the number of orbits to complete a repeating ground track and the number of orbits of the non-repeating ground track over the period of the repeating ground track. Constraint (22) ensures the selected period duration, M, satisfies the limit on the period duration. Constraint (23) requires the semi-major axis associated with the selected L:M pair remains within the specified semi-major axis range. Constraints (24) and (25) require that the selected L:M pair be co-prime positive integers. Enumeration

rapidly identifies the optimal L:M pair for the mathematical program.

Two *very* important caveats exist regarding the semi-major axis range of the repeating ground track orbits. First, the lower bound a_{min} on the semi-major axis of the selected repeating ground track orbit should be much smaller than the semi-major axis of the current orbit. Second, the upper bound of the semi-major axis should be much larger than the semi-major axis of the current non-repeating ground track orbit. The presented method may result in an erroneous solution if the semi-major axis range borders the semi-major axis of the current orbit. Such an erroneous solution may result if no repeating ground track within the specified semi-major axis range properly reflects the ground track of the original orbit. It is entirely appropriate, and perhaps best practice, to set the lower bound of the semi-major axis range to the radius of the Earth. Although setting the lower bound of the semi-major axis range may result in a repeating ground track orbit that is not physically realizable, any such solution suggests that there does not exist a repeating ground track orbit reflective of the current orbit, and it may be better to leave the non-repeating ground track orbit as a non-repeating ground track orbit as a result.

After selecting an L:M resonance pair, any repeating ground track development method can be used to adjust the orbital parameters of the original non-repeating ground track orbit into a repeating ground track orbit [55, 177, 179, 180, 39]. The work in this chapter adopts the iterative method presented by Vallado [39] for approximating the semi-major axis of a repeating ground track orbit, given a set of orbital parameters and desired L:M pair. Vallado's [39] iterative method for finding the orbital parameters of a repeating ground track orbit is capable of handling both circular and elliptical orbits considering perturbations due to Earth's oblateness.

4.3 Examples: Modifying Non-Repeating Ground Tracks into Repeating Ground Tracks

This section uses several examples to demonstrate the usefulness of the *orbit metric* defined by Equation (21) to identify the appropriate L:M resonance pair for modifying non-repeating ground track orbits into repeating ground track orbits when the desired parameters are unknown. Each example limits the maximum number of orbits per sidereal day to $L_{\text{max-per-M}} = 17$ orbits per sidereal day and the maximum period duration to $M_{max} = 10$ sidereal days. Additionally, the semi-major axis of the orbit associated with any considered repeating ground track must remain within $a_{range} = (6378, 100{,}000]$ km.

The eight examples shown in this section modify non-repeating ground track orbits at varying semi-major axes of $a_{original} \in \{6550, 8500, 11{,}500, 17{,}500, 20{,}000, 40{,}000, 50{,}000, 51{,}000\}$, respectively. These eight semi-major axis values are chosen to represent orbits from low Earth orbit through Supersynchronous Earth orbit, and to demonstrate the method's performance is independent of ground track shape. The Appendix provides a more comprehensive list of examples for non-repeating ground track orbits with semi-major axis values between 6550 km and 65,000 km sampled every 500 km after 7000 km. The Appendix only considers semi-major axis values above 6545 km since the world record for the lowest altitude for a successful satellite orbit is 167.4 km [182]. All examples use randomly selected inclinations between 0^o and 180^o (*excluding* 0^o and 180^o) to represent both prograde and retrograde orbits, while avoiding the special case of Equatorial orbits.

Table 12 identifies the inclination and semi-major axis of the original non-repeating ground track orbits, the inclination and semi-major axis of the modified now repeating ground track orbits, the selected L:M resonance pairs used to make the adjustments, as well as the computation times associated with identifying the optimal L:M reso-

nance pairs using the method described in Section 4.2. The terms i and a represent the orbital inclination and the semi-major axis, respectively. Figures 15-22 illustrate the ground tracks defined by the orbital parameters in Table 12. Figures 15-22 use a longitude and latitude of 0^o as the starting point for each ground track since the selected L:M pairs are independent of the starting coordinates of the ground tracks.

Table 12: Parameter Modification from Non-Repeating to Repeating Ground Tracks ($M_{max} = 10$ sidereal days)

Example	**Non-Repeating** (i, a)	**Repeating** (i, a)	**Selected L:M** L:M	**Comp. Time** minutes
1	$(37^o, 6550)$	$(37^o, 6564)$	16 : 1	0.001
2	$(50^o, 8500)$	$(50^o, 8491)$	11 : 1	0.006
3	$(130^o, 11{,}500)$	$(130^o, 11{,}542)$	7 : 1	0.005
4	$(130^o, 17{,}500)$	$(130^o, 17{,}476)$	15 : 4	0.007
5	$(155^o, 20{,}000)$	$(155^o, 20{,}281)$	3 : 1	0.006
6	$(55^o, 40{,}000)$	$(55^o, 42{,}164)$	1 : 1	0.006
7	$(65^o, 50{,}000)$	$(65^o, 49{,}854)$	7 : 9	0.007
8	$(65^o, 51{,}000)$	$(65^o, 51{,}078)$	3 : 4	0.007

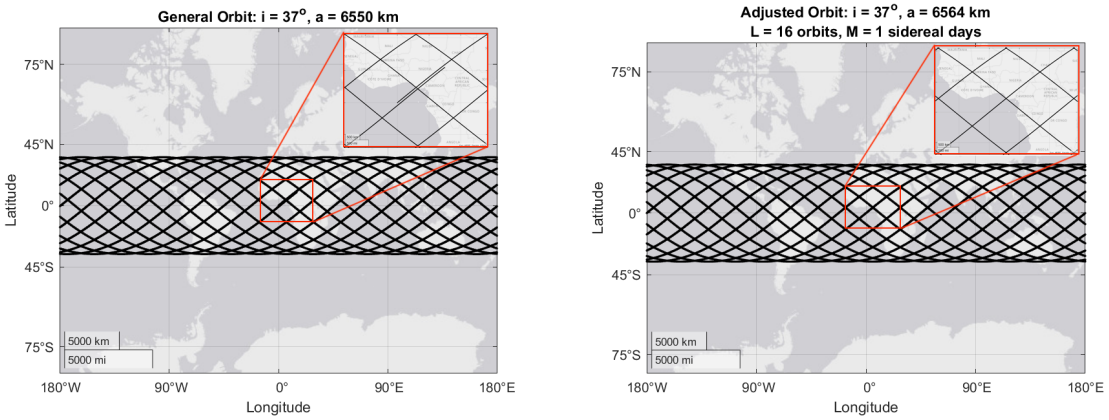

(a) Non-Repeating Ground Track

(b) Repeating Ground Track

Figure 15: Example 1 of Finding a Repeating Ground Track Orbit from a Non-Repeating Ground Track Orbit (Simulated Duration = 1 Sidereal Day)

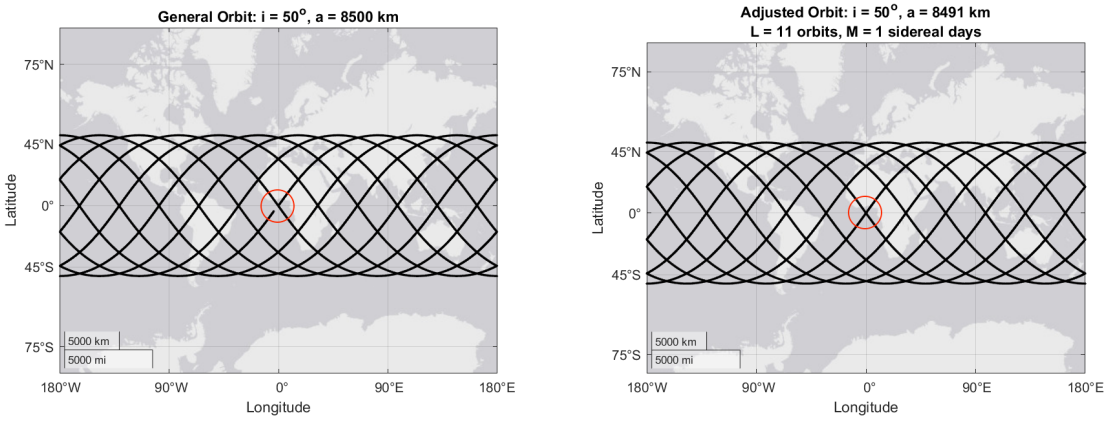

(a) Non-Repeating Ground Track (b) Repeating Ground Track

Figure 16: Example 2 of Finding a Repeating Ground Track Orbit from a Non-Repeating Ground Track Orbit (Simulated Duration = 1 Sidereal Day)

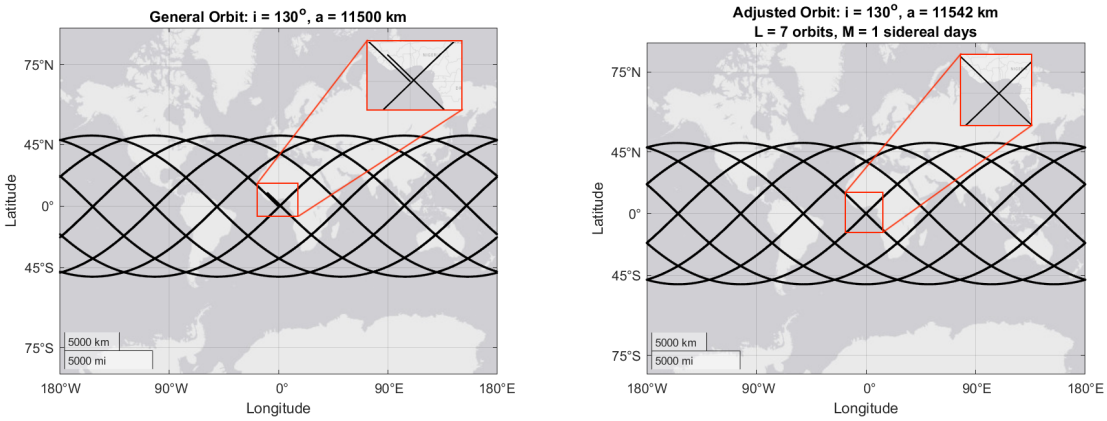

(a) Non-Repeating Ground Track (b) Repeating Ground Track

Figure 17: Example 3 of Finding a Repeating Ground Track Orbit from a Non-Repeating Ground Track Orbit (Simulated Duration = 1 Sidereal Day)

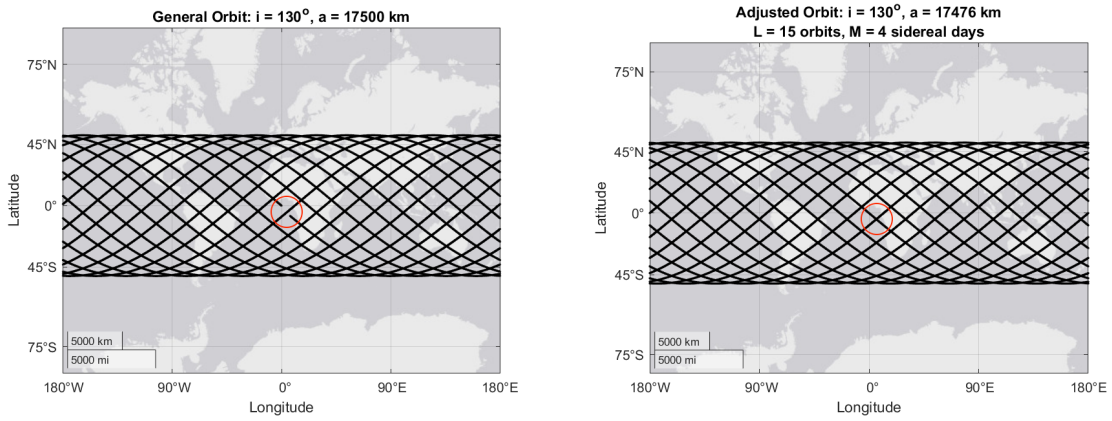

(a) Non-Repeating Ground Track (b) Repeating Ground Track

Figure 18: Example 4 of Finding a Repeating Ground Track Orbit from a Non-Repeating Ground Track Orbit (Simulated Duration = 4 Sidereal Days)

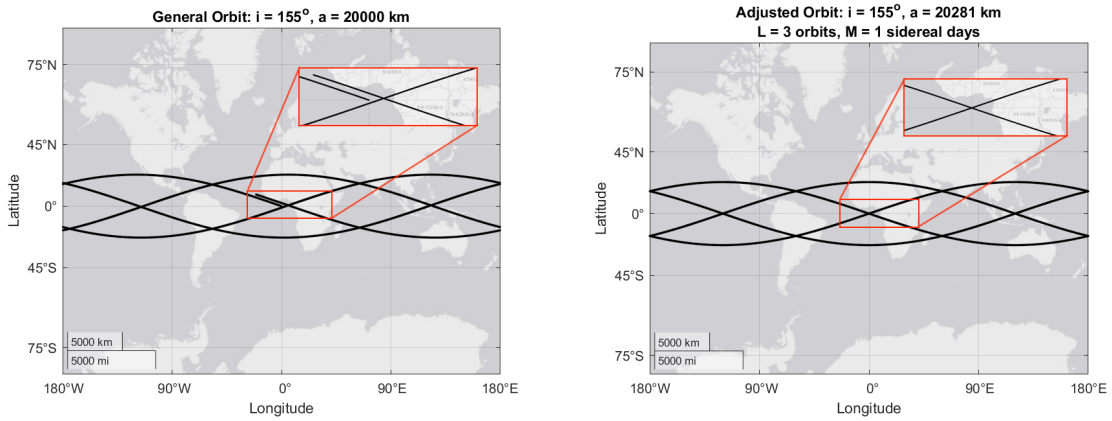

(a) Non-Repeating Ground Track (b) Repeating Ground Track

Figure 19: Example 5 of Finding a Repeating Ground Track Orbit from a Non-Repeating Ground Track Orbit (Simulation Duration = 1 Sidereal Day)

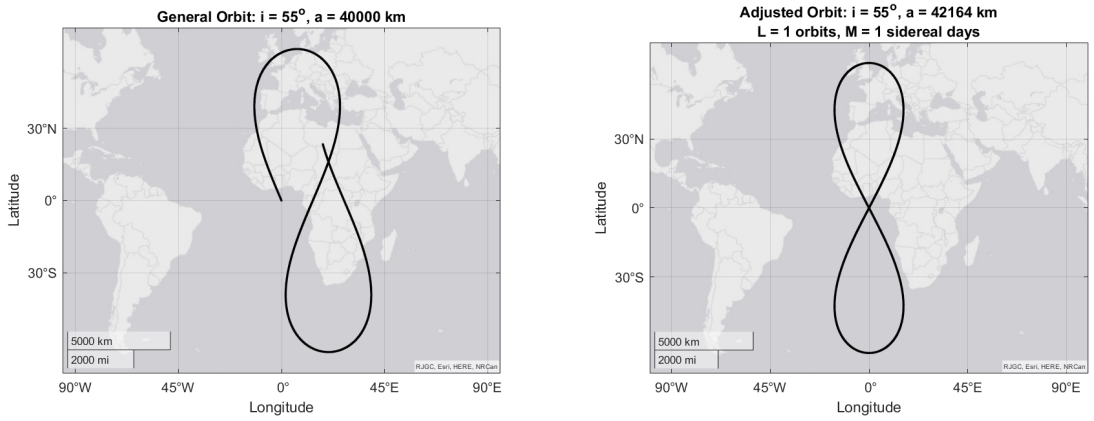

(a) Non-Repeating Ground Track (b) Repeating Ground Track

Figure 20: Example 6 of Finding a Repeating Ground Track Orbit from a Non-Repeating Ground Track Orbit (Simulation Duration = 1 Sidereal Days)

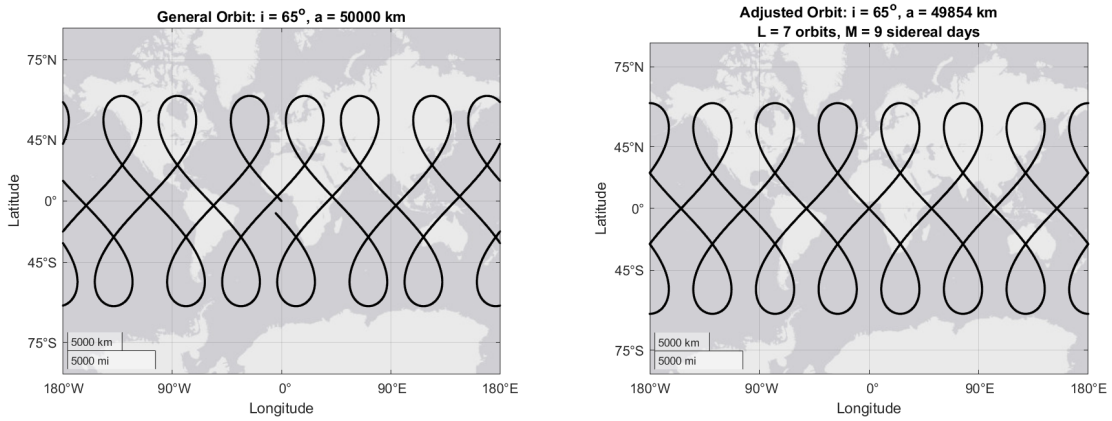

(a) Non-Repeating Ground Track (b) Repeating Ground Track

Figure 21: Example 7 of Finding a Repeating Ground Track Orbit from a Non-Repeating Ground Track Orbit (Simulated Duration = 9 Sidereal Days)

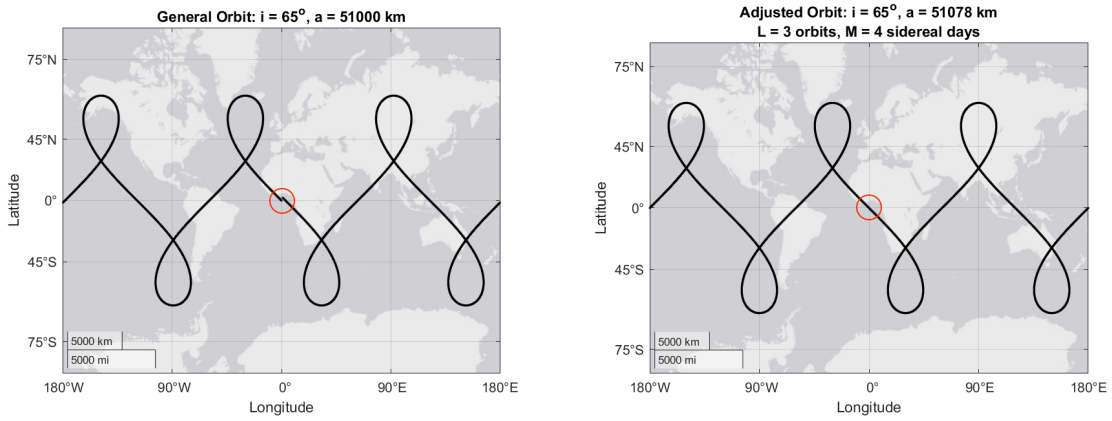

(a) Non-Repeating Ground Track (b) Repeating Ground Track

Figure 22: Example 8 of Finding a Repeating Ground Track Orbit from a Non-Repeating Ground Track Orbit (Simulated Duration = 4 Sidereal Days)

The methodology using the orbit metric identified an appropriate L:M resonance pair for each example consistently under half of a second. Visually, the repeating ground tracks closely resemble their original ground tracks in each example. Recall that the selected repeating ground tracks depend on the maximum period duration, M_{max}. Resolving Example 6 demonstrates that using a longer maximum period duration may result in a different repeating ground track. In Example 6, the selected L:M pair equals 1:1 when $M_{max} = 10$ sidereal days; however, the selected L:M pair equals 13:12 when $M_{max} = 20$ sidereal days. Figure 23 shows the selected repeating ground track when the maximum period duration is increased to $M_{max} = 20$ sidereal days. This result emphasizes the importance of appropriately selecting the maximum period duration when selecting repeating ground tracks.

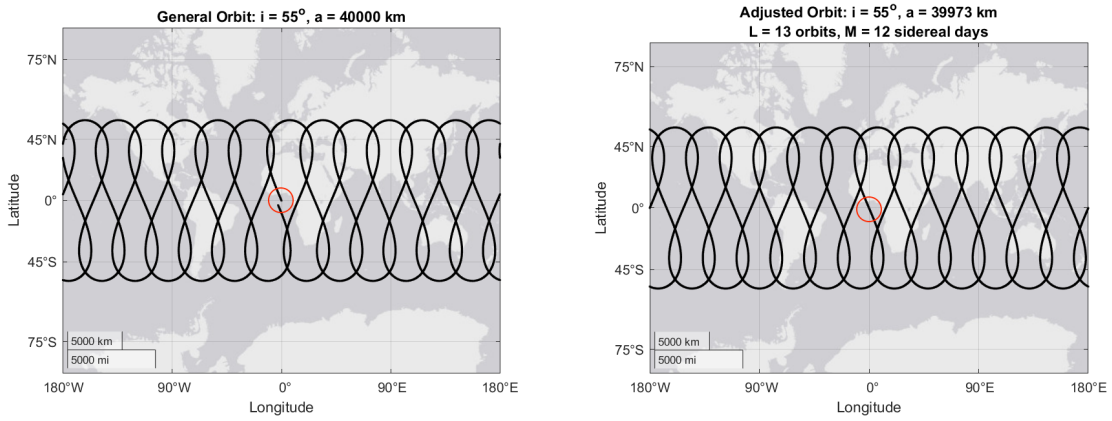

(a) Non-Repeating Ground Track (b) Repeating Ground Track

Figure 23: Revisiting Example 6 (M_{max} = 20 sidereal days) of Finding a Repeating Ground Track Orbit from a Non-Repeating Ground Track Orbit (Simulated Duration = 12 Sidereal Days)

The orbital parameters of the adjusted orbits remain relatively close to the orbital parameters of the original orbits for many of the examples. The difference in the semi-major axis values between the original and adjusted orbits for Examples 1, 2, 3, 4, and 8 were approximately 14.0 km, 8.7 km, 42.1 km, 23.8 km, and 77.8 km, respectively. The difference in the semi-major axis values is larger in Examples 5, 6, and 7 with differences of approximately 281.3 km, 2163.9 km, and 145.8 km, respectively. The larger adjustments observed at the higher semi-major axis values may be a result of fewer orbits with repeating ground tracks near those semi-major axis values with periods under the specified limit, M_{max}. Overall, the examples demonstrate that non-repeating ground track orbits can be modified into repeating ground track orbits when the parameters of the adjusted track are unknown prior to orbital adjustment attained by solving the mathematical program set forth in Equations (21)-(25).

Although the presented method identifies an appropriate L:M resonance pair for the non-repeating ground track orbits in the examples above, the question of whether or not the best L:M resonance pair was selected remains. Computing the average angular separation between the original tracks and each repeating ground track con-

sidered over the duration of the respective repeating ground track period demonstrates that the orbit metric appropriately identifies the best L:M resonance pair. Table 13 identifies the L:M pair associated with the smallest average angular separation between its respective repeating ground track and the original ground track for each L:M pair considered in each example (i.e., the repeating ground track that most reflects the ground track of the non-repeating ground track orbit).

Table 13: L:M Pair Associated with the Smallest Average Angular Separation Between its Respective Repeating Ground Track and the Original Ground Track ($M_{max} = 10$ sidereal days)

Example	**Best L:M Pair (L:M)**	**Computation Time** (min.)
1	16 : 1	38.3
2	11 : 1	34.4
3	7 : 1	39.7
4	15 : 4	35.6
5	3 : 1	36.0
6	1 : 1	35.1
7	7 : 9	35.3
8	3 : 4	35.3

The L:M pairs associated with the repeating ground tracks with the least average angular separation with the original ground tracks match the L:M pairs found by solving the mathematical program represented via Equations (21)-(25), identified in Table 13. These results indicate that solving the mathematical program does find the repeating ground track that most resembles the original ground non-repeating ground track when the design space is sufficiently large. Additionally, the L:M pairs identified by the two methods matched for each example explored in Table 14 of the Appendix. Therefore, the optimal solution to the mathematical program indeed finds the L:M resonance pair associated with the repeating ground track that most resembles the

original ground track with an appropriate design space.

The average computation time used by the deterministic simulations that approximated the average angular separation is approximately 36.1 minutes, which is much greater than the average computation time associated with the orbit metric of approximately 0.0057 minutes. Therefore, the orbit metric is much more computationally efficient than the average angular separation metric. The simulations used discretized time steps of one-second intervals to obtain good approximations of the average angular separation. The computer used for this experiment has an Intel Core i5 processor with 16 GB of RAM.

Figures 24-32 illustrate the average angular separation between each considered repeating ground track and the original ground track for each example to demonstrate the importance of selecting the optimal L:M pair as well as the consequences of selecting a sub-optimal L:M pair. The vertical axis represents the average angular separation and the horizontal axis represents the semi-major axis value associated with each repeating ground track orbit. The green diamond represents the repeating ground track that has the least average angular separation between it and the original ground track of the example (i.e., the repeating ground track that most resembles the original ground track within the specified design space), corresponding to the respective L:M pair in Table 13. The black dots represent the repeating ground tracks that do not resemble the original ground track as well as the best repeating ground track.

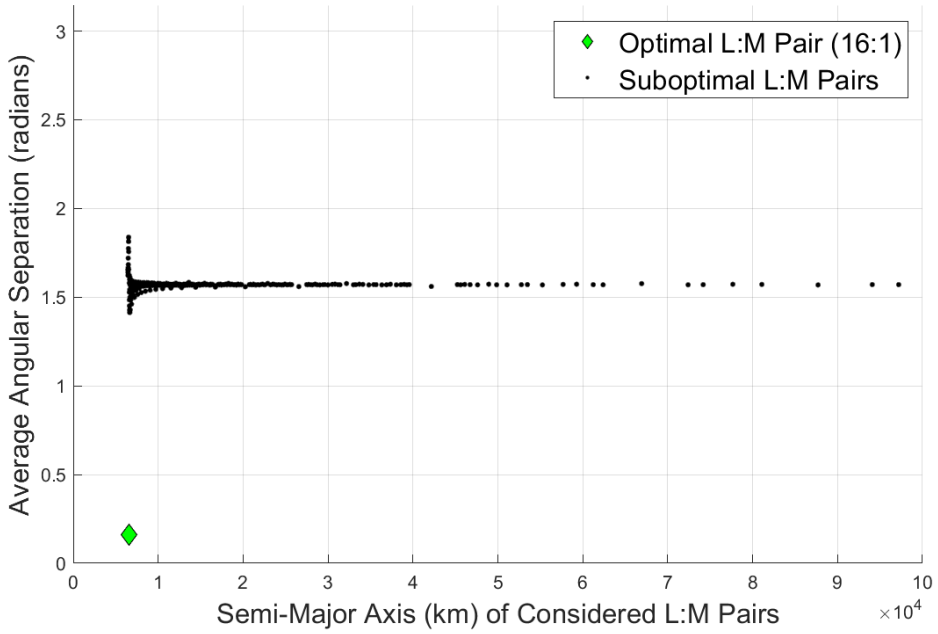

Figure 24: Average Angular Separation Between Considered Repeating Ground Tracks and Original Ground Track: Example 1

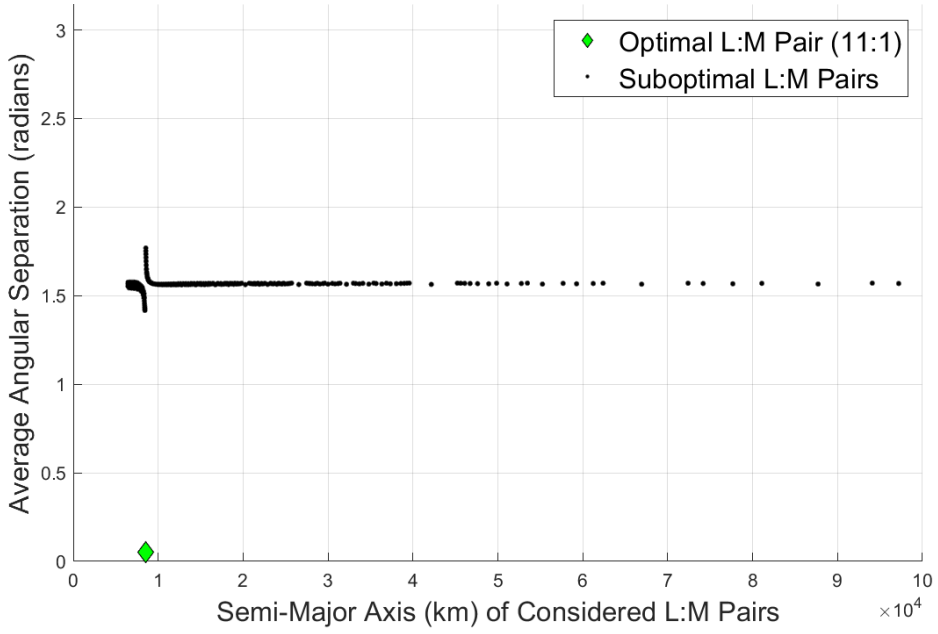

Figure 25: Average Angular Separation Between Considered Repeating Ground Tracks and Original Ground Track: Example 2

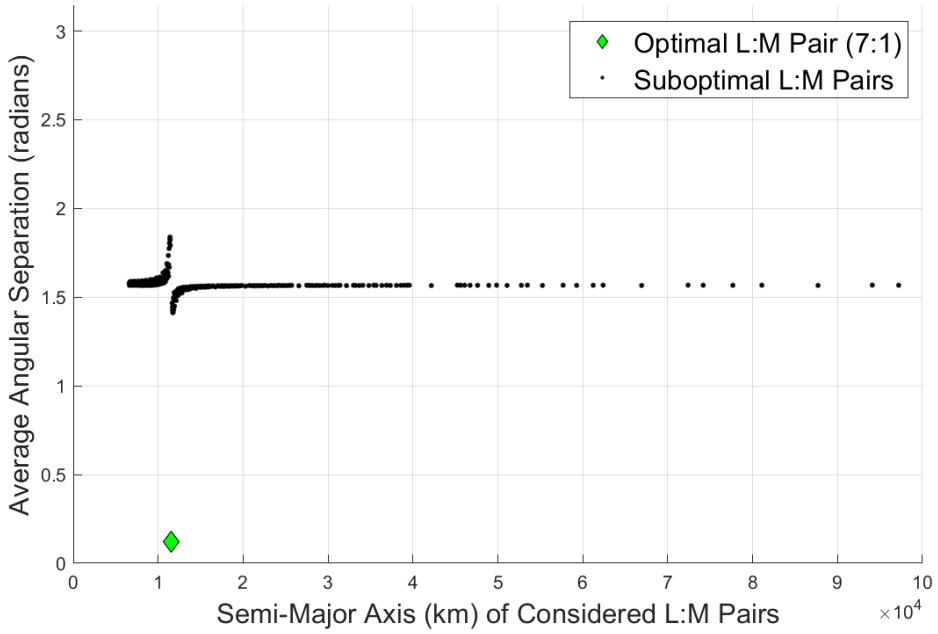

Figure 26: Average Angular Separation Between Considered Repeating Ground Tracks and Original Ground Track: Example 3

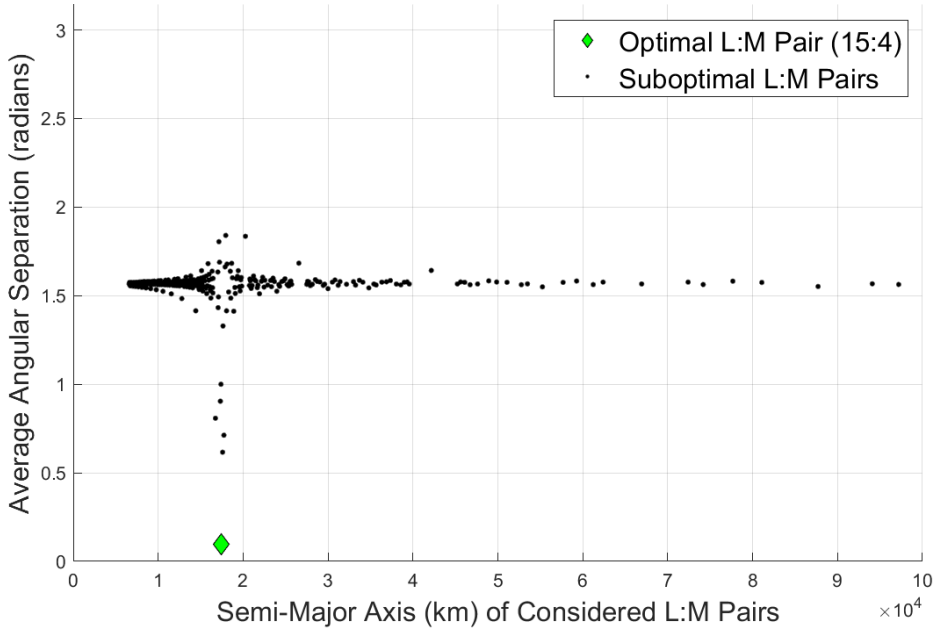

Figure 27: Average Angular Separation Between Considered Repeating Ground Tracks and Original Ground Track: Example 4

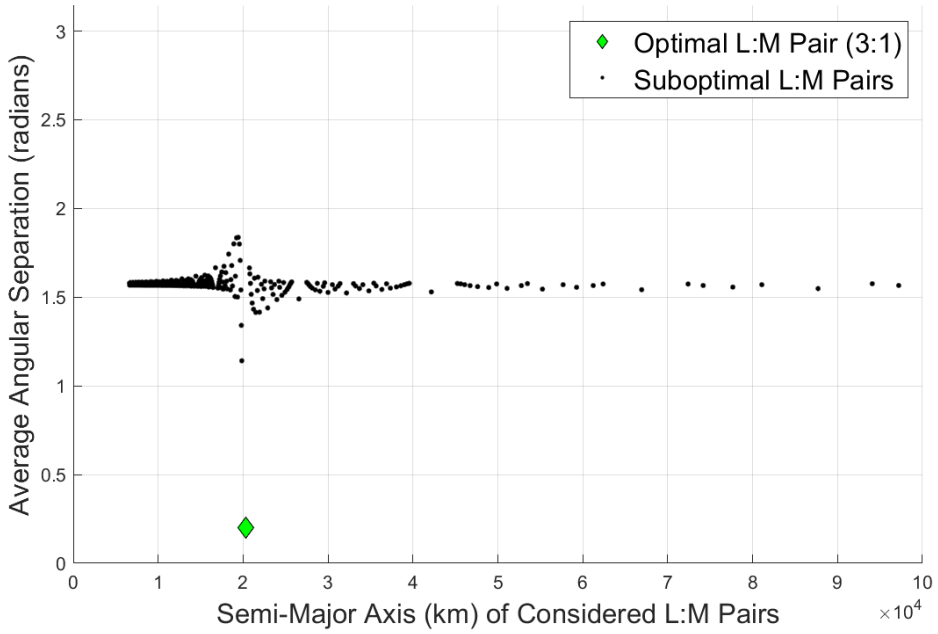

Figure 28: Average Angular Separation Between Considered Repeating Ground Tracks and Original Ground Track: Example 5

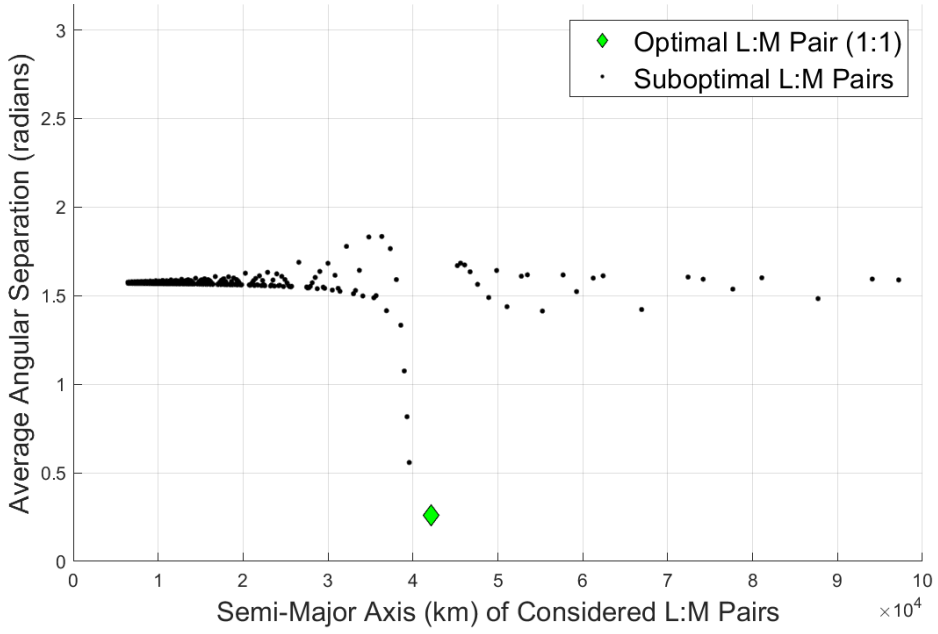

Figure 29: Average Angular Separation Between Considered Repeating Ground Tracks and Original Ground Track: Example 6

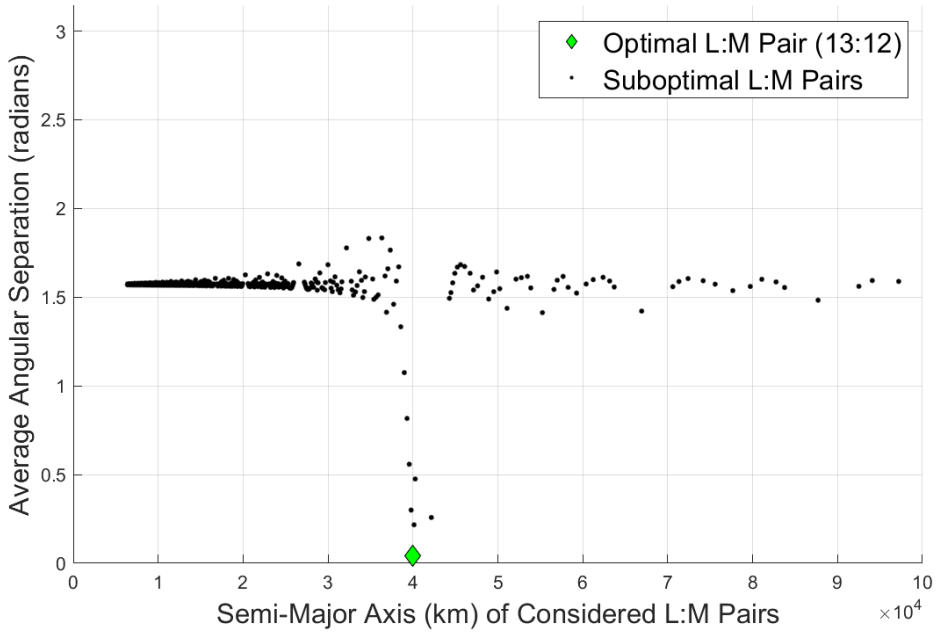

Figure 30: Average Angular Separation Between Considered Repeating Ground Tracks and Original Ground Track: Example 6 Revisited ($M_{max} = 20$ sidereal days)

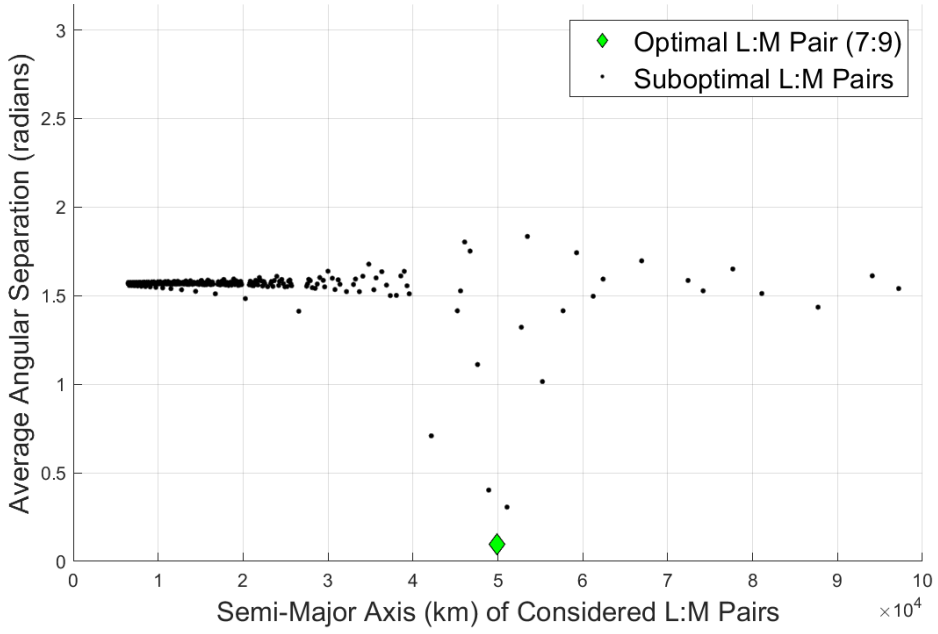

Figure 31: Average Angular Separation Between Considered Repeating Ground Tracks and Original Ground Track: Example 7

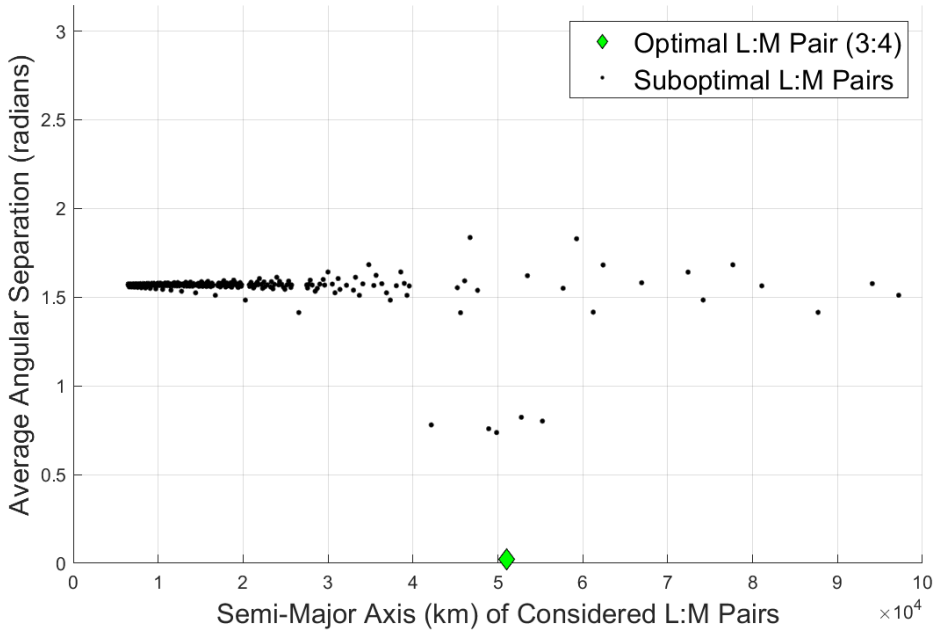

Figure 32: Average Angular Separation Between Considered Repeating Ground Tracks and Original Ground Track: Example 8

The average angular separation between the explored repeating ground tracks and the respective original ground tracks appear to approach $\pi/2$ as the difference between the semi-major axis of the repeating ground track orbit and the respective original orbit increases. This suggests that circular orbits with drastically different semi-major axis values will not have similar ground tracks. Additionally, the repeating ground track orbits that have semi-major axis values similar to the respective original orbit have a tendency to have ground tracks that are either more similar to or opposite from the original ground track, but still may be very different from the original ground track. These observations emphasize the importance of properly identifying the optimal L:M pair for orbital adjustments.

Overall, the experimental results suggest that solving the mathematical program defined in Equations (21) to (25) with the orbit metric identifies the L:M pair associated with the repeating ground track that most resembles the original ground

track from the set of considered repeating ground tracks, and it does so in much less computation time than using the average angular separation metric.

4.4 Conclusion

Satellite orbits may have perturbed non-repeating ground tracks. This chapter presents a simple approach to identify the optimal repeat parameters to modify a non-repeating ground track orbit into a repeating ground track orbit. Multiple examples demonstrate that the method identifies the repeat parameters associated with the repeating ground track that most closely resembles the ground track of the original non-repeating ground track orbit. Additionally, the methodology removes the need to run computationally expensive simulations to identify the repeating ground track that best resembles the ground track of an existing non-repeating ground track orbit. This result is not only important from a design viewpoint, but also with the operational perspective of orbital maintenance, as there may exist a repeating ground track orbit that closely resembles a current non-repeating ground track orbit. Additionally, these modified ground tracks can be longitudinally shifted to provide coverage to the desired area of interest.

Currently, improper selection of the parameter ranges used for identifying the parameters of the optimal repeating ground track may result in erroneous solutions if these ranges exclude the optimal solution. Although the current method of using large parameter ranges suffices to capture the optimal solution within the parameter ranges, future research addressing optimal parameter range selection could improve the computational efficiency of the proposed procedure, while ensuring avoidance of sub-optimal solutions.

4.5 Appendix

Table 14: L:M Pair Selections (Maximum Considered Period Duration: $M_{max} = 10$ Sidereal Days) [Note: Selections by both the orbit metric and the average angular separation metric matched in all examples]

Original Orbit Semi-Major Axis (km)	Original Orbit Inclination (degrees)	L:M Pair Selections (L:M)
6550	146	117:7
7000	163	121:8
7500	23	79:6
8000	164	86:7
8500	114	11:1
9000	18	10:1
9500	50	28:3
10000	98	26:3
10500	172	81:10
11000	173	68:9
11500	29	7:1
12000	174	33:5
12500	172	56:9
13000	87	35:6
13500	144	11:2
14000	26	47:9
14500	76	5:1
15000	164	33:7
15500	142	9:2
16000	172	30:7
16500	118	4:1
17000	7	39:10
17500	152	15:4
18000	168	18:5

Table 14: L:M Pair Selections (Maximum Considered Period Duration: $M_{max} = 10$ Sidereal Days) [Note: Selections by both the orbit metric and the average angular separation metric matched in all examples]

Original Orbit Semi-Major Axis (km)	Original Orbit Inclination (degrees)	L:M Pair Selections (L:M)
18500	122	31:9
19000	136	10:3
19500	134	19:6
20000	71	3:1
20500	118	3:1
21000	31	17:6
21500	127	11:4
22000	6	8:3
22500	50	18:7
23000	9	5:2
23500	18	12:5
24000	148	7:3
24500	125	9:4
25000	57	11:5
25500	171	17:8
26000	7	2:1
26500	79	2:1
27000	69	2:1
27500	138	19:10
28000	143	13:7
28500	34	9:5
29000	88	7:4
29500	80	12:7
30000	116	5:3
30500	127	13:8
31000	136	8:5

Table 14: L:M Pair Selections (Maximum Considered Period Duration: $M_{max} = 10$ Sidereal Days) [Note: Selections by both the orbit metric and the average angular separation metric matched in all examples]

Original Orbit Semi-Major Axis (km)	Original Orbit Inclination (degrees)	L:M Pair Selections (L:M)
31500	50	14:9
32000	122	3:2
32500	118	3:2
33000	30	13:9
33500	22	7:5
34000	90	11:8
34500	172	4:3
35000	61	4:3
35500	105	13:10
36000	41	5:4
36500	135	5:4
37000	46	11:9
37500	91	6:5
38000	126	7:6
38500	160	8:7
39000	172	9:8
39500	98	11:10
40000	25	1:1
40500	27	1:1
41000	47	1:1
41500	151	1:1
42000	46	1:1
42500	146	1:1
43000	44	1:1
43500	167	1:1
44000	63	1:1

Table 14: L:M Pair Selections (Maximum Considered Period Duration: $M_{max} = 10$ Sidereal Days) [Note: Selections by both the orbit metric and the average angular separation metric matched in all examples]

Original Orbit Semi-Major Axis (km)	Original Orbit Inclination (degrees)	L:M Pair Selections (L:M)
44500	36	1:1
45000	45	9:10
45500	111	8:9
46000	85	7:8
46500	63	6:7
47000	149	6:7
47500	105	5:6
48000	99	5:6
48500	165	4:5
49000	52	4:5
49500	136	4:5
50000	135	7:9
50500	69	3:4
51000	102	3:4
51500	14	3:4
52000	10	3:4
52500	96	5:7
53000	140	5:7
53500	168	7:10
54000	24	2:3
54500	102	2:3
55000	85	2:3
55500	3	2:3
56000	61	2:3
56500	30	2:3
57000	143	5:8

Table 14: L:M Pair Selections (Maximum Considered Period Duration: $M_{max} = 10$ Sidereal Days) [Note: Selections by both the orbit metric and the average angular separation metric matched in all examples]

Original Orbit Semi-Major Axis (km)	Original Orbit Inclination (degrees)	L:M Pair Selections (L:M)
57500	56	5:8
58000	95	5:8
58500	30	3:5
59000	108	3:5
59500	48	3:5
60000	118	3:5
60500	124	4:7
61000	134	4:7
61500	81	4:7
62000	16	5:9
62500	41	5:9
63000	164	5:9
63500	28	1:2
64000	148	1:2
64500	97	1:2
65000	179	1:2

V. Investigating an Asymmetric Satellite Constellation Design Framework: A Case Study of Regional Communication Network Robustness

Abstract

Appropriate selection of a satellite constellation design framework for a particular mission set requires *a priori* knowledge about the relative merits and shortcomings of different frameworks. Symmetric satellite constellation frameworks exhibit good properties for missions requiring continuous global coverage, whereas asymmetric satellite constellation frameworks benefit missions focusing on regional coverage. This research compares the performance of an asymmetric "string-of-pearls" common repeating ground track constellation design framework against a Walker constellation design framework for maintaining continuous connectivity between regions of interest. Several examples illustrate that the asymmetric string of pearls constellation framework requires an average of approximately 1.67 fewer satellites than the Walker constellation, whereas the Walker constellation appears approximately $9 \pm 4.5\%$ more robust to satellite failures.

5.1 Introduction

Satellite constellation design often relies on predefined geometric frameworks, such as Walker [1] and Star Pattern [16] constellations. Choo *et al.* [160] provide a comprehensive survey of satellite constellation design frameworks and design methodologies. Each satellite constellation design framework exhibits properties that make it more suitable for certain mission objectives. Several studies examine the performance differences between satellite constellation design frameworks to identify the designs appropriate for certain missions.

Many studies compare satellite constellation design frameworks for missions requiring continuous global coverage [15, 31, 17, 183]. These studies often focus on the number of satellites required to achieve this continuous global coverage. Walker [15] compares the minimum number of satellites required for Walker and Star Pattern constellations to provide continuous global coverage. Ulybyshev [17] examines and compares the minimum number of satellites required for Near-Polar, Polar, and Walker constellations to provide continuous global coverage. Other studies focus on the mission performance and challenges associated with certain satellite constellations. Lang and Adams [31] compare the overall system costs of using Walker and Polar Orbit constellations for continuous global coverage. Vatalaro *et al.* [183] analyze the performance differences between satellite constellations in low Earth orbit (LEO), medium Earth orbit (MEO), and geosynchronous equatorial orbit (GEO) for continuous global coverage in the presence of signal interference. Multiple studies focus on the performance of specific satellite constellation systems being considered by industry, e.g., SpaceX, Telesat, OneWeb, and Amazon [184, 185, 186].

Satellite constellation design literature also compares satellite constellation design frameworks for regional coverage. Lang [34] compares the minimum number of satellites required by Walker and Polar Orbit constellations to provide continuous coverage between 20^o-60^o latitude. Muri *et al.* [187] compare the ability of a sun-synchronous repeating ground track orbit against a Flower constellation to provide communications throughput for regional coverage. Many studies find that asymmetric satellite constellations require fewer satellites for regional coverage than symmetric satellite constellations [38, 188, 60]. Ullock and Schoen [38] examine the difference in the minimum number of satellites required for asymmetric and symmetric Polar Orbit constellations to provide continuous regional coverage. Ma *et al.* [188] examine the minimum number of satellites required for a Walker constellation and asymmetric

constellations to provide continuous regional communications coverage to Taiwan. Lee *et al.* [60] present a method to design asymmetric satellite constellations and found they use fewer satellites than the explored symmetric satellite constellations for regional coverage. Although asymmetric satellite constellations may require fewer satellites than symmetric satellite constellations to provide regional coverage, unaddressed within the literature is the relative robustness of the resulting asymmetric constellations, compared to their symmetric alternatives.

The robustness of a satellite constellation and its ability to operate under the presence of satellite failures has been examined for global coverage. Shake *et al.* [189] examine different operational strategies for maintaining the ability of a Walker constellation of 360 satellites to provide continuous global communications in the presence of randomly occurring satellite failures. It may be beneficial to examine the worst-case scenario for a given number of satellite failures. Network interdiction models can analyze the worst-case degradation of a network. Network interdiction has been extensively studied in the literature for a variety of applications, including wireless communications vulnerability [190, 191], evader detection [192, 193], water distribution vulnerability [194, 195], robustness of computing networks [196], and illicit network disruption [197, 198]. Smith and Song [199] present a thorough survey of network interdiction.

This research investigates the robustness of an asymmetric satellite constellation designed to maintain connectivity between two regions against satellite failures using network interdiction approaches. It evaluates a sparse (minimum satellite) asymmetric constellation having a common repeating ground track. As a benchmark, testing compares its communications robustness to that of a (symmetric) Walker constellation.

This research makes three contributions to the satellite constellation design literature. First, it presents and demonstrates a heuristic to design an asymmetric satellite constellation with all satellites following a common repeating ground track for continuous regional coverage. Second, it formulates a network interdiction model to evaluate the worst-case degradation of the average connectivity a satellite constellation provides between two regions. Third, it analyzes the relative robustness of an asymmetric satellite constellation design framework and a symmetric satellite constellation design framework for realistic, representative scenarios.

The remainder of the chapter is organized as follows. Section 5.2 presents the heuristic for designing an asymmetric common repeating ground track satellite constellation for continuous regional coverage, as well as the formulation for optimal satellite network interdiction. Section 5.3 provides several illustrative examples comparing the performance between the two satellite constellation design frameworks. Finally, Section 5.4 provides concluding remarks.

5.2 Methodology

Comparison of the performance of satellite constellation frameworks requires the design of satellite constellations. These satellite constellations should represent the best designs of their respective design frameworks. Alternative optimization criterion used to design the satellite constellations may yield different constellations. Since satellite constellations are expensive to deploy, manage, and operate, it is often of interest to identify the fewest number of satellites to achieve mission success. Within this context, the analysis herein designs satellite constellations focused on minimizing the number of satellites required to provide continuous coverage to all regions of interest. In order to develop a methodology, this research employs the following assumptions which simplify the mathematical modeling and analysis as follows: 1)

satellite coverage considers a spherical Earth, 2) a satellite's field of regard (possible coverage) is equal to its field of view (focused coverage), 3) the satellite's field of regard is conical and remains normal to the surface of the Earth, 4) latency is not considered (connectivity is instantaneous), 5) there is no limit on data transfer rate through a satellite, 6) satellite sensor performance is independent of semi-major axis, 7) geographic masking is not considered, 8) all locations within a satellites field of regard receive coverage, 9) the satellite orbit only considers perturbations due to a non-spherical Earth, and 10) other environmental factors, including debris and the Van Allen radiation belts, are not considered for the constellation's performance. Section 5.2.1 presents a heuristic to design asymmetric satellite constellations wherein all satellites follow a common repeating ground track.

This analysis uses robustness to the number of satellite failures as a metric to compare satellite constellation design frameworks. The robustness of a satellite constellation can be examined by analyzing how well the satellite constellation functions in the event of worst-case scenario satellite failures. Section 5.2.2 presents a formulation to find this worst-case degradation to the performance of the satellite constellation for a given number of satellite failures.

5.2.1 Asymmetric Satellite Constellation Design Heuristic

This research addresses satellite constellations that have all satellites following a single repeating ground track using irregular intersatellite phasing, referred to as an asymmetric "string-of-pearls" common repeating ground track constellation. Although a "pure" string-of-pearls approach (equally-phased satellites) simplifies constellation design, the flexibility of asymmetry enables the design of more efficient constellations. Lee *et al.* [60] present a binary mathematical program to minimize the number of satellites required for such an asymmetric satellite constellation to provide

regional coverage. However, Lee *et al.* [60] acknowledge that their reliance on integer variables limits the scalability of their method and recommend designing heuristics to obtain initial feasible solutions. This research embraces their recommendation, and this section presents a heuristic to identify an initial feasible satellite constellation, as well as a minor modification to their formulation that cuts the design space to reduce computational costs associated with demonstrating optimality. Algorithm 2 outlines this research's approach to designing asymmetric satellite constellations.

Algorithm 2 Designing an Asymmetric Satellite Constellation

1: Select a repeating ground track
2: Initialize satellite constellation design
3: Refine orbits and remove unnecessary satellites from constellation

Algorithm 2 has three main steps. The first two steps identify an initial feasible satellite constellation that satisfies the regional coverage requirements. Line 1 selects a repeating ground track, and Line 2 uses this repeating ground track to design an initial satellite constellation. Line 3 repositions and removes satellites from the satellite constellation using a modified version of the formulation presented by Lee *et al.* [60]. The subsequent discussion details each of these steps.

5.2.1.1 Select a repeating ground track

Algorithm 3 outlines the procedure for selecting a repeating ground track in Step 1 of Algorithm 2.

Algorithm 3 Selecting a Repeating Ground Track

1: Define satellite orbit design problem
2: Optimize single-satellite orbit
3: Modify and refine orbit into a repeating ground track orbit

Algorithm 3 has three parts. The first part defines the orbital design space used to search for an optimal single-satellite orbit, as well as the optimality metric. The

tuple (i, λ_0, a) can represent the design space of circular orbits. The parameter i represents the orbital inclination, λ_0 represents the longitude of the satellite's first ascension across the equatorial plane within the simulation (i.e., the first time the satellite crosses the equator from south to north), and a represents the semi-major axis of the circular orbit. This research uses the minimum average coverage over each of the regions of interest as the objective metric for selecting a single-satellite orbit. Equation (26) defines the coverage function, which represents when a satellite provides coverage to a region of interest.

$$c(r,t) = \begin{cases} 1 & \text{satellite covers region } r \text{ at time } t \\ 0 & \text{otherwise} \end{cases} \tag{26}$$

Equation (27) defines the minimium average coverage over the regions of interest. The parameter T represents the time duration, and the set R represents the set of regions of interest.

$$f = \min_{r \in R} \left\{ \frac{1}{T} \int_{t=0}^{T} c(r,t) dt \right\} \tag{27}$$

Deterministic simulations approximate Equation (27) using Equation (28). The parameter D represents the number of discretized time points, and Δt represents the time step length between discretized time points.

$$f \approx \min_{r \in R} \left\{ \frac{1}{D\Delta t} \sum_{d=0}^{D-1} c(r, d\Delta t)\Delta t \right\} \tag{28}$$

The second part of Algorithm 3 actively searches the orbital design space to optimize the single-satellite orbit. Solving the following mathematical program will identify the optimal circular orbit for a single-satellite to provide coverage to the regions of interest.

$$\max_{i,\lambda_0,a} \quad z \tag{29}$$

$$\text{s.t.} \quad z \leq \frac{1}{T}\int_{t=0}^{T} c(r,t)dt, \quad \forall r \in R, \tag{30}$$

$$i_{min} \leq i \leq i_{max}, \tag{31}$$

$$\lambda_0^{min} \leq \lambda_0 \leq \lambda_0^{max}, \tag{32}$$

$$a_{min} \leq a \leq a_{max}. \tag{33}$$

Objective function (29) maximizes the minimum average coverage received by any of the regions of interest from a single satellite using Constraint (30). Constraints (31)-(33) ensure each of the orbital parameters remains within the desired design space. The nonlinearity of the objective function warrants the use of a metaheuristic to search the design space for the optimal orbit; however, a metaheuristic will not always identify the optimal orbit. Choo *et al.* [200] demonstrate that response surface analysis and particle swarm optimization are both useful methodologies for handling similar design problems to the mathematical program described above, with the response surface analysis quickly identifying good regions of the design space and the particle swarm optimization excelling in converging to good solutions.

The metaheuristic finding good solutions to the mathematical program defined by Objective function (29) and Constraints (31)-(33) uses both response surface analysis and particle swarm optimization to leverage the beneficial properties of both search methods. First, response surface analysis explores the design space to identify a promising location in the design space. Next, particle swarm optimization explores the design space informed by the location identified in the response surface analysis.

The third part of Algorithm 3 modifies the selected single-satellite orbit into a repeating ground track orbit and refines the repeating ground track to improve its

coverage properties. This modification first identifies the repeat parameters, L:M, that correspond to a repeating ground track closely resembling the ground track of the current satellite orbit. The repeating parameters L and M signify that a satellite repeats its ground track using L orbits in M sidereal days. L and M must be co-prime integers, (i.e., their greatest common divisor is 1) [1]. Choo *et al.* [201] present an efficient method for identifying an L:M pair associated with a repeating ground track that closely resembles a non-repeating ground track.

Arbitrarily modifying the orbit into a repeating ground track orbit may result in a suboptimal modification (i.e., the best coverage is not achieved). Solving a second optimization problem will address this concern. Let $g(\mathrm{L}, \mathrm{M}, i)$ be a function identifying the semi-major axis necessary for a circular orbit with an inclination i to produce a repeating ground track that repeats using L orbits in M sidereal days. Restricting the semi-major axis to $g(\mathrm{L}, \mathrm{M}, i)$ results in the adjusted mathematical program.

$$\max_{i,\lambda_0,a} \quad z \tag{34}$$

$$\text{s.t.} \quad z \leq \frac{1}{T} \int_{t=0}^{T} c(r,t)dt, \quad \forall r \in R, \tag{35}$$

$$i_{min} \leq i \leq i_{max}, \tag{36}$$

$$\lambda_0^{min} \leq \lambda_0 \leq \lambda_0^{max}, \tag{37}$$

$$a = g(\mathrm{L}, \mathrm{M}, i). \tag{38}$$

Objective function (34) and Constraints (35)-(37) match Objective function (29) and Constraints (30)-(32), respectively. Constraint (38) ensures the selected satellite orbit remains a repeating ground track orbit associated with the desired L:M pair. The same metaheuristic used to find the original single-satellite orbit can also be applied to this mathematical program. The newly selected repeating ground track orbit provides the ground track used to design the satellite constellation.

5.2.1.2 Initialize satellite constellation design

Line 2 of Algorithm 2 uses the heuristic outlined in Algorithm 4 to identify an initial feasible common repeating ground track satellite constellation that provides continuous coverage to the region(s) of interest.

Algorithm 4 Initial Satellite Constellation Design Heuristic

1: Identify region of interest receiving least amount of coverage
2: **while** coverage of identified region is not continuous **do**
3: Add satellite to the constellation using identified region
4: **while** coverage of every region is not continuous **do**
5: Identify region receiving least amount of coverage
6: Add satellite to the constellation using identified region

Line 1 of Algorithm 4 identifies the region of interest, r_l, that receives the least amount of coverage from a single satellite following the selected repeating ground track. Solving Equation (39) identifies the region of interest that receives the least amount of coverage from a single satellite.

$$r_l \in \arg\min_{r \in R} \left\{ \frac{1}{T} \int_{t=0}^{T} c(r,t)dt \right\} \tag{39}$$

Line 2 of Algorithm 4 checks whether the identified region of interest, r_l, receives continuous coverage from the current satellite constellation. If r_l does not receive continuous coverage, a satellite is added to the constellation (Line 3 of Algorithm 4). The following paragraphs explain the steps of adding a satellite to the constellation.

Equation (40) defines a function representing the coverage function for a region of interest from a satellite placed at different locations along the repeating ground track. Equation (41) defines an *OR gate* function.

$$c_{t_i}(r,t,t_i,c) = \begin{cases} c(r,t+t_i) & t+t_i \leq T \\ c(r,t+t_i-T) & t+t_i > T \end{cases} \tag{40}$$

$$\mathrm{OR}(a,b) = \begin{cases} 1 & a = 1 \text{ or } b = 1 \\ 0 & a = b = 0 \end{cases} \tag{41}$$

Let $C_i(r,t,t_i)$ represent the cumulative coverage function of region of interest r from a constellation of i satellites following the repeating ground track at time t. Together, Equations (42) and (43) define $C_i(r,t,t_i)$.

$$C_1(r,t,0) = c_0(r,t,0,c) \tag{42}$$

$$C_i(r,t,t_i) = \mathrm{OR}(c_{t_i}(r,t,t_i,c), C_{i-1}(r,t,t_{i-1})) \tag{43}$$

Solving Equation (44) identifies the placement of an additional satellite along the repeating ground track.

$$\tilde{t}_i \in \underset{t_i \in [0,T)}{\arg\max} \left\{ \int_{t=0}^{T} C_i(r_l,t,t_i)dt \right\} \tag{44}$$

Equation (44) identifies the placement of a satellite along the repeating ground track to maximize the marginal benefit of the added satellite in providing coverage to the region of interest that receives the least amount of coverage from a single satellite. Satellites are added until the region of interest, r_l, receives continuous coverage. Let $\mathcal{T}_{opt}$ represent a set of optimal solutions to Equation (44). If $\mathcal{T}_{opt}$ is not a singleton (i.e., if alternative optimal solutions exist with respect to Equation (44)), Equation (45) discriminates among them, identifying the placement that maximizes the average marginal benefit of the satellite placement across *all* regions of interest.

$$\tilde{t}_i \in \underset{t_i \in \mathcal{T}_{opt}}{\arg\max} \left\{ \frac{1}{R} \sum_{r=1}^{R} \int_{t=0}^{T} C_i(r,t,t_i)dt \right\} \tag{45}$$

Once the region of interest that receives the least amount of coverage from a single satellite receives continuous coverage, it remains important to ensure that every region of interest also receives continuous coverage. Line 4 evaluates whether if every region

of interest receives continuous coverage from the current satellite constellation. If at least one region of interest does not receive continuous coverage, Line 5 identifies the region of interest currently receiving the least amount of coverage (i.e., identifying a new r_l). Line 6 also uses Equation (44) to identify the placement of a new satellite, and, if necessary, Equation (45). This process continues until every region of interest receives continuous coverage.

5.2.1.3 Refine satellite placement and remove unnecessary satellites from constellation

The satellite constellation produced by Algorithm 4 may not have the minimum number of satellites. Line 3 of Algorithm 2 adjusts the placement of the satellites in the constellation and removes excess satellites. Lee *et al.* [60] present a mathematical programming approach to design asymmetric satellite constellations for regional coverage focused on minimizing the number of satellites in the satellite constellation. Their formulation for a single repeating ground track is presented as follows. Let v_r represent a discretized coverage function provided to a region r by a single satellite following a repeating ground track. The function v_r will have D discretized time points. Let T represent the period of the repeating ground track and define $\Delta t_d = T/D$. Using Equation (26), Equation (46) defines v_r, where $d = 0, 1, ..., D-1$.

$$v_r(d) = c(r, d\Delta t_d) \tag{46}$$

Equation (47) uses Equation (46) to create a coverage matrix $\boldsymbol{V}_r$ for each region of interest r.

$$\boldsymbol{V}_r = \begin{bmatrix} \upsilon_r(0) & \upsilon_r(D-1) & \upsilon_r(D-2) & \dots & \upsilon_r(1) \\ \upsilon_r(1) & \upsilon_r(0) & \upsilon_r(D-1) & \dots & \upsilon_r(2) \\ \upsilon_r(2) & \upsilon_r(1) & \upsilon_r(0) & \dots & \vdots \\ \vdots & \vdots & \ddots & \ddots & \vdots \\ \upsilon_r(D-1) & \upsilon_r(D-2) & \dots & \dots & \upsilon_r(0) \end{bmatrix} \tag{47}$$

Let $\boldsymbol{f}_r$ be the coverage requirements of the r^{th} region of interest over the period of the repeating ground track. Let $\boldsymbol{x} = [x_0, x_1, ..., x_{D-1}]'$ be a column vector of decision variables indicating where satellites are placed along the repeating ground track, wherein x_d is 1 if a satellite is placed along the repeating ground track at time slot d and 0 otherwise. The formulation to minimize the number of satellites in an asymmetric satellite constellation where all satellites follow the same repeating ground track is presented by Lee *et al.* [60] as follows.

$$\min_{\boldsymbol{x}} \quad \sum_{d=0}^{D-1} x_d \tag{48}$$

$$\text{s.t.} \quad \boldsymbol{V}_r \boldsymbol{x} \geq \boldsymbol{f}_r, \quad \forall r \in R, \tag{49}$$

$$x_d \in \{0, 1\}, \quad \forall d = 0, 1, ..., D-1. \tag{50}$$

Objective function (48) seeks to minimize the number of satellites used within the satellite constellation. Constraint (49) ensures all coverage requirements satisfy the demands of each region of interest. Constraint (50) requires that at most a single satellite may be placed at any point along the repeating ground track. This formulation consists entirely of binary variables, which may result in tractability issues for large problem instances. The following two constraints can reduce the size of the design space. The number of satellites used in the initial design of the satellite constellation establishes an upper bound for the formulation. Additionally, examining

the coverage provided to each region of interest by a single satellite identifies a lower bound on the minimum number of satellite required for continuous regional coverage. Consider a single satellite following a repeating ground track and a single region of interest, r. Solving Equation (51) finds the proportion of time a region of interest receives coverage from an individual satellite.

$$\psi^r_{total} = \frac{1}{T} \int_{t=0}^{T} c(r,t)dt \tag{51}$$

The minimum number of satellites achievable for a satellite constellation to provide continuous coverage to a single region is bounded by $\lceil 1/\psi^r_{total} \rceil$. Therefore, the minimum number of satellites achievable for a satellite constellation to provide continuous coverage to multiple regions of interest is the maximum of the minimum number of satellites achievable for a satellite constellation to provide continuous coverage to any of the regions of interest. Equation (52) determines a lower bound, lb, on the minimum number of satellites achievable for a common repeating ground track satellite constellation to provide continuous coverage to multiple regions of interest.

$$lb = \max_{r \in R} \left\{ \left\lceil \frac{1}{\psi^r_{total}} \right\rceil \right\} \tag{52}$$

The mathematical program presented by Lee *et al.* [60] can be expanded into the following mathematical program. Let ub represent the number of satellites used in the initial satellite constellation.

$$\min_{\boldsymbol{x}} \quad \sum_{d=0}^{D-1} x_d \tag{48}$$

$$\text{s.t.} \quad \boldsymbol{V}_r \boldsymbol{x} \geq \boldsymbol{f}_r, \quad \forall r \in R, \tag{49}$$

$$\sum_{d=0}^{D-1} x_d \leq ub, \tag{53}$$

$$\sum_{d=0}^{D-1} x_d \geq lb, \tag{54}$$

$$x_d \in \{0,1\}, \quad \forall d = 0,1,...,D-1. \tag{50}$$

Constraints (53)-(54) reduce the feasible region of the design space of the previously discussed formulation (i.e., (48)-(50)). In preliminary testing, instances of this problem were too large to solve to optimality using a leading commercial solver (CPLEX [202]) within a practical time limit (i.e., 12 hours). However, the identified, often suboptimal solutions did demonstrably help refine the satellite constellation and remove satellites, improving the sparsity of the satellite constellation. As such, the binary math program yields computationally challenging instances, but even suboptimal solutions provide value to refining the satellite constellation design.

5.2.2 Optimal Satellite Constellation Interdiction Models

This research evaluates the robustness of a satellite constellation by observing its ability to maintain continuous connectivity between a ground station (or headquarters location) and regions of interest in the presence of satellite failures. A satellite constellation achieves the connectivity between a headquarters location and a region of interest when at least one path exists from the headquarters location to the region of interest through the satellite constellation. The headquarters location and regions of interest establish connectivity with satellites that exist above a predeter-

mined elevation angle relative to the plane tangent to the surface of a spherical Earth. Direct line of sight informs inter-satellite connectivity. Although latency in communications exists in real systems, this research assumes the instantaneous transfer of communications.

This research models the robustness of a satellite constellation's ability to maintain connectivity as a network interdiction problem. The network interdiction problem approach identifies the worst-case scenario for a bounded number of satellite failures as a representation of the robustness of the constellation. This research considers the state of the satellite constellation only after a fixed number of satellites have failed.

From a game theoretic perspective, this network interdiction problem can be modeled as a Stackleberg game (two-player, two-stage, sequential game with complete and perfect information). The first player attempts to maximize the degradation of connectivity to the satellite constellation by appropriately selecting the satellites to fail. The second player attempts to maximize the connectivity between the headquarters location and the regions of interest using the remaining satellite constellation. Although this research develops the network interdiction model for the dynamic satellite network, it is illustrative to first consider a static satellite network (i.e., one time instance).

5.2.2.1 Static Network Configuration

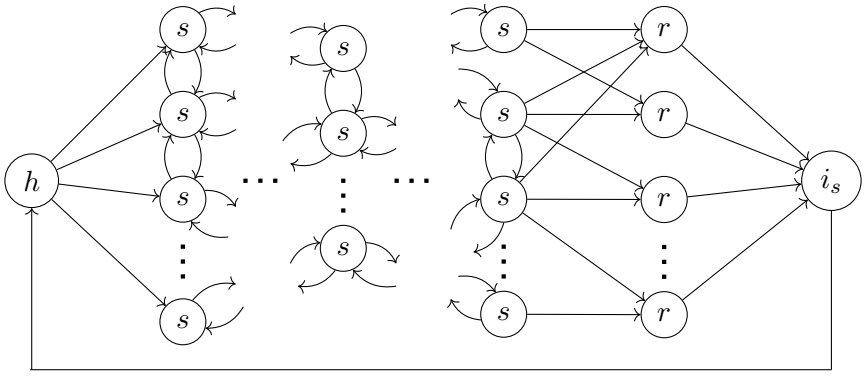

Figure 33: Static Network Problem Structure

The static model focuses on the ability of a satellite constellation to provide continuous connectivity between a headquarters location and region(s) of interest at a single instance in time. Figure 33 shows the general structure of this static network model. The model uses four groups of nodes. The node labeled h represents the headquarters location, the nodes labeled s represent the satellites, the nodes labeled r represent the regions of interest, and the sink node labeled i_s simplifies the network model. The arcs represent the connectivity between the nodes. Arcs are directed from the headquarters location to the satellites currently accessible to it. No directional arcs exist from the satellite nodes into the headquarters node. Two directed arcs in opposite directions represent all intersatellite connections. Arcs directed from satellites to the region(s) of interest represent satellite coverage. No directional arcs exist from the region of interest nodes to the satellite nodes. All of the regions of interest nodes have arcs directed towards the sink node, and the sink node has an arc directed towards the headquarters location. Tables 15-17 establish the sets, parameters, and variables for the static model.

Table 15: Bilevel Program Symbol Description (Sets)

Symbol	Description
N	Set of nodes in the static network
$\{h\} \subset N$	Node representing the headquarters location
$R \subset N$	Set of nodes representing the regions of interest
$S \subset N$	Set of nodes representing the satellites
$\{i_s\} \subset N$	Artificial node required to establish model
A_s	The set of arcs in the network representing connectivity between pairs of satellites i and j, informed by line-of-sight between satellites and inducing pairs of directed arcs (i,j) and (j,i), $i,j \in S$
A_h	The set of arcs in the network representing connectivity between the headquarters location and satellites capable of immediate data-link with the headquarters location, inducing directed arcs $(h,i), h \in \{h\}, i \in S$
A_r	The set of arcs in the network representing connectivity between satellites and the regions of interest informed by a satellite's immediate coverage, inducing directed arcs $(i,r), i \in S, r \in R$
A_{i_s}	The set of arcs associated with the artificial sink node establishing arcs between the region of interest nodes and the sink node, as well as the sink node to the headquarters node. Inducing (r,i_s) and (i_s,h), $r \in R$,$i_s \in \{i_s\}$, and $h \in \{h\}$
$A = A_s \cup A_h \cup A_r \cup A_{i_s}$	Set of all arcs
$G(N,A)$	The satellite constellation network when all satellites are functioning

Table 16: Bilevel Program Symbol Description (Parameters)

Symbol	Description
Γ	The maximum number of satellite failures (interdictions)
u_{ij}	The maximum flow through arc $(i,j) \in A$

Table 17: Bilevel Program Symbol Description (Decision Variables)

Symbol	Description
γ_i	Binary decision variable equal to 1 if interdicts flow through node $i \in N$, and 0 otherwise
γ_{ij}	Binary decision variable equal to 1 if interdicts flow through arc $(i,j) \in A$, and 0 otherwise
x_{ij}	Non-negative decision variable representing (communications) flow between any pair of nodes $(i,j) \in A$

The flow through the network represents an abstraction of communications; flow identifies the regions of interest that connect to the headquarters location, but lacks any representation of data transfer. For each arc $(i,j) \in A$, the flow x_{ij} is limited to a maximum amount of flow, u_{ij}. Equation (55) defines the maximum flow for each arc.

$$u_{(i,j)} = \begin{cases} |R| & i \notin R \\ 1 & i \in R \end{cases} \quad \forall (i,j) \in A \setminus \{(i_s,h)\} \tag{55}$$

The parameter Γ represents the largest number of satellite failures. The variable γ_i identifies which satellites fail. The following bilevel mathematical program represents the static network interdiction model.

$$\min_{\boldsymbol{\gamma}} \max_{\boldsymbol{x}} \quad x_{i_s h} \tag{56}$$

$$\text{s.t.} \quad \sum_{i \in N} \gamma_i \leq \Gamma, \tag{57}$$

$$\gamma_i \in \{0,1\}, \ \forall i \in N, \tag{58}$$

$$\sum_{(j,i) \in A} x_{ji} - \sum_{(i,j) \in A} x_{ij} = 0, \quad \forall i \in N, \tag{59}$$

$$x_{ij} \leq u_{ij}(1 - \gamma_{ij}), \quad \forall (i,j) \in A \setminus \{(i_s, h)\}, \tag{60}$$

$$\gamma_{ij} = \gamma_i, \quad \forall (i,j) \in A \setminus \{(i_s, h)\}, \tag{61}$$

$$\gamma_i = 0, \quad \forall i \in N \setminus S, \tag{62}$$

$$x_{ij} \geq 0, \quad \forall (i,j) \in A. \tag{63}$$

Objective function (56) minimizes the maximum flow through the network. Constraint (57) limits the number of interdictions (failures). Constraint (58) ensures the complete interdiction of nodes. Constraint (59) ensures the flow passes through a node. Constraints (60) and (61) ensure that the flow only passes through non-interdicted nodes. Constraint (62) limits the interdictions to only the satellite nodes. Constraint (63) ensures only positive flows are possible. Constraints (57)-(58) and (61)-(62) define the upper-level problem (player deciding which satellites fail), and Constraints (59)-(60) and (63) define the lower-level problem (player maximizing connectivity with the remaining satellite network).

Similar to Wood [203], the bilevel mathematical program can be reformulated as a single-level problem by replacing the lower-level problem with its dual. Table 18 identifies the dual variables used to take the dual of the lower-level problem.

Table 18: Associated Primal Variables for the Dual of the Lower-level Problem

Primal Constraint	**Dual Variable**
(59)	$\alpha_i,\ \forall\ i \in N$
(60)	$\theta_{ij} \geq 0,\ \forall\ (i,j) \in A \setminus \{(i_s,h)\}$

Since the lower-level problem is identical to Wood's [203] formulation, each α_i and θ_{ij} can be replaced with binary decision variables. Therefore, the bilevel mathematical program can be reformulated as the following single-level problem.

$$\min_{\boldsymbol{\gamma}} \min_{\boldsymbol{\alpha},\boldsymbol{\theta}} \sum_{(i,j)\in A\setminus\{(i_s,h)\}} u_{ij}(1-\gamma_{ij})\theta_{ij} \tag{64}$$

$$\text{s.t.}\ \ \alpha_i - \alpha_j + \theta_{ij} \geq 0, \quad \forall (i,j) \in A \setminus \{(i_s,h)\}, \tag{65}$$

$$\alpha_{i_s} - \alpha_h \geq 1, \tag{66}$$

$$\gamma_{ij} = \gamma_i, \quad \forall (i,j) \in A \setminus \{(i_s,h)\}, \tag{67}$$

$$\gamma_i = 0, \quad \forall i \in N \setminus S, \tag{68}$$

$$\sum_{i\in N} \gamma_i \leq \Gamma, \tag{69}$$

$$\theta_{ij} \in \{0,1\}, \quad \forall (i,j) \in A \setminus \{(i_s,h)\}, \tag{70}$$

$$\alpha_i, \gamma_i \in \{0,1\}, \quad \forall i \in N. \tag{71}$$

Since Constraints (67) and (68) are only related to γ_i and γ_{ij}, the formulation can be further reduced to transform it from a mixed (binary) integer nonlinear program to a binary integer program, the latter of which is directly solvable using a larger number of commercial solvers. Define a binary variable $\beta_{ij} \in \{0,1\}$ for each $(i,j) \in A\setminus\{(i_s,h)\}$ such that it satisfies Constraint (72).

$$\beta_{ij} \geq \theta_{ij} - \gamma_{ij}, \quad \forall (i,j) \in A \setminus \{(i_s,h)\} \tag{72}$$

Wood [203] demonstrates that including β_{ij} into the model can eliminate Constraint (72) and each decision variable θ_{ij} from the formulation. Additionally, replacing each decision variable γ_{ij} with γ_i using Constraint (67) eliminates γ_{ij} and Constraint (67) from the formulation. The static network interdiction problem can be reformulated as the following mathematical program.

$$\min_{\boldsymbol{\gamma},\boldsymbol{\alpha},\boldsymbol{\beta}} \quad \sum_{(i,j)\in A\setminus\{(i_s,h)\}} u_{ij}\beta_{ij} \tag{73}$$

$$\text{s.t.} \quad \alpha_i - \alpha_j + \beta_{ij} + \gamma_i \geq 0, \quad \forall (i,j) \in A \setminus \{(i_s,h)\}, \tag{74}$$

$$\alpha_{i_s} - \alpha_h \geq 1, \tag{75}$$

$$\gamma_i = 0, \quad \forall i \in N \setminus S, \tag{76}$$

$$\sum_{i\in N} \gamma_i \leq \Gamma, \tag{77}$$

$$\beta_{ij} \in \{0,1\}, \quad \forall (i,j) \in A \setminus \{(i_s,h)\}, \tag{78}$$

$$\alpha_i, \gamma_i \in \{0,1\}, \quad \forall i \in N. \tag{79}$$

This static network interdiction model closely resembles the work by Kennedy *et al.* [204]. Kennedy *et al.* [204] also derive their formulation from Wood [203] to include nodal interdictions into the network interdiction model. The primary difference between Kennedy's *et al.* [204] formulation and the present formulation are Constraints (74) and (76). Kennedy's *et al.* [204] formulation allows for arc interdictions as well as nodal interdictions for every node, whereas this formulation does not allow for arc interdictions and restricts interdictions to specific nodes.

Dynamic Network Formulation

The formulation for the static network model is extended to model the dynamic nature of a satellite constellation. The dynamic satellite network model considers the unique network configurations observed throughout the period of interest. The degradation to the satellite network is measured as the weighted average degradation

to each network configuration for predefined satellite failures. The time duration the network remains in a particular configuration informs the weight applied to the configuration. Tables 19-21 define the sets, parameters, and decision variables for the dynamic network interdiction model formulation.

Table 19: Dynamic Program Symbol Description (Sets)

Symbol	Description
C	Set of network configurations
N	Set of nodes in the static network
$\{h\} \subset N$	Node representing the headquarters location
$R \subset N$	Set of nodes representing the regions of interest
$S \subset N$	Set of nodes representing the satellites
$\{i_s\} \subset N$	Artificial node required to establish model
A_s^c	The set of arcs in the network representing connectivity between pairs of satellites i and j, informed by line-of-sight between satellites and inducing pairs of directed arcs (i,j) and (j,i), $i,j \in S$ in network configuration $c \in C$
A_h^c	The set of arcs in the network representing connectivity between the headquarters location and satellites capable of immediate data-link with the headquarters location, inducing directed arcs $(h,i), h \in \{h\}, i \in S$ in network configuration $c \in C$
A_r^c	The set of arcs in the network representing connectivity between satellites and the regions of interest informed by a satellite's immediate coverage, inducing directed arcs $(i,r), i \in S, r \in R$ in network configuration $c \in C$
$A_{i_s}^c$	The set of arcs associated with the artificial sink node establishing arcs between the region of interest nodes and the sink node, as well as the sink node to the headquarters node. Inducing (r,i_s) and (i_s,h), $r \in R$,$i_s \in \{i_s\}$, and $h \in \{h\}$ in network configuration $c \in C$
$A^c = A_s^c \cup A_h^c \cup A_r^c \cup A_{i_s}^c$	Set of all arcs in network configuration $c \in C$
$G^c(N, A^c)$	The satellite constellation network when all satellites are functioning in network configuration $c \in C$

Table 20: Dynamic Program Symbol Description (Parameters)

Symbol	Description
Γ	The maximum number of satellite failures (interdictions)
u_{ij}^c	The maximum flow through arc $(i,j) \in A$ in network configuration $c \in C$
v^c	Time weight provided to $G^c(N, A^c)$

Table 21: Dynamic Program Symbol Description (Decision Variables)

Symbol	Description
γ_i	Binary decision variable equal to 1 if interdicts node $i \in N$, and 0 otherwise
x_{ij}^c	Non-negative decision variable representing (communications) flow between any pair of nodes $(i,j) \in A^c$
β_{ij}^c	Binary decision variable indicating if arc $(i,j) \in A^c$ is limiting flow through the network, and 0 otherwise

Using the sets, parameters, and variable definitions defined in Tables Table 19-21, the following formulation models the dynamic network interdiction problem.

$$\min_{\boldsymbol{\gamma},\boldsymbol{\alpha},\boldsymbol{\beta}} \quad \frac{1}{\sum_{c\in C} v^c} \sum_{c\in C} \left(v^c \sum_{(i,j)\in A\setminus\{(i_s,h)\}} u_{ij}^c \beta_{ij}^c \right) \tag{80}$$

$$\text{s.t.} \quad \alpha_i^c - \alpha_j^c + \beta_{ij}^c + \gamma_i \geq 0, \quad \forall (i,j) \in A^c \setminus \{(i_s,h)\}, c \in C, \tag{81}$$

$$\alpha_{i_s}^c - \alpha_h^c \geq 1, \quad \forall c \in C, \tag{82}$$

$$\gamma_i = 0, \quad \forall i \in N \setminus S, \tag{83}$$

$$\sum_{i\in N} \gamma_i \leq \Gamma, \tag{84}$$

$$\beta_{ij}^c \in \{0,1\}, \quad \forall (i,j) \in A^c \setminus \{(i_s,h)\}, c \in C, \tag{85}$$

$$\alpha_i^c \in \{0,1\}, \quad \forall i \in N, c \in C, \tag{86}$$

$$\gamma_i \in \{0,1\}, \quad \forall i \in N, \tag{87}$$

for which Equation (88) defines the u_{ij}^c-parameters.

$$u_{(i,j)}^c = \begin{cases} |R| & i \notin R \\ 1 & i \in R \end{cases} \quad \forall c \in C \tag{88}$$

Objective function (80) minimizes the weighted average of flow through the network. Constraints (81) and (82) correspond to Constraints (74) and (75) for each network configuration. Constraints (83) and (84) limit the number of satellite failures. Satellite failures are independent of the satellite configuration. Finally, Constraints

(85)-(87) ensure that all the decision variables remain binary decision variables.

5.2.3 Analyzing Sunlight Exposure

Thus far, discussion has focused on procedures to design a communications satellite network to cover regions of interest with a minimal number of satellites, followed by models to assess the robustness of the network. Also of interest is the sunlight exposure to satellite constellations. This characteristic is important to assess because satellite functionality depends on a reliable source of energy.

This research examines sunlight exposure to satellite constellations using the following assumptions. First, the subsatellite direction of each satellite remains normal to the surface of the Earth. Second, each satellite uses fixed solar panels that remain perpendicular to the subsatellite direction (i.e., parallel to the plane tangent to the Earth's surface). Third, the solar panels capture sunlight on both sides of the panels (bifacial solar panels).

The angle sunlight hits solar panels changes its intensity of exposure. Equation (89) measures this intensity, $\eta(t)$, of sunlight provided to a satellite at time t by checking its angle of exposure. The unit vector $\boldsymbol{s}_{sunlight}(t)$ represents the sunlight direction and the unit vector $\boldsymbol{n}(t)$ represents the direction normal to the surface of the solar panels on a satellite at time t.

$$\eta(t) = \begin{cases} |\boldsymbol{s}_{sunlight}(t) \cdot \boldsymbol{n}(t)| & \text{Satellite is exposed to sunlight at time } t \\ 0 & \text{Otherwise} \end{cases} \tag{89}$$

5.3 Illustrative Examples

Several examples compare the performance of the presented asymmetric satellite constellation design framework that ensures all satellites follow a common repeating ground track against the performance of a symmetric satellite constellation design

framework. The performance of each constellation considers its number of satellites, its robustness to satellite failures, and its average sun exposure experienced over a calendar year.

Walker constellations establish the symmetric constellation performance benchmarks in each example. Six parameter $P/S/F$, a, δ, and Ω_0^{ref} define Walker constellations. The triplet $P/S/F$ represent the number of equally spaced orbital planes, the number of equally spaced satellites within each plane, and the inter-satellite spacing between adjacent planes, respectively. The parameters a, δ, and Ω_0^{ref} represent the semi-major axis, the common orbital inclination, and the right ascension of the ascending node of the reference satellite, respectively. A genetic algorithm [163] provided by MATLAB [173] minimizes the number of satellites each Walker constellation uses to maintain continuous coverage to all locations of interest in each example.

Problem Scenario

In each example, the satellite constellations attempt to maintain continuous connectivity between a headquarters location (ground terminal) and a region of interest. Each example uses the same headquarters location but different regions of interest to examine the impact of relative coordinate positioning on the ability of satellite constellations to maintain the desired connectivity between the locations. Each example uses Dayton, Ohio (OH) as the headquarters location and one or more discretized representations of countries as the region of interest. The discretized representation of each country (excluding Australia) uses approximately 1^o meshgrid sampling to represent its respective region. The discretized representation of Australia uses approximately 2^o meshgrid sampling to help manage the size of the mathematical programs used for its analysis.

The following assumptions define connectivity in each example. A satellite provides connectivity to a point on the Earth's surface (i.e., the headquarters location or

regions of interest) when the satellite exists above an elevation angle of 35^o relative to the plane tangent to the spherical Earth's surface intersecting the point. Intersatellite connectivity becomes available between two satellites when a direct line-of-sight exists between the satellites above approximately 100 km of atmosphere (a radius of approximately 6478 km from the center of the Earth).

The following two assumptions apply to the design and analysis of satellite constellations in each example. First, semi-major axis values remain under 35,000 km to ensure that all satellites remain in either low Earth orbit or medium Earth orbit. Second, the analysis disregards the impact of environmental factors on the performances of the satellite constellations. These factors include the effect of latency, as well as the environmental hazards posed by the Van Allen radiation belts commonly experienced by satellites in medium Earth orbit [13]. This analysis also disregards additional drawbacks associated with higher orbits, including higher power antennas required for communications or larger optics required to achieve desired resolutions.

Examples: Number of Satellites

Tables 22 and 23 list the satellite constellations designed for each example. Table 22 identifies the number of satellites and the repeating ground track used to design each common repeating ground track constellation. Algorithm 2 designs the common repeating ground track constellations in each example. Table 23 identifies the corresponding Walker constellation designs.

Table 22: Common Repeating Ground Tracks used for Constellations

Example	**L**	**M**	**a (km)**	**i (degrees)**	**λ_0 (degrees)**	**Number of Satellites**
Ecuador	4	3	34,808	6.6	28.3	6
Falkland Islands	4	3	34,804	85.9	70.2	7
Uruguay	4	3	34,804	75.9	61.6	7
Norway	4	3	34,804	86.1	73.4	7
Egypt	3	2	32,177	49	61	8
Kenya	2	1	26,562	33.1	50.8	6
Madagascar	2	1	26,562	34.7	57.4	6
Malaysia	2	1	26,562	37.3	50.9	6
New Zealand	2	1	26,561	102.1	127.9	7
Japan	2	1	26,561	104.6	169.9	7
Australia	2	1	26,562	33	19.6	6
SKJMP*	2	1	26,561	40.7	79.7	6

*South Korea, Japan, Malaysia, Philippines

Table 23: Walker Constellations

Example	**S**	**P**	**F**	**a (km)**	**i (degrees)**	**Ω_0^{ref} (degrees)**	**Number of Satellites**
Ecuador	7	1	0	34,246	179.9	114.7	7
Falkland Islands	4	2	1	34,140	51.6	10.6	8
Uruguay	7	1	0	34,856	0.1	6.5	7
Norway	5	2	1	33,491	115.5	64.5	10
Egypt	1	7	0	34,976	180	359.2	7
Kenya	7	1	0	34,992	180	360	7
Madagascar	7	1	0	34,988	179.9	0.5	7
Malaysia	1	7	0	34,864	0.2	356.3	7
New Zealand	3	3	0	34,702	122.1	294.9	9
Japan	5	2	0	28,985	146	19.3	10
Australia	5	2	1	30,426	33.5	304.6	10
SKJMP*	5	2	0	32,731	32.2	83	10

*South Korea, Japan, Malaysia, Philippines

The orbital inclinations used in the common repeating ground track constellations range from approximately 6.6^o to 104.6^o. Roughly half of the Walker constellations use near-equatorial orbits (inclinations of approximately 0^o or 180^o). It appears that the common repeating ground track constellations use higher inclinations than the Walker constellations. Two factors may account for this difference. First, the design method for the common repeating ground track constellation selects a repeating ground track to maximize the minimum coverage provided to any of the regions of interest using a single satellite. This criteria rewards the ground tracks that pass near the regions of interest, resulting in equal consideration of all regions regardless of latitude. The

selected repeating ground track must balance regions both near and far from the equator. In contrast, the design of the Walker constellations only considers the ability of the entire constellation to provide coverage to the regions of interest. The Walker constellation design method does not provide equal consideration to all regions of interest, so long as it achieves continuous coverage. Second, the combination of a moderately low elevation angle of 35^o and large semi-major axis values up to 35,000 km allows the Walker constellation to use near-equatorial orbits. This combination allows satellite coverage to span large surfaces of the Earth, removing the need to use inclined orbits. The use of equatorial orbits would likely diminish as either the elevation angle increases or the limit on the semi-major axis decreases.

The common repeating ground track constellation uses fewer satellites than the Walker constellation in 10 of the 12 examples and uses the same number of satellites in one of the examples. The Walker constellation only uses fewer satellites than the common repeating ground track constellation in one of the examples. This suggests that the added flexibility of asymmetric satellite constellation design frameworks may help reduce the number of satellites used in constellations.

Examples: Satellite Constellation Robustness

The ability of each satellite constellation to maintain continuous connectivity between the headquarters location and its region of interest under an increasing number of satellite failures acts as a measure of its robustness. The number of satellite failures used to evaluate each constellation begins with zero failures to measure the performance of fully-functional satellite constellations. The number of satellite failures increases until every satellite fails within the constellation. The specific combination of satellite failures used to optimally degrade the performance of a satellite constellation is independent of previous combinations of failures used on the same constellation (i.e., satellite constellations reset to full functionality prior to considering each number

of satellite failures).

Figures 34-36 show a few examples of the average remaining connectivity each satellite constellation maintains between the the headquarters location and the region of interest before and after satellite failures degrade the network. Figures 39-47 in the Appendix show this network degradation for the remaining examples. Table 24 provides summary statistics on the differences of the common repeating ground track constellations against the baseline Walker constellations for each considered number of satellite failures. The maximum, average, and minimum represent the largest difference, the average difference, and the minimum difference in the proportion of regions of interest observed with communications connectivity to the headquarters location for any number of satellite failures.

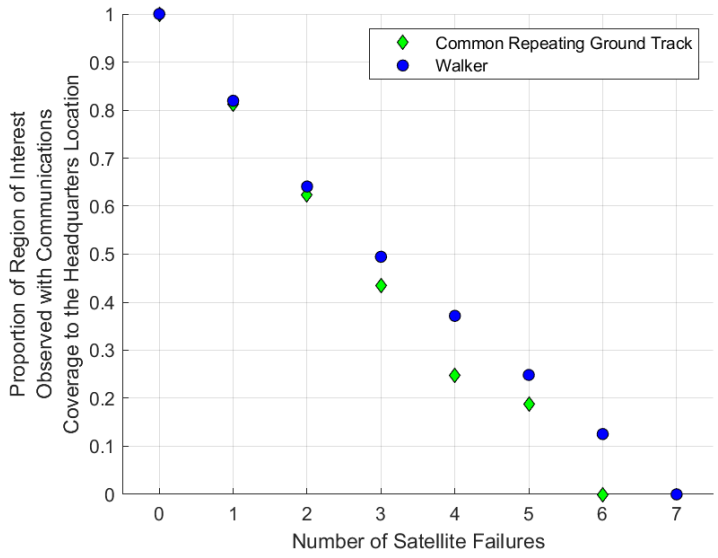

Figure 34: Example: Dayton, OH - Ecuador, Under 35,000 km (Semi-Major Axis) Comparing Communications Survivability
Common Repeating Ground Track = 6 total satellites; Walker = 7 total satellites

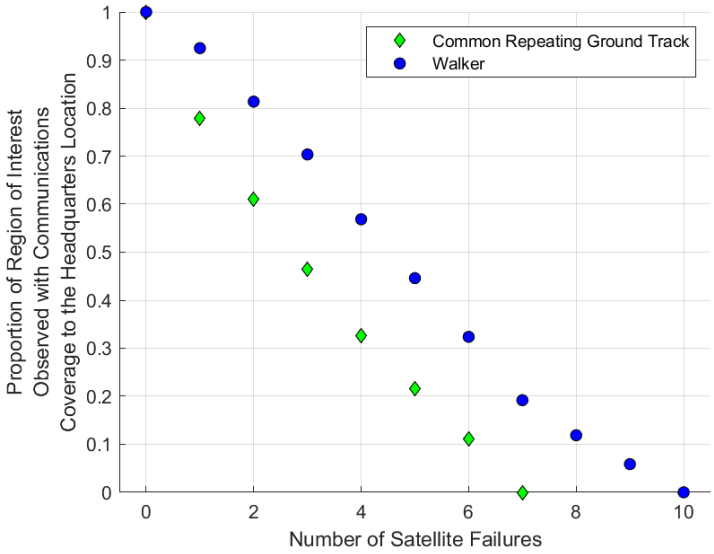

Figure 35: Example: Dayton, OH - Norway, Under 35,000 km (Semi-Major Axis) Comparing Communications Survivability
Common Repeating Ground Track = 7 total satellites; Walker = 10 total satellites

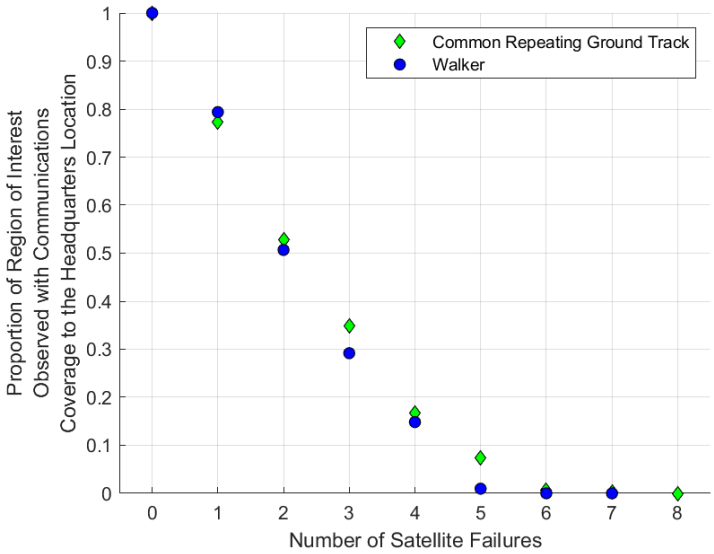

Figure 36: Example: Dayton, OH - Egypt, Under 35,000 km (Semi-Major Axis) Comparing Communications Survivability
Common Repeating Ground Track = 8 total satellites; Walker = 7 total satellites

Figures 34-36 and Figures 39-47 in the Appendix show all fully functional satellite constellations provide continuous or near-continuous connectivity between the head-

Table 24: Relative Performance of Satellite Constellations for Each Number of Satellite Failures (Common Repeating Ground Track Constellation - Walker Constellation)

Example	**Number of Satellite Savings**	**Relative Difference (%) in Satellite Constellation Performance over the Range of Satellite Failures**		
		Max.	**Avg.**	**Min.**
Ecuador	-1	0.00	-0.05	-0.13
Falkland Islands	-1	0.00	-0.07	-0.20
Uruguay	0	0.00	-0.10	-0.19
Norway	-3	0.00	-0.15	-0.24
Egypt	1	0.06	0.02	-0.02
Kenya	-1	0.00	-0.11	-0.28
Madagascar	-1	0.00	-0.09	-0.24
Malaysia	-1	0.00	-0.09	-0.29
New Zealand	-2	0.00	-0.10	-0.26
Japan	-3	0.00	-0.12	-0.34
Australia	-4	0.00	-0.14	-0.37
SKJMP	-4	0.00	-0.13	-0.44
Average	-1.67	0.01	-0.09	-0.25

quarters location and its region of interest. Differences in the robustness between the two constellation frameworks becomes apparent in the presence of satellite failures. The connectivity maintained by the common repeating ground track constellations degrade faster than the connectivity provided by the Walker constellations in all but one example. Figure 36 shows the similar degradation rate of the common repeating ground track constellation and the Walker constellation in the example of providing connectivity between Dayton, OH, and Egypt.

Table 24 provides summary statistics comparing the relative performance of the common repeating ground track constellations against the Walker constellations over the range of disruptions. The relative data uses the Walker constellation as the baseline constellation (i.e., the performance metric of the Walker constellation is subtracted from the performance metric of the common repeating ground track constellation). Most of the maximum relative values are 0 and the averages are negative, indicating that the common repeating ground track constellation rarely performs better than the Walker constellation for any number of satellite failures. The relative performance of the common repeating ground track constellation was similar to the

Walker constellation in a single example (the example using Egypt as the region of interest). Therefore, the Walker constellations appear more robust than the common repeating ground track constellations; the Walker constellations provide an average of approximately 9% more communications connectivity between the headquarters location and the region of interest than the common repeating ground track constellations for any number of satellite failures. The use of fewer satellites by the common repeating ground track constellation likely makes it less robust than the Walker constellations that tend to use more satellites.

Examples: Sunlight Exposure

Investigating the sun exposure received by satellites provides insights into the reliability of energy available to satellites throughout different seasons of the year. Such consideration of energy availability will inform engineering requirements for satellite design. The daily average intensity of sun exposure for each satellite informs the exposure of the entire constellation. Figure 37-38 show two examples of the average intensity of sunlight exposure of satellites in the constellation, as well as the minimum daily average intensity of sunlight experienced by any of the satellites in the constellation throughout the year. Figures 48-57 in the Appendix show the sunlight exposure of the satellites in the remaining satellite constellations. To summarize the results in Figures 37-38 and Figures 48-57 in the Appendix, Tables 25 and 26 list the average and minimum daily average intensity of sunlight experienced by the satellite constellations on March 20th and June 21st, which correspond to vernal equinox and the summer solstice, respectively.

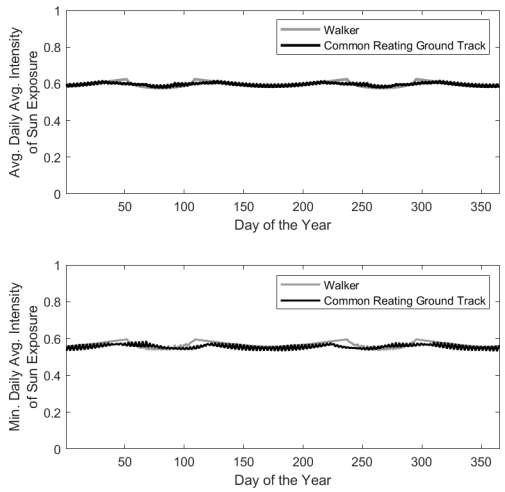

Figure 37: Example: Dayton, OH - Ecuador, Under 35,000 m (Semi-Major Axis)
Daily Average Sun Exposure to Satellite Constellation

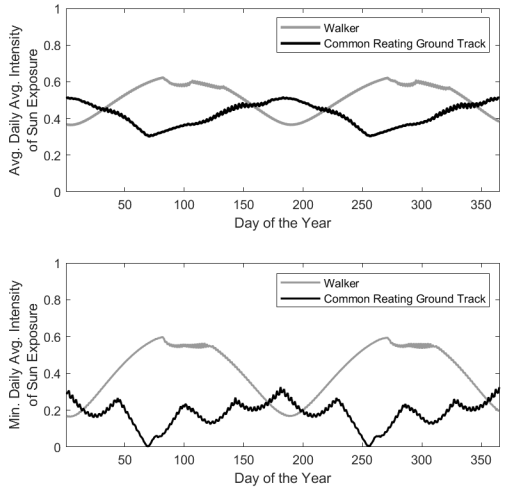

Figure 38: Example: Dayton, OH - Falkland Islands, Under 35,000 m (Semi-Major Axis)
Daily Average Sun Exposure to Satellite Constellation

Table 25: Average Daily Average Intensity of Sun Exposure of Satellites in the Satellite Constellation

	Walker		**Common Repeating Ground Track**	
Example	**March 20**	**June 21**	**March 20**	**June 21**
Ecuador	0.58	0.58	0.58	0.58
Falkland Islands	0.62	0.41	0.32	0.49
Uruguay	0.58	0.58	0.47	0.45
Norway	0.34	0.57	0.37	0.46
Egypt	0.58	0.58	0.52	0.59
Kenya	0.58	0.58	0.58	0.52
Madagascar	0.58	0.58	0.57	0.52
Malaysia	0.58	0.58	0.56	0.52
New Zealand	0.48	0.51	0.41	0.43
Japan	0.6	0.47	0.4	0.46
Australia	0.58	0.51	0.58	0.52
SKJMP	0.54	0.6	0.56	0.51

Table 26: Minimum Daily Average Intensity of Sun Exposure of Any Satellite in the Constellation

	Walker		**Common Repeating Ground Track**	
Example	**March 20**	**June 21**	**March 20**	**June 21**
Ecuador	0.56	0.56	0.55	0.56
Falkland Islands	0.59	0.23	0.06	0.26
Uruguay	0.56	0.55	0.24	0.21
Norway	0.33	0.54	0.05	0.21
Egypt	0.55	0.55	0.42	0.56
Kenya	0.55	0.55	0.54	0.35
Madagascar	0.54	0.55	0.52	0.34
Malaysia	0.54	0.55	0.51	0.31
New Zealand	0.41	0.48	0.14	0.17
Japan	0.56	0.35	0.18	0.13
Australia	0.55	0.44	0.53	0.38
SKJMP	0.53	0.58	0.48	0.32

The following observations regarding sunlight exposure relates the satellite constellation information in Tables 22-23 to the results in Figures 37-38, Figures 48-57 in the Appendix, and Tables 25-26. First, the time of year impacts the average intensity of sun exposure experienced by the satellite constellations due to the change in the relative positioning of the sun and Earth.

Second, orbital inclination amplifies the impact of the seasons on sunlight exposure

experienced by the satellite constellations. The satellite constellations using high-inclination orbits experience greater fluctuations in daily average intensity of sunlight exposure than the constellations using orbits with low-inclination orbits. A two-sample t-test shows a significant difference exists between the average of the variances of sunlight exposure to satellite constellations using high-inclination orbits ($45^o - 135^o$) and low-inclination orbits throughout the year with a p-value of approximately 0.026. Therefore, the common repeating ground track constellations *appear* to experience more sunlight exposure variability than the Walker constellations throughout the year because they tend to use a more highly-inclined orbits than the Walker constellations (6 of the common repeating ground track constellations use inclinations between $45^o - 135^o$, while only 3 Walker constellations use inclinations between $45^o - 135^o$).

Third, orbital inclination also influences the minimum daily average intensity of exposure experienced by any of the satellites in the constellation. Satellites in constellations using highly-inclined orbits will remain nearly perpendicular to the direction of sunlight occasionally throughout the year, resulting in low sunlight exposure. In contrast, satellites in constellations using low inclinations will always remain relatively aligned with the sunlight direction each day throughout the year. Therefore, the common repeating ground track constellations experience more variability of daily average intensity of sunlight throughout the year, as well as more satellites that receive near-zero (< 0.1) exposure to sunlight occasionally throughout the year than the Walker constellations because they tend to use more highly-inclined orbits than the Walker constellations in each of the examples. In the examples, none of the satellites in the Walker constellations received less than a daily-average minimum exposure of 0.1 any time throughout the year, while five of the common repeating ground track constellations had satellites receiving less than a daily average minimum exposure of 0.1 multiple times throughout the year. Using the data presented in Tables 25-26, the

p-values associated with paired t-tests on the difference between the average-intensity and minimum-intensity of exposure provided to the Walker and common repeating ground tack constellations were approximately 0.033 and 0.009, respectively, further demonstrating a significant difference between the sun exposure experienced by the two constellations.

5.4 Conclusion

This research investigates the performance of an asymmetric "string-of-pearls" common repeating ground track constellation design framework. Three metrics evaluate the performance of the satellite constellation design framework: the number of satellites used to establish continuous regional coverage, the constellation's ability to maintain connectivity between a headquarters location and its region of interest in the presence of satellite failures (i.e., robustness), and the daily average exposure to sunlight. This research presents a heuristic focused on minimizing the number of satellites used in an asymmetric string of pearls constellation to provide continuous regional coverage, as well as a network interdiction model to identify the worst-case degradation inflicted onto the satellite network given specified numbers of satellite failures.

Several illustrative examples compare the performance of asymmetric "string-of-pearls" common repeating ground track constellations designed using the presented heuristic against the performance of baseline Walker constellations in medium Earth orbit. The asymmetric design aspect of the string-of-pearls constellation enables it to use fewer satellites than the Walker constellation to maintain continuous connectivity between the headquarters location and its region of interest. However, the use of fewer satellites makes the asymmetric string-of-pearls constellation less robust to satellite failures than the Walker constellation. Additionally, the asymmetric string-

of-pearls constellations tends to use orbits with higher inclinations than the Walker constellation, resulting in greater variability of sunlight exposure throughout the year.

Future research should examine the performance differences between these two satellites constellation design frameworks in low Earth orbit. Additionally, more efficient design methods for the asymmetric common repeating ground track constellations, as well as generalizing the methods to include elliptical orbits will benefit the satellite constellation design process. Future research should also include the effects of latency into the calculations evaluating the robustness of the satellite networks.

5.5 Appendix

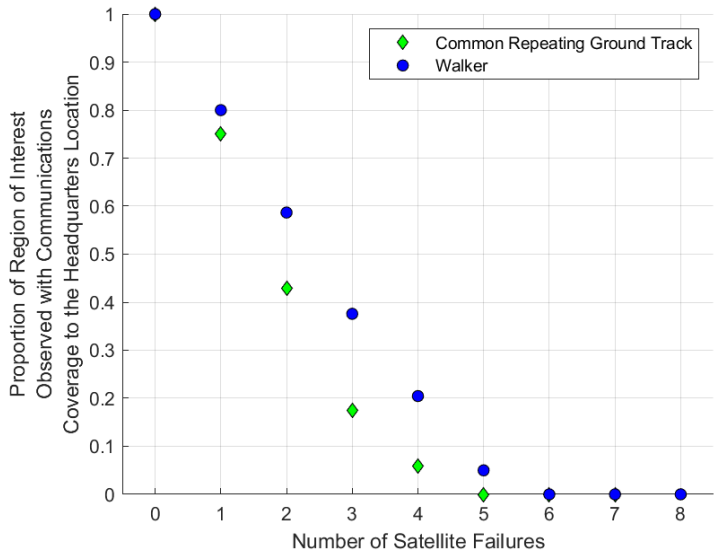

Figure 39: Example: Dayton, OH - Falkland Islands, Under 35,000 km (Semi-Major Axis)
Comparing Communications Survivability
Common Repeating Ground Track = 7 total satellites; Walker = 8 total satellites

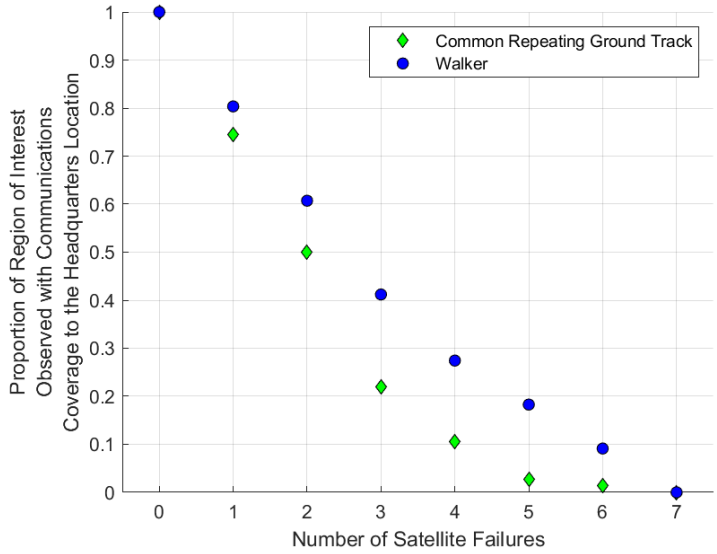

Figure 40: Example: Dayton, OH - Uruguay, Under 35,000 km (Semi-Major Axis) Comparing Communications Survivability
Common Repeating Ground Track = 7 total satellites; Walker = 7 total satellites

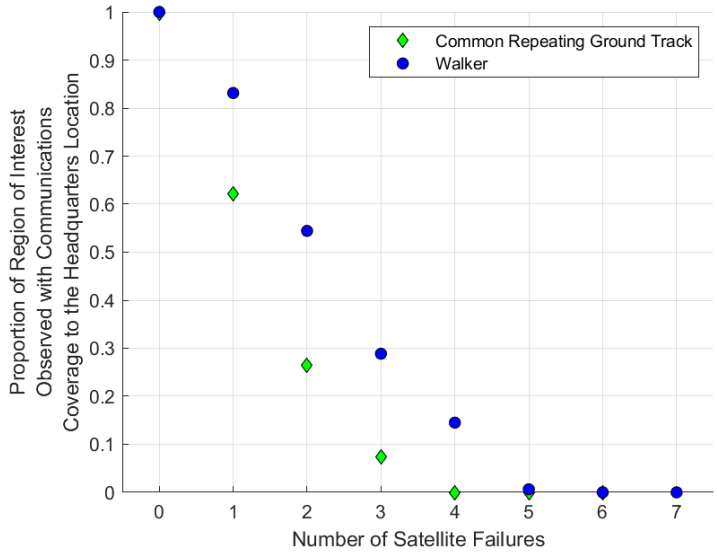

Figure 41: Example: Dayton, OH - Kenya, Under 35,000 km (Semi-Major Axis) Comparing Communications Survivability
Common Repeating Ground Track = 6 total satellites; Walker = 7 total satellites

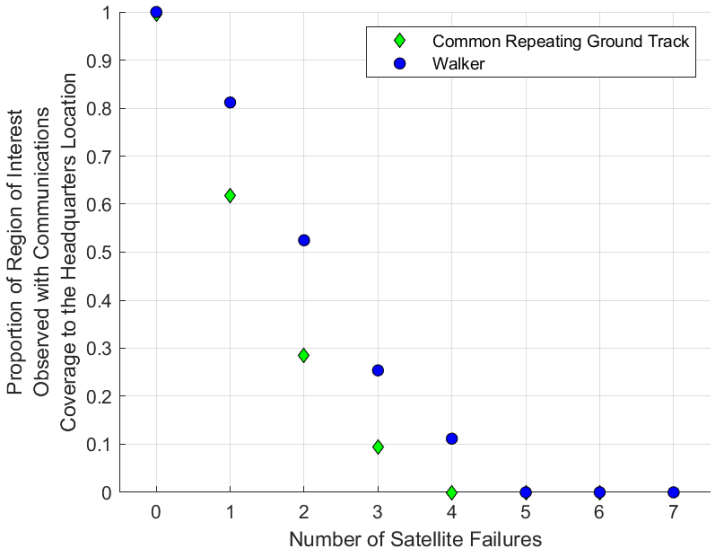

Figure 42: Example: Dayton, OH - Madagascar, Under 35,000 km (Semi-Major Axis) Comparing Communications Survivability
Common Repeating Ground Track = 6 total satellites; Walker = 7 total satellites

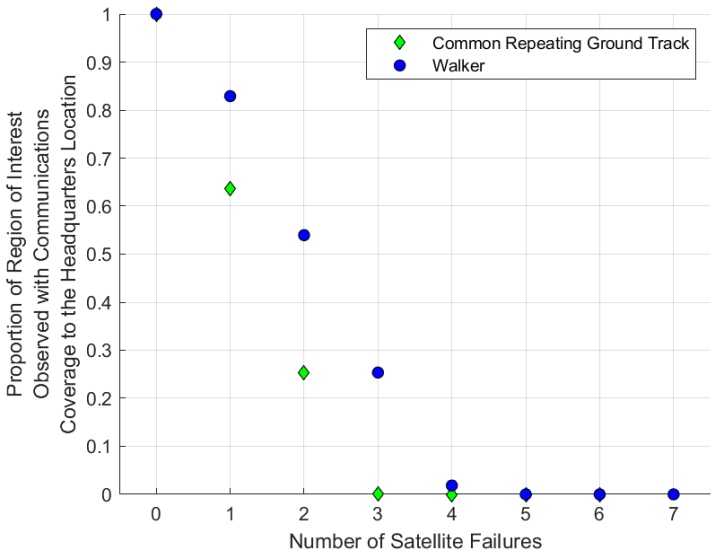

Figure 43: Example: Dayton, OH - Malaysia, Under 35,000 km (Semi-Major Axis) Comparing Communications Survivability
Common Repeating Ground Track = 6 total satellites; Walker = 7 total satellites

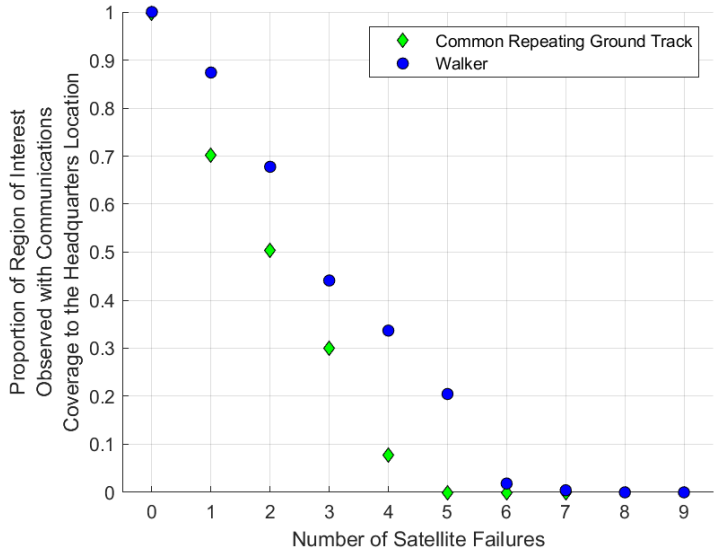

Figure 44: Example: Dayton, OH - New Zealand, Under 35,000 km (Semi-Major Axis)
Comparing Communications Survivability
Common Repeating Ground Track = 7 total satellites; Walker = 9 total satellites

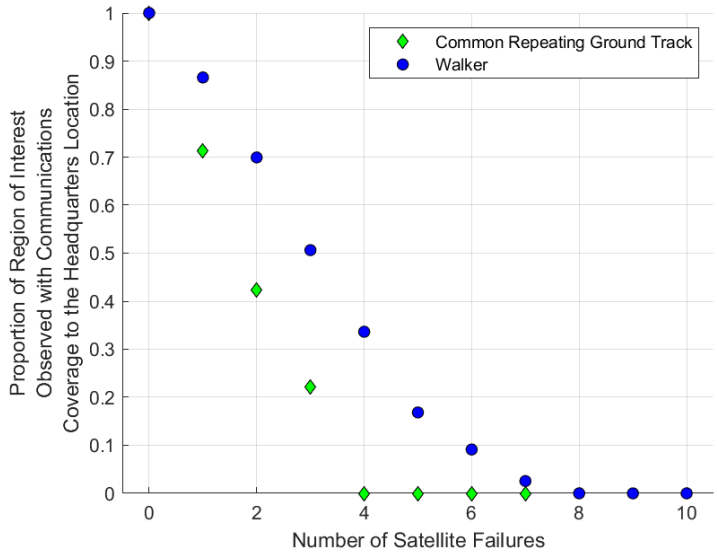

Figure 45: Example: Dayton, OH - Japan, Under 35,000 km (Semi-Major Axis)
Comparing Communications Survivability
Common Repeating Ground Track = 7 total satellites; Walker = 10 total satellites

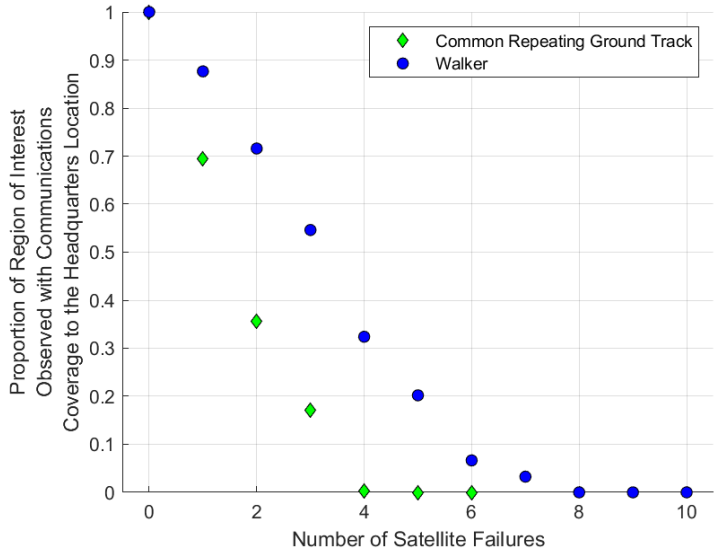

Figure 46: Example: Dayton, OH - Australia, Under 35,000 km (Semi-Major Axis) Comparing Communications Survivability
Common Repeating Ground Track = 6 total satellites; Walker = 10 total satellites

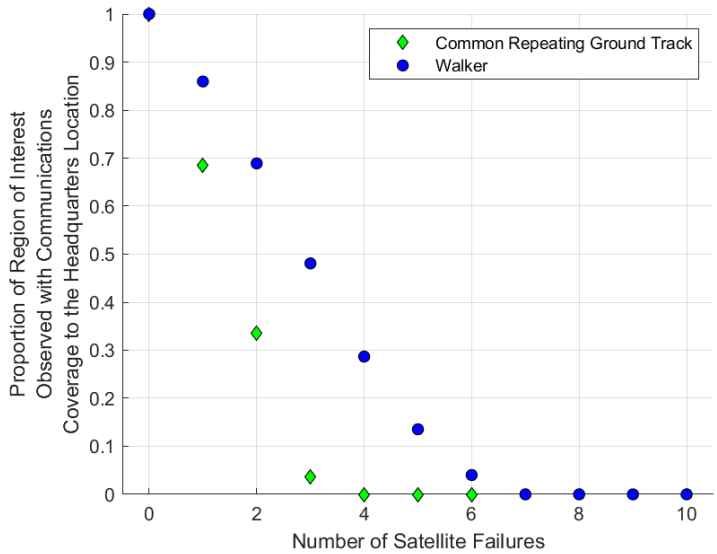

Figure 47: Example: Dayton, OH - South Korea Japan Malaysia Philippines, Under 35,000 km (Semi-Major Axis)
Comparing Communications Survivability
Common Repeating Ground Track = 6 total satellites; Walker = 10 total satellites

Daily Average Sun Exposure

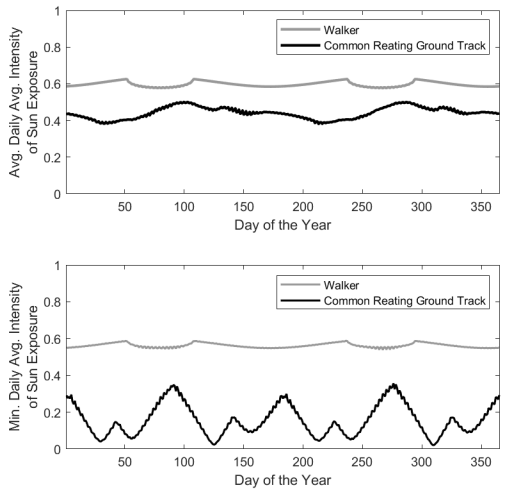

Figure 48: Example: Dayton, OH - Uruguay, Under 35,000 m (Semi-Major Axis) Daily Average Sun Exposure to Satellite Constellation

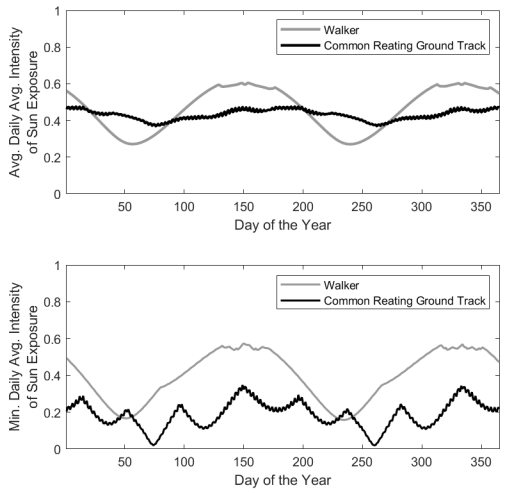

Figure 49: Example: Dayton, OH - Norway, Under 35,000 m (Semi-Major Axis) Daily Average Sun Exposure to Satellite Constellation

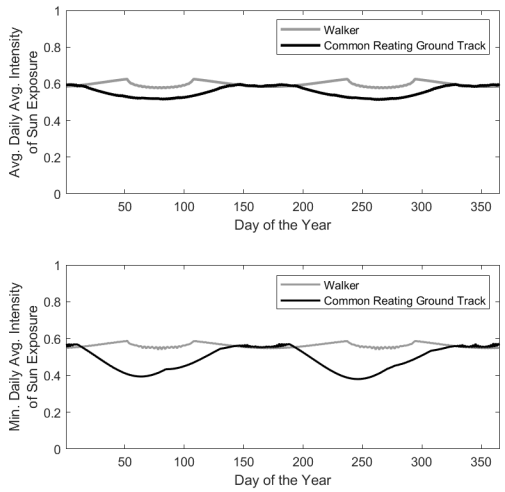

Figure 50: Example: Dayton, OH - Egypt, Under 35,000 m (Semi-Major Axis) Daily Average Sun Exposure to Satellite Constellation

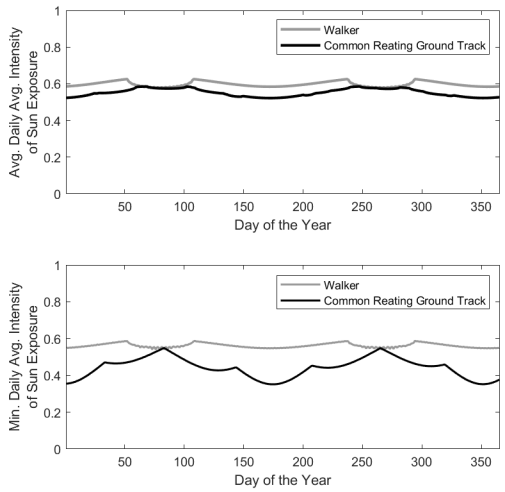

Figure 51: Example: Dayton, OH - Kenya, Under 35,000 m (Semi-Major Axis) Daily Average Sun Exposure to Satellite Constellation

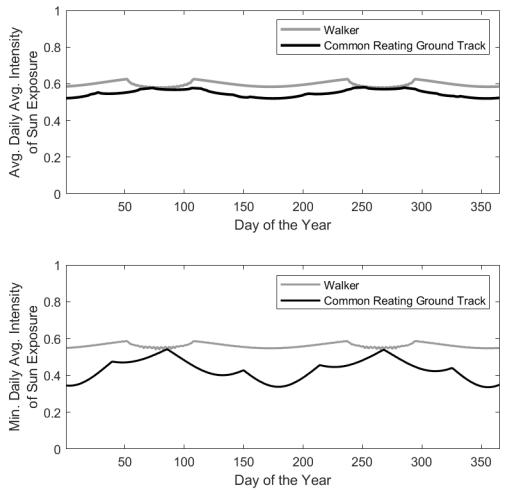

Figure 52: Example: Dayton, OH - Madagascar, Under 35,000 m (Semi-Major Axis) Daily Average Sun Exposure to Satellite Constellation

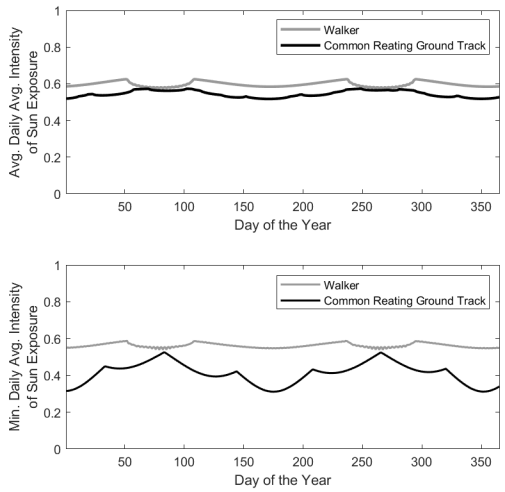

Figure 53: Example: Dayton, OH - Malaysia, Under 35,000 m (Semi-Major Axis) Daily Average Sun Exposure to Satellite Constellation

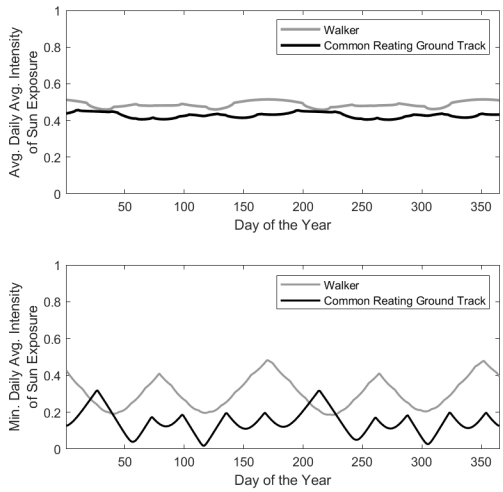

Figure 54: Example: Dayton, OH - New Zealand, Under 35,000 m (Semi-Major Axis) Daily Average Sun Exposure to Satellite Constellation

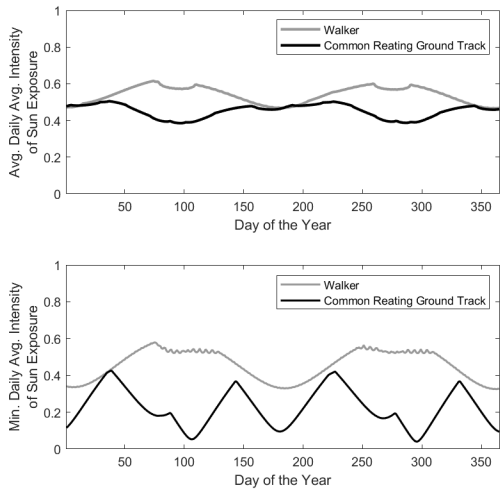

Figure 55: Example: Dayton, OH - Japan, Under 35,000 m (Semi-Major Axis) Daily Average Sun Exposure to Satellite Constellation

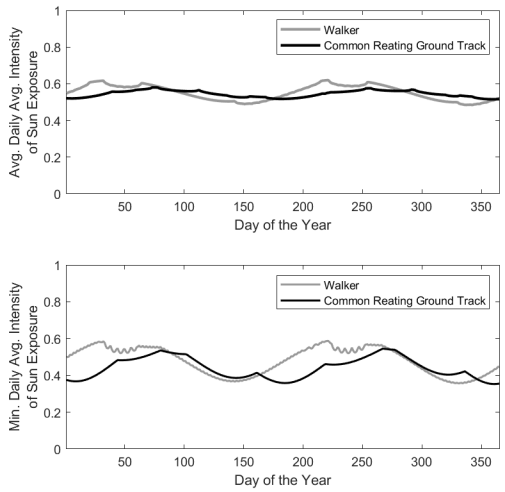

Figure 56: Example: Dayton, OH - Australia, Under 35,000 m (Semi-Major Axis) Daily Average Sun Exposure to Satellite Constellation

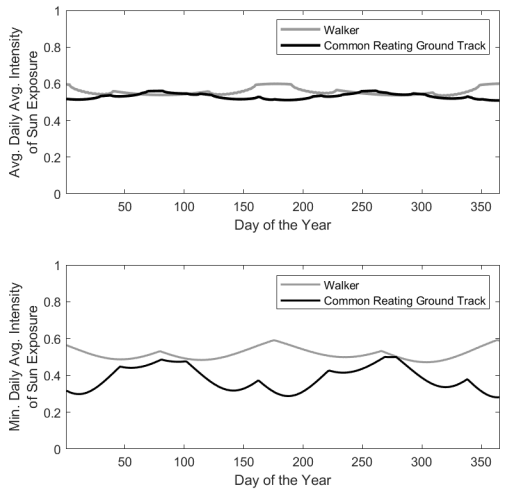

Figure 57: Example: Dayton, OH - South Korea Japan Malaysia Philippines, Under 35,000 m (Semi-Major Axis)
Daily Average Sun Exposure to Satellite Constellation

VI. Conclusion

This dissertation considers the problem of 'optimal' satellite constellation design. Satellite constellation design often relies on predefined geometric frameworks to simplify the design problem. However, using predefined geometric frameworks raises the question: *which geometric framework performs best for each mission set?* This research leverages simulations, metaheuristics, and mathematical programming techniques to help address this question for regional Earth-observation missions by focusing on the following main research questions.

1. What is an appropriate construct to better understand the satellite constellation design literature with a focus on frameworks and methods presented?

2. What orbit allows for a single satellite to best provide Earth-observation coverage to one or more distinct regions?

3. What is the best satellite constellation design for Earth-observation missions of one or more distinct regions?

This research is of interest to satellite constellation designers and researchers. The organization of the satellite constellation design literature directs designers to specific design methods and identifies potential research opportunities to researchers. The developed metaheuristics and procedures support satellite constellation design and research processes. Finally, the analysis of the performance of the investigated satellite constellation design frameworks informs designers about their potential utility for certain mission sets.

6.1 Conclusions

Chapter II addresses the first major research question by investigating the satellite constellation design literature. An abundant amount of literature exists examining different factors of satellite constellation design. Organizing the literature in an appropriate manner improves its benefit to the satellite constellation design community by directing designers to specific design approaches and identifying potential research opportunities.

Chapter II makes the following contributions. First, it presents a novel topology approach to analyze the current state of the satellite constellation design literature. Second, it organizes and discusses some of the most cited literature according to the topology's classification scheme. Finally, it maps articles in the satellite constellation design literature to a topology for better understanding of the state of the art and state of practice.

Chapter III addresses the second major research question by examining the problem of optimal orbit selection. The chapter focuses on the selecting the circular repeating ground track orbit that maximizes the coverage provided to a region of interest using a single satellite. The example provided in the this chapter focuses on selecting a circular repeating ground track orbit to provide coverage to a discretized representation of New Zealand.

Chapter III makes the following contributions. First, it develops a customized metaheuristic for designing an optimal circular repeating ground track orbit for a single satellite focused on maximizing the satellite's coverage to a region of interest. The metaheuristic applies a methodical application of designed experiments and response surface analysis to explore the orbital design space. Second, it evaluates its performance against the performance of a genetic algorithm, a simulated annealing approach, and particle swarm optimization. The results suggest that the metaheurstic

is more computationally efficient than the genetic algorithm and simulated annealing approaches, and achieves comparable quality solutions as all three of these baseline methods.

Chapter IV addresses the second major research question by examining the problem of modifying existing non-repeating ground track orbits into repeating ground track orbits. Such non-repeating ground track orbits may exist conceptually in design methods, or may have been an existing orbit that became perturbed. Although the satellite constellation design literature presents methods capable of optimally converting non-repeating ground track orbits into repeating ground track orbits, the methods rely on *a priori* knowledge about the desired repeating parameters of the repeating ground track. This chapter address the scenario where the desired repeating parameters of the repeating ground track are unknown prior to orbit modification.

Chapter IV makes the following contributions. First, it presents a objective metric capable of quantifying the similarities between two ground tracks. Using the objective metric directly can be computationally expensive since it is evaluated using simulations. Second, it presents an alternative objective metric and procedure to identify the repeating ground track that most resembles the ground track of the non-repeating ground track orbit via geometric adjustment minimization. The presented procedure is computationally efficient and foregoes the need for simulations. Third, several illustrative examples demonstrate the procedure appropriately identifies the repeating ground track most resembling a non-repeating ground track.

Chapter V addresses the third major research question by examining the performance of two satellite constellation design frameworks, asymmetric "string-of-pearls" and the Walker-delta approaches, using several illustrative examples. The satellite constellations focus on providing continuous coverage to a headquarters location and a region of interest using the minimum number of satellites. A single point represents

the headquarters location and discretized representations of one or more country define the regions of interest. The objective of the satellite constellations is to maintain continuous connectivity between the headquarters location and its regions of interest. The satellite constellations are evaluated considering the number of satellites required to provide continuous regional coverage, their ability to maintain continuous connectivity between the headquarters location and its regions of interest in the presence of satellite failures, and the average exposure to sunlight throughout the year.

Chapter V makes the following contributions. First, it presents a heuristic to design asymmetric "string-of-pearls" common repeating ground track constellations focusing on providing continuous regional coverage using the fewest number of satellites. Second, it presents a mathematical program modeling the dynamic satellite network interdiction problem to identify the worst-case degradation to the satellite network in the presence of a specified number of satellite failures. Third, several illustrative examples compare the performance of the asymmetric "string-of-pearls" constellation framework against a Walker-delta constellation framework considering the number of satellites used, the robustness of the constellation, as well as the average exposure to sunlight throughout the year.

6.2 Recommendations for Future Research

Although the research in this dissertation provides useful insights into satellite constellation design, several opportunities exist for future development. Many of these potential improvements address the following research assumptions.

First, the model of the field of regard of a satellite uses a conic section that remains normal to the Earth, resulting in circular satellite coverage. Investigating different shapes of satellite coverage would expand the applicability of this research. Second, a satellite simultaneously provides coverage to all locations within its field

of regard. Modeling a more realistic field of view would improve the realism of the research. Third, the model of sensor coverage considers a spherical Earth. Incorporating geographic shielding into the model, as well as the oblate shape of the Earth, into the sensor coverage models would make the simulations more realistic. Fourth, the orbital models only consider perturbations due to the oblate shape of the Earth. Effects from other environmental factors, such as atmospheric drag at low altitudes, the effects of latency in communications, or hazards from the Van Allen radiation belts, are assumed to be absent. Such assumptions further reduce the realism of the simulation models.

Aside from making the simulations more realistic, future research should also focus on improving the tractability of methods designing large satellite constellations, especially in low Earth orbit. Low Earth orbit satellite constellations are of increasing interest as the cost to deploy satellites to space continues to decrease. The relative speed of satellites in low Earth orbit to the Earth's surface makes optimal design of these satellite constellations even more challenging than medium Earth orbit. Incorporating latency and queuing of communications into the satellite network interdiction model will improve representation of the satellite network and its identification of worst-case scenario satellite failures. Perhaps the most promising extension of this research will be the use of multiple distinct repeating ground tracks in constellation construction.

Bibliography

1. John G Walker. Continuous Whole-Earth Coverage by Circular-Orbit Satellite Patterns. Technical report, Royal Aircraft Establishment Farnborough (United Kingdom), 1977. https://apps.dtic.mil/sti/citations/ADA044593.

2. Alan C O'Connor, Michael P Gallaher, Kyle Clark Sutton, Daniel Lapidus, Zack T Oliver, Troy J Scott, Dallas W Wood, Manuel A Gonzalez, Elizabeth G Brown, and Joshua Fletcher. Economic Benefits of the Global Positioning System (gps). 2019.

3. Michael Sheetz. Spacex's Starlink Satellite Internet Surpases 400,000 Subscribers Globally. https://www.cnbc.com/2022/05/25/spacexs-starlink-surpasses-400000-subscribers-globally.html, March 2022.

4. Micah Maidenberg and Alison Sider. Delta Air Lines Tested Spacex's Starlink Internet for Planes, Delta Ceo Says. https://www.wsj.com/articles/delta-air-lines-tested-spacexs-starlink-internet-for-planes-delta-ceo-says-11650316287?page=1, April 2022.

5. Zoe Thomas. Space Manufacturing: Building an Economy Beyond Earth. https://www.wsj.com/podcasts/google-news-update/space-manufacturing-building-an-economy-beyond-earth/ea925ca1-2e44-4cf7-9c19-dd4618d4fc46, June 2022.

6. Sarah Lewin. Making Stuff in Space: Off-Earth Manufacturing Is Just Getting Started. https://www.space.com/40552-space-based-manufacturing-just-getting-started.html, May 2018.

7. Alastair Gale. How the U.s. and South Korea Predict a North Korean Weapons Test. https://www.wsj.com/articles/how-the-u-s-and-south-korea-

predict-a-north-korean-weapons-test-11653640572?mod=world_major_1_pos6, May 2022.

8. Mariella Moon. China's Military Scientist Call for Development of Anti-Starlink Measures. https://finance.yahoo.com/news/china-military-scientists-anti-starlink-measures-060518398.html?guccounter=1&guce_referrer=aHR0cHM6Ly93d3cuZ29vZ2xlLmNvbS8&guce_referrer_sig=AQAAABPMxBhkLlpVPHWV0YL9h3oodz47eW4St1HvJLmIHUTG3p_LNZAmkts-w2OXByZKyRY0esx6i3VNXfBuPCSG622QuAZM7CTTXtIyDPeSC18ndwJxVqqYeQR2KxvlJ-BJHch6Fhg_fDeoE7LL-GCGfaZLetsl5U0E2KHas-xlH6xO, June 2022.

9. Sandra Erwin. Space Force General: Commercial Satellite Internet in Ukraine Showing Power of Megaconstellations. https://spacenews.com/space-force-general-commercial-satellite-internet-in-ukraine-showing-power-of-megaconstellations/, May 2022.

10. Kevin Collier. Starlink Internet Becomes a Lifeline for Ukrainians. https://www.nbcnews.com/tech/security/elon-musks-starlink-internet-becomes-lifeline-ukrainians-rcna25360, April 2022.

11. Harry Jones. The Recent Large Reduction in Space Launch Cost. 48th International Conference On Environmental Systems, 2018.

12. David Jarvis. Satellite Broadband: Time for Liftoff. https://deloitte.wsj.com/articles/satellite-broadband-time-for-liftoff-01584385327#:~:text=With%20the%20advent%20of%20new,%2C%20or%20about%2085%25%20less., March 2020.

13. James R Wertz, David F Everett, and Jeffery J Puschell. *Space Mission Engineering: the New SMAD*. Microcosm Press, 2011.

14. François Dufour. Coverage Optimization of Elliptical Satellite Constellations With an Extended Satellite Triplet Method. In *54th International Astronautical Congress of the International Astronautical Federation, the International Academy of Astronautics, and the International Institute of Space Law*, pages A–3, 2003.

15. JG Walker. Circular Orbit Patterns Providing Continuous Whole Earth Coverage, Royal Aircraft Establishment. *Technical Report 70211*, 1970.

16. WS Adams and L Rider. Circular Polar Constellations Providing Continuous Single Or Multiple Coverage Above a Specified Latitude. *Journal of the Astronautical Sciences*, 35:155–192, 1987.

17. Yuri Ulybyshev. Near-Polar Satellite Constellations for Continuous Global Coverage. *Journal of Spacecraft and Rockets*, 36(1):92–99, 1999.

18. Daniele Mortari, Matthew P Wilkins, and Christian Bruccoleri. The Flower Constellations. *The Journal of the Astronautical Sciences*, 52(1):107–127, 2004.

19. Daniele Mortari and Matthew P Wilkins. Flower Constellation Set Theory. Part I: Compatibility and Phasing. *IEEE Transactions On Aerospace and Electronic Systems*, 44(3):953–962, 2008.

20. Martin E Avendano and Daniele Mortari. New Insights On Flower Constellations Theory. *IEEE Transactions On Aerospace and Electronic Systems*, 48(2):1018–1030, 2012.

21. Jeremy J Davis and Daniele Mortari. Reducing Walker, Flower, and Streets-of-Coverage Constellations to a Single Constellation Design Framework. *Adv. Astronaut. Sci*, 143:697–712, 2012.

22. Martín E Avendaño, Jeremy J Davis, and Daniele Mortari. The 2-D Lattice Theory of Flower Constellations. *Celestial Mechanics and Dynamical Astronomy*, 116(4):325–337, 2013.

23. Jeremy J Davis, Martín E Avendaño, and Daniele Mortari. The 3-D Lattice Theory of Flower Constellations. *Celestial Mechanics and Dynamical Astronomy*, 116(4):339–356, 2013.

24. David Arnas, Daniel Casanova, and Eva Tresaco. 4d Lattice Flower Constellations. *Advances in Space Research*, 67(11):3683–3695, 2021.

25. John G Walker. Satellite Constellations. *Journal of the British Interplanetary Society*, 37:559, 1984.

26. Arthur H Ballard. Rosette Constellations of Earth Satellites. *IEEE Transactions On Aerospace and Electronic Systems*, (5):656–673, 1980.

27. Meiqian Guan, Tianhe Xu, Fan Gao, Wenfeng Nie, and Honglei Yang. Optimal Walker Constellation Design of Leo-Based Global Navigation and Augmentation System. *Remote Sensing*, 12(11):1845, 2020.

28. William R Whittecar and Matthew P Ferringer. Global Coverage Constellation Design Exploration Using Evolutionary Algorithms. In *AIAA/AAS Astrodynamics Specialist Conference*, page 4159, 2014.

29. HAN Yi, WANG Lei, FU Wenju, ZHOU Haitao, LI Tao, XU Beizhen, and CHEN Ruizhi. Leo Navigation Augmentation Constellation Design With the Multi-Objective Optimization Approaches. *Chinese Journal of Aeronautics*, 34(4):265–278, 2021.

30. S Huang, C Colombo, and F Bernelli Zazzera. Multi-Criteria Design of Continuous Global Coverage Walker and Street-of-Coverage Constellations Through Property Assessment. *Acta Astronautica*, 188:151–170, 2021.

31. Thomas J Lang and William S Adams. A Comparison of Satellite Constellations for Continuous Global Coverage. In *Mission Design & Implementation of Satellite Constellations*, pages 51–62. Springer, 1998.

32. Daniel Casanova, Martin Avendano, and Daniele Mortari. Optimizing Flower Constellations for Global Coverage. In *AIAA/AAS Astrodynamics Specialist Conference*, page 4805, 2012.

33. David C Beste. Design of Satellite Constellations for Optimal Continuous Coverage. *IEEE Transactions On Aerospace and Electronic Systems*, (3):466–473, 1978.

34. Thomas Lang. Low Earth Orbit Satellite Constellations for Continuous Coverage of the Mid-Latitudes. In *Astrodynamics Conference*, page 3638, 2013.

35. L Rider. Optimized Polar Orbit Constellations for Redundant Earth Coverage. *Journal of the Astronautical Sciences*, 33:147–161, 1985.

36. L Rider. Analytic Design of Satellite Constellations for Zonal Earth Coverage Using Inclined Circular Orbits. *Journal of the Astronautical Sciences*, 34:31–64, 1986.

37. Yu P Ulybyshev. Design of Satellite Constellations With Continuous Coverage On Elliptic Orbits of Molniya Type. *Cosmic Research*, 47(4):310–321, 2009.

38. MH Ullock and AH Schoen. Optimum Polar Satellite Networks for Continuous Earth Coverage. *AIAA Journal*, 1(1):69–72, 1963.

39. David A Vallado. *Fundamentals of Astrodynamics and Applications*. Microcosm Press, Hawthorne, CA, 4 edition, 2013.

40. Jeannette Heiligers, Matteo Ceriotti, Colin R McInnes, and James D Biggs. Displaced Geostationary Orbit Design Using Hybrid Sail Propulsion. *Journal of Guidance, Control, and Dynamics*, 34(6):1852–1866, 2011.

41. Matteo Ceriotti and Colin R McInnes. Systems Design of a Hybrid Sail Pole-Sitter. *Advances in Space Research*, 48(11):1754–1762, 2011.

42. Cuiqin Dai, Guimin Zheng, and Qianbin Chen. Satellite Constellation Design With Multi-Objective Genetic Algorithm for Regional Terrestrial Satellite Network. *China Communications*, 15(8):1–10, 2018.

43. Nadav Mailhot and Pini Gurfil. Constellation Design for Regional Space-Borne Geolocation. *Journal of Guidance, Control, and Dynamics*, 45(5):795–814, 2022.

44. Matthew P Ferringer and David B Spencer. Satellite Constellation Design Tradeoffs Using Multiple-Objective Evolutionary Computation. *Journal of Spacecraft and Rockets*, 43(6):1404–1411, 2006.

45. Juan A Fraire, Santiago Henn, Fabio Dovis, Roberto Garello, and Giorgio Taricco. Sparse Satellite Constellation Design for Lora-Based Direct-to-Satellite Internet of Things. In *GLOBECOM 2020-2020 IEEE Global Communications Conference*, pages 1–6. IEEE, 2020.

46. Matthew P Ferringer, Ronald S Clifton, and Timothy G Thompson. Efficient and Accurate Evolutionary Multi-Objective Optimization Paradigms for Satellite Constellation Design. *Journal of Spacecraft and Rockets*, 44(3):682–691, 2007.

47. Pau Garcia Buzzi, Daniel Selva, Nozomi Hitomi, and William J Blackwell. Assessment of Constellation Designs for Earth Observation: Application to the Tropics Mission. *Acta Astronautica*, 161:166–182, 2019.

48. Mahdi Jafari Nadoushan and Nima Assadian. Repeat Ground Track Orbit Design With Desired Revisit Time and Optimal Tilt. *Aerospace Science and Technology*, 40:200–208, 2015.

49. Tania Savitri, Youngjoo Kim, Sujang Jo, and Hyochoong Bang. Satellite Constellation Orbit Design Optimization With Combined Genetic Algorithm and Semianalytical Approach. *International Journal of Aerospace Engineering*, 2017, 2017.

50. Ossama Abdelkhalik and Daniele Mortari. Orbit Design for Ground Surveillance Using Genetic Algorithms. *Journal of Guidance, Control, and Dynamics*, 29(5):1231–1235, 2006.

51. Ossama Abdelkhalik and Ahmed Gad. Optimization of Space Orbits Design for Earth Orbiting Missions. *Acta Astronautica*, 68(7-8):1307–1317, 2011.

52. Yury N Razoumny. Fundamentals of the Route Theory for Satellite Constellation Design for Earth Discontinuous Coverage. Part 1: Analytic Emulation of the Earth Coverage. *Acta Astronautica*, 128:722–740, 2016.

53. Emiliano Ortore, Marco Cinelli, and Christian Circi. A Ground Track-Based Approach to Design Satellite Constellations. *Aerospace Science and Technology*, 69:458–464, 2017.

54. Prasenjit Sengupta, Srinivas R Vadali, and Kyle T Alfriend. Satellite Orbit Design and Maintenance for Terrestrial Coverage. *Journal of Spacecraft and Rockets*, 47(1):177–187, 2010.

55. Sharon D Vtipil and Brett Newman. Determining an Earth Observation Repeat Ground Track Orbit for an Optimization Methodology. *Journal of Spacecraft and Rockets*, 49(1):157–164, 2012.

56. Soung Sub Lee. Closed-Form Solution of Repeat Ground Track Orbit Design and Constellation Deployment Strategy. *Acta Astronautica*, 180:588–595, 2021.

57. Sung Wook Paek, Sangtae Kim, and Olivier De Weck. Optimization of Reconfigurable Satellite Constellations Using Simulated Annealing and Genetic Algorithm. *Sensors*, 19(4):765, 2019.

58. Christian Circi, Emiliano Ortore, and Federico Bunkheila. Satellite Constellations in Sliding Ground Track Orbits. *Aerospace Science and Technology*, 39:395–402, 2014.

59. Yuri Ulybyshev. Satellite Constellation Design for Complex Coverage. *Journal of Spacecraft and Rockets*, 45(4):843–849, 2008.

60. Hang Woon Lee, Seiichi Shimizu, Shoji Yoshikawa, and Koki Ho. Satellite Constellation Pattern Optimization for Complex Regional Coverage. *Journal of Spacecraft and Rockets*, 57(6):1309–1327, 2020.

61. Ahan Kak and Ian F Akyildiz. Large-Scale Constellation Design for the Internet of Space Things/cubesats. In *2019 IEEE Globecom Workshops (GC Wkshps)*, pages 1–6. IEEE, 2019.

62. Ruoqi Deng, Boya Di, Hongliang Zhang, and Lingyang Song. Ultra-Dense Leo Satellite Constellation Design for Global Coverage in Terrestrial-Satellite Networks. In *GLOBECOM 2020-2020 IEEE Global Communications Conference*, pages 1–6. IEEE, 2020.

63. Akram Al-Hourani. Optimal Satellite Constellation Altitude for Maximal Coverage. *IEEE Wireless Communications Letters*, 10(7):1444–1448, 2021.

64. Katherine M Wagner and Jonathan T Black. Genetic-Algorithm-Based Design for Rideshare and Heterogeneous Constellations. *Journal of Spacecraft and Rockets*, 57(5):1021–1032, 2020.

65. Cyrus D Jilla and David W Miller. Multi-Objective, Multidisciplinary Design Optimization Methodology for Distributed Satellite Systems. *Journal of Spacecraft and Rockets*, 41(1):39–50, 2004.

66. Eliad Peretz, Christine Hamilton, John C Mather, Simone D'Amico, Adam Michaels, Robert Pritchett, Wayne Yu, and Peter Wizinowich. Astrostationary Orbits for Hybrid Space and Ground-Based Observatories. *Journal of Astronomical Telescopes, Instruments, and Systems*, 8(1):014004, 2022.

67. Adam W Koenig, Simone D'Amico, Eliad Peretz, Wayne Yu, Sun Hur Diaz, and John Mather. Optimal Spacecraft Orbit Design for Inertial Alignment With Ground Telescopes. In *2021 IEEE Aerospace Conference (50100)*, pages 1–12. IEEE, 2021.

68. Ryan P Russell and Martin Lara. Long-Lifetime Lunar Repeat Ground Track Orbits. *Journal of Guidance, Control, and Dynamics*, 30(4):982–993, 2007.

69. MT Ozimek, DJ Grebow, and KC Howell. Design of Solar Sail Trajectories With Applications to Lunar South Pole Coverage. *Journal of Guidance, Control, and Dynamics*, 32(6):1884–1897, 2009.

70. GV Mozhaev. Capabilities of Kinematically Regular Satellite Systems With Symmetry Groups of the Second Type in the Problem of Continuous Single Coverage of the Earth. *Cosmic Research*, 43(3):205–212, 2005.

71. T Ely. Satellite Constellation Design for Zonal Coverage Using Genetic Algorithms. *Spaceflight Mechanics 1998*, pages 443–460, 1998.

72. John Draim. The Ellipso™ Satellite-Application of Small Satellite Principles to the Space Segment of a Global Mobile Personal Communications System. 1998.

73. VK Saulskiy. Multisatellite Systems With Linear Structure and Their Application for Continuous Coverage of the Earth. *Cosmic Research*, 43(1):34–51, 2005.

74. Hosam E Emara and Cornelius T Leondes. Minimum Number of Satellites for Three-Dimensional Continuous Worldwide Coverage. *IEEE Transactions On Aerospace and Electronic Systems*, (2):108–111, 1977.

75. Yu P Ulybyshev and VN Doniants. Dynamic Communication Networks Using Satellite Constellations and Ground Stations. In *53rd Int. Astronautical Congress, Houston (USA)*, 2002.

76. Thomas J Lang and John M Hanson. Orbital Constellations Which Minimize Revisit Time. *Advances in the Astronautical Sciences*, 54:1071–1086, 1984.

77. Thomas J Lang and Janet L Meyer. A New Six Satellite Constellation for Optimal Continuous Global Coverage. *Spaceflight Mechanics 1995*, pages 1451–1458, 1995.

78. Chris Sabol. *Application of Sun-Synchronous, Critically Inclined Orbits to Global Personal Communications Systems*. PhD thesis, Massachusetts Institute of Technology, 1995.

79. Thomas J Lang. Optimal Low Earth Orbit Constellations for Continuous Global Coverage. *Astrodynamics 1993*, pages 1199–1216, 1994.

80. Thomas J Lang. Symmetric Circular Orbit Satellite Constellations for Continuous Global Coverage. *Astrodynamics 1987*, pages 1111–1132, 1988.

81. John M Hanson and William Burley Higgins. Designing Good Geosynchronous Constellations. *Journal of the Astronautical Sciences*, 38:143–159, 1990.

82. LG Vargo. Orbital Patterns for Satellite Systems. *The Journal of the Astronautical Sciences*, 7(4):78–86, 1960.

83. YP Ulybyshev and VN Donianz. Elliptic Orbit Constellations for Regional Communication and Molniya–Zond Satellite Constellation, 53rd Intern. Astronautical Congress, Houston (usa), Oct. 10–19, 2002. Technical report, Paper IAC-02-M. 4.05.

84. PV Suder Oli, N Nagarajan, and HR Rayan. Global Communication Using a Constellation of Low Earth Meridian Orbits. *IEEE Transactions On Aerospace and Electronic Systems*, 29(3):696–705, 1993.

85. John E Draim, P Cefola, and D Castrel. Elliptical Orbit Constellations-a New Paradigm for Higher Efficiency in Space Systems? In *2000 IEEE Aerospace Conference. Proceedings (Cat. No. 00TH8484)*, volume 7, pages 27–35. IEEE, 2000.

86. RL Easton and R Brescia. Continuously Visible Satellite Constellations. Technical report, Naval Research Lab Washington DC, 1969.

87. R David Luders. Satellite Networks for Continuous Zonal Coverage. *ARS Journal*, 31(2):179–184, 1961.

88. Ryutaro Suzuki. A Study of Leo Constellation With Figure-of-Eight Shape Ring Network. In *57th International Astronautical Congress*, pages B3–1.

89. VN Doniants, Yu P Ulybyshev, and EF Zemskov. Satellite Networks Using Mid-Altitude Elliptical Orbit Constellation\molniya-Zond\"". In *55th International Astronautical Congress of the International Astronautical Federation, the International Academy of Astronautics, and the International Institute of Space Law*, pages M–5.

90. Serena Chan, Ayanna Samuels, Nirav Shah, Jennifer Underwood, and Olivier De Weck. Optimization of Hybrid Satellite Constellations Using Multiple Layers and Mixed Circular-Elliptical Orbits. In *22nd AIAA International Communications Satellite Systems Conference & Exhibit 2004 (ICSSC)*, page 3205, 2004.

91. Andrew Turner. Non-Geo Constellations for Commercial Telecommunications Applications. In *22nd AIAA International Communications Satellite Systems Conference & Exhibit 2004 (ICSSC)*, page 3164, 2004.

92. Muhamad Asvial, Rahim Tafazolli, and Barry G Evans. Genetic Hybrid Satellite Constellation Design. In *21st International Communications Satellite Systems Conference and Exhibit*, page 2283, 2003.

93. Juan Zhang, Xingsuo He, Fengyan Deng, and Liexia Zhang. Designing Twin-Station Leo Satellite Constellation for Zonal Coverage. In *42nd AIAA Aerospace Sciences Meeting and Exhibit*, page 325, 2004.

94. William Mason, Victoria Coverstone Carroll, and John Hartmann. Optimal Earth Orbiting Satellite Constellations Via a Pareto Genetic Algorithm. In *AIAA/AAS Astrodynamics Specialist Conference and Exhibit*, page 4381, 1998.

95. Eric Frayssinhes. Investigating New Satellite Constellation Geometries With Genetic Algorithms. In *Astrodynamics Conference*, page 3636, 1996.

96. Giovanni Palmerini. Design of Global Coverage Constellations Based On Elliptical Orbits. In *Astrodynamics Conference*, page 3637, 1996.

97. John Draim and David Castiel. Elliptic Constellations for Optimal Coverage of Selected Geographical Areas. In *16th International Communications Satellite Systems Conference*, page 1075, 1996.

98. C Byron Winn and Paul Mennemeyer. Coverage Obtained by Controlled Satellite Constellations for Regional Communications. *Journal of Spacecraft and Rockets*, 9(2):92–95, 1972.

99. Alexandr Andreevich Gutenev. Optimization of Low-Altitude Global Communication Constellations. *Journal of Guidance, Control, and Dynamics*, 15(4):871–877, 1992.

100. John E Draim. Continuous Global N-Tuple Coverage With (2n+ 2) Satellites. *Journal of Guidance, Control, and Dynamics*, 14(1):17–23, 1991.

101. John M Hanson and Alexander N Linden. Improved Low-Altitude Constellation Design Methods. *Journal of Guidance, Control, and Dynamics*, 12(2):228–236, 1989.

102. John E Draim. A Common-Period Four-Satellite Continuous Global Coverage Constellation. *Journal of Guidance, Control, and Dynamics*, 10(5):492–499, 1987.

103. John E Draim. Three-and Four-Satellite Continuous-Coverage Constellations. *Journal of Guidance, Control, and Dynamics*, 8(6):725–730, 1985.

104. Yuri Ulybyshev. Geometric Analysis of Low-Earth-Orbit Satellite Communication Systems: Covering Functions. *Journal of Spacecraft and Rockets*, 37(3):385–391, 2000.

105. L Ya Kantor and VN Kheifets. Optimal Choice of a Satellite Broadcasting System Based On High-Elliptic Orbits. *Cosmic Research*, 40(6):587–593, 2002.

106. GV Mozhaev. The Problem of the Continuous Earth Coverage and the Kinematically Regular Satellite Networks. I. *Cosmic Research*, 11:755, 1973.

107. Erick Lansard, Eric Frayssinhes, and Jean-Luc Palmade. Global Design of Satellite Constellations: a Multi-Criteria Performance Comparison of Classical Walker Patterns and New Design Patterns. *Acta Astronautica*, 42(9):555–564, 1998.

108. John E Draim, Paul J Cefola, and Kenneth J Ernandes. Seamless Handovers in Cobra Teardrop Satellite Arrays. *Acta Astronautica*, 61(1-6):139–150, 2007.

109. Yanbo Wei, Huaijian Li, and Xiaojing Du. An Efficient Leo Global Navigation Constellation Design Based On Walker Constellation. In *2020 IEEE Computing, Communications and IoT Applications (ComComAp)*, pages 1–6. IEEE, 2020.

110. Katherine Mott and Jonathan Black. Model-Based Heterogeneous Optimal Space Constellation Design. In *2018 21st International Conference On Information Fusion (FUSION)*, pages 602–609. IEEE, 2018.

111. Ossama Abdelkhalik, Daniele Mortari, and Keun Joo Park. Satellite Constellation Design for Earth Observation. In *15th AAS/AIAA Space Flight Mechanics Meeting, Copper Mountain, CO*, pages 05–148, 2005.

112. Ben Gorr, Alan Aguilar, Daniel Selva, Vinay Ravindra, Mahta Moghaddam, and Sreeja Nag. Heterogeneous Constellation Design for a Smart Soil Moisture Radar Mission. In *2021 IEEE International Geoscience and Remote Sensing Symposium IGARSS*, pages 7799–7802. IEEE, 2021.

113. Matthew Ferringer, Ronald Clifton, and Timothy Thompson. Constellation Design With Parallel Multi-Objective Evolutionary Computation. In *AIAA/AAS Astrodynamics Specialist Conference and Exhibit*, page 6015, 2006.

114. Katherine E Mott and Jonathan T Black. Heterogeneous Constellation Design Methodology Applied to a Mars-Orbiting Communications and Positioning Constellation. In *AAS/AIAA Astrodynamics Conference*, pages 2383–2396, 2017.

115. Pengfei Wang, Boya Di, and Lingyang Song. Multi-Layer Leo Satellite Constellation Design for Seamless Global Coverage. In *2021 IEEE Global Communications Conference (GLOBECOM)*, pages 01–06. IEEE, 2021.

116. Wenzhe Ding, Xinhong Li, and Hong Yang. Quick-Response Microsatellite Constellation Design. In *2020 IEEE 4th Information Technology, Networking, Electronic and Automation Control Conference (ITNEC)*, volume 1, pages 262–267. IEEE, 2020.

117. Tengyue Mao, Zhengquan Xu, and Rui Hou. Efficient Constellation Design Based On Improved Non-Dominated Sorting Genetic Algorithm-Ii. *J. Comput.*, 7(6):1337–1344, 2012.

118. Alan L Jennings and Heather Diniz. Global Navigation Satellite System Design Exploration Using a Multi-Objective Genetic Algorithm. In *AIAA SPACE 2015 Conference and Exposition*, page 4622, 2015.

119. Yasin Tamer. Electro-Optic Satellite Constellation Design Using Multi-Objective Genetic Algorithm. 2020.

120. Sung Wook Paek. *Reconfigurable Satellite Constellations for Geo-Spatially Adaptive Earth Observation Missions*. PhD thesis, Massachusetts Institute of Technology, 2012.

121. Heather C Diniz. Navigation Constellation Design Using a Multi-Objective Genetic Algorithm. 2015.

122. Afreen Siddiqi, Jason Mellein, and Olivier De Weck. Optimal Reconfigurations for Increasing Capacity of Communication Satellite Constellations. In *46th AIAA/ASME/ASCE/AHS/ASC Structures, Structural Dynamics and Materials Conference*, page 2065, 2005.

123. Dawei Yan, Peng You, Cong Liu, Shaowei Yong, and Dongfang Guan. Constellation Multi-Objective Optimization Design Based On Qos and Network Stability in Leo Satellite Broadband Networks. *KSII Transactions On Internet and Information Systems (TIIS)*, 13(3):1260–1283, 2019.

124. Ibrahim Sanad and David G Michelson. A Framework for Heterogeneous Satellite Constellation Design for Rapid Response Earth Observations. In *2019 IEEE Aerospace Conference*, pages 1–10. IEEE, 2019.

125. Xiangyue He, Haiyang Li, Luyi Yang, and Jian Zhao. Reconfigurable Satellite Constellation Design for Disaster Monitoring Using Physical Programming. *International Journal of Aerospace Engineering*, 2020, 2020.

126. Ji Jiang, Shi Yan, and Mugen Peng. Regional Leo Satellite Constellation Design Based On User Requirements. In *2018 IEEE/CIC International Conference On Communications in China (ICCC)*, pages 855–860. IEEE, 2018.

127. Aaron B Hoskins, Hugh R Medal, and Eghbal Rashidi. Satellite Constellation Design for Forest Fire Monitoring Via a Stochastic Programing Approach. *Naval Research Logistics (NRL)*, 64(8):642–661, 2017.

128. Sabine Frey, Vassilis Angelopoulos, Manfred Bester, John Bonnell, Tai Phan, and Daniel Rummel. Orbit Design for the Themis Mission. *Space Science Reviews*, 141(1):61–89, 2008.

129. AT Takano and Belinda G Marchand. Optimal Constellation Design for Space Based Situational Awareness Applications. In *AAS/AIAA Astrodynamics Specialist Conference*, volume 142, pages 2011–543, 2011.

130. Ashley D Biria and Belinda G Marchand. Constellation Design for Space-Based Space Situational Awareness Applications: an Analytical Approach. *Journal of Spacecraft and Rockets*, 51(2):545–562, 2014.

131. Peng Zong and Saeid Kohani. Optimal Satellite Leo Constellation Design Based On Global Coverage in One Revisit Time. *International Journal of Aerospace Engineering*, 2019, 2019.

132. Dawei Yan, Cong Liu, Peng You, and Shaowei Yong. Multi-Objective Optimization Design of Extended Walker Constellation for Global Coverage Services. In *2016 2nd IEEE International Conference On Computer and Communications (ICCC)*, pages 1309–1313. IEEE, 2016.

133. Pau Garcia Buzzi and Daniel Selva. Evolutionary Formulations for Design of Heterogeneous Earth Observing Constellations. In *2020 IEEE Aerospace Conference*, pages 1–10. IEEE, 2020.

134. Behnam Saboori, Ahmad Monemi Bidgoli, and Bahareh Saboori. Multiobjective Optimization in Repeating Sun-Synchronous Orbits Design for Remote-Sensing Satellites. *Journal of Aerospace Engineering*, 27(5):04014027, 2014.

135. Giacomo Taini, Andrea Pietropaolo, and Anna Notarantonio. Criteria and Trade-Offs for Leo Orbit Design. In *2008 IEEE Aerospace Conference*, pages 1–11. IEEE, 2008.

136. Muhamad Asvial, Rahim Tafazolli, and Barry Evans. Non-Geo Satellite Constellation Design With Satellite Diversity Using Genetic Algorithm. In *20th AIAA International Communication Satellite Systems Conference and Exhibit*, page 2018, 2002.

137. Gregory A Orndorff and Bruce F Zink. A Constellation Architecture for National Security Space Systems. *Johns Hopkins APL Technical Digest*, 29(3):273–282, 2010.

138. Joseph R Gagliano. Orbital Constellation Design and Analysis Using Spherical Trigonometry and Genetic Algorithms: A Mission Level Design Tool for Single Point Coverage On Any Planet. 2018.

139. Mark Bolden, Timothy Craychee, and Erin Griggs. An Evaluation of Observing Constellation Orbit Stability, Low Signal-to-Noise, and the Too-Short-Arc Challenges in the Cislunar Domain. In *Advanced Maui Optical and Space Surveillance Technologies Conference (AMOS)*, 2020.

140. Sharon Vtipil and Brett Newman. Designing a Constrained Optimal Orbit for Earth Observation Satellites Based On User Requirements. In *AIAA/AAS Astrodynamics Specialist Conference*, page 7520, 2010.

141. Matthew Wilkins and Daniele Mortari. Constellation Design Via Projection of an Arbitrary Shape Onto a Flower Constellation Surface. In *AIAA/AAS Astrodynamics Specialist Conference and Exhibit*, page 4975, 2004.

142. Martín Lara. Searching for Repeating Ground Track Orbits: a Systematic Approach. *The Journal of the Astronautical Sciences*, 47(3):177–188, 1999.

143. Charles H Lee, Kar-Ming Cheung, Chad Edwards, Stuart J Kerridge, Gary K Noreen, and Arvydas Vaisnys. Orbit Design Based On Global Maps of Telecom Metrics. In *2005 IEEE Aerospace Conference*, pages 846–854. IEEE, 2005.

144. Ossama Abdelkhalik. Initial Orbit Design From Ground Track Points. *Journal of Spacecraft and Rockets*, 47(1):202–205, 2010.

145. Taibo Li, Junhua Xiang, Zhaokui Wang, and Yulin Zhang. Circular Revisit Orbits Design for Responsive Mission Over a Single Target. *Acta Astronautica*, 127:219–225, 2016.

146. Roberto Armellin, Yanchao He, and Ming Xu. Design And Control Of Repeat Ground Track Orbits In High Fidelity Dynamical Model Via High Order Poincar E Mapping. *Advances in the Astronautical Sciences*, AAS 19-270(99513195602346):27, 2019.

147. Ante Barišić, Andrea Crnković, and Željko Hećimović. Satellite Orbits Optimized for Satellite Supported Services On the Territory of Croatia. *Tehnički Vjesnik*, 18(2):179–186, 2011.

148. Martin Lara and Ryan P Russell. Fast Design of Repeat Ground Track Orbits in High-Fidelity Geopotentials. *The Journal of the Astronautical Sciences*, 56(3):311–324, 2008.

149. Yingguo Chen, Vladimir Mahalec, Yingwu Chen, Renjie He, and Xiaolu Liu. Optimal Satellite Orbit Design for Prioritized Multiple Targets With Threshold Observation Time Using Self-Adaptive Differential Evolution. *Journal of Aerospace Engineering*, 28(2):04014066, 2015.

150. Martin W Lo. The Coverage of Elliptical Orbits Using Ergodic Theory. In *2004 IEEE Aerospace Conference Proceedings (IEEE Cat. No. 04TH8720)*, volume 1. IEEE, 2004.

151. Chao Han, Yujin Zhang, and Shengzhou Bai. Geometric Analysis of Ground-Target Coverage From a Satellite by Field-Mapping Method. *Journal of Guidance, Control, and Dynamics*, 44(8):1469–1480, 2021.

152. Robert L Forward. Statite-a Spacecraft That Does Not Orbit. *Journal of Spacecraft and Rockets*, 28(5):606–611, 1991.

153. Ariadna Farrés. Catalogue On the Dynamics of a Solar Sail Around L1 and L2. In *Proceedings of the 4th International Symposium On Solar Sailing*, 2017.

154. Generoso Aliasi, Giovanni Mengali, and Alessandro A Quarta. Artificial Equilibrium Points for a Generalized Sail in the Circular Restricted Three-Body Problem. *Celestial Mechanics and Dynamical Astronomy*, 110(4):343–368, 2011.

155. Generoso Aliasi, Giovanni Mengali, and Alessandro A Quarta. Artificial Equilibrium Points for a Generalized Sail in the Elliptic Restricted Three-Body Problem. *Celestial Mechanics and Dynamical Astronomy*, 114(1):181–200, 2012.

156. AK de Almeida, AFBA Prado, T Yokoyama, and DM Sanchez. Spacecraft Motion Around Artificial Equilibrium Points. *Nonlinear Dynamics*, 91(3):1473–1489, 2018.

157. Generoso Aliasi, Giovanni Mengali, and Alessandro A Quarta. Artificial Lagrange Points for Solar Sail With Electrochromic Material Panels. *Journal of Guidance, Control, and Dynamics*, 36(5):1544–1550, 2013.

158. Generoso Aliasi, Giovanni Mengali, and Alessandro A Quarta. Artificial Periodic Orbits Around L 1-Type Equilibrium Points for a Generalized Sail. *Journal of Guidance, Control, and Dynamics*, 38(9):1847–1852, 2015.

159. John E Draim, Richard Inciardi, Ron Proulx, Paul J Cefola, David Carter, and Duane E Larsen. Beyond Geo—using Elliptical Orbit Constellations to Multiply the Space Real Estate. *Acta Astronautica*, 51(1-9):467–489, 2002.

160. Nathaniel Choo, Darryl Ahner, and Bryan Little. Investigating the Building Blocks of Satellite Constellation Design: A Survey of Orbit Design and Selection Methodologies. Technical report, Air Force Institute of Technology, 2023.

161. Yingguo Chen, Vladimir Mahalec, Yingwu Chen, Xiaolu Liu, Renjie He, and Kai Sun. Reconfiguration of Satellite Orbit for Cooperative Observation Using Variable-Size Multi-Objective Differential Evolution. *European Journal of Operational Research*, 242(1):10–20, 2015.

162. Xiaohui Wang, Hao Zhang, Shengzhou Bai, and Yuxian Yue. Design of Agile Satellite Constellation Based On Hybrid-Resampling Particle Swarm Optimization Method. *Acta Astronautica*, 178:595–605, 2021.

163. John H Holland. Genetic Algorithms-John H. Holland. *Computer Programs That Evolve in Ways That Resemble Natural Selection can Solve Complex Problems Even Their Creators do Not Fully Understand*, pages 1–4, 1975.

164. Suleyman Simsek and Samet Uslu. Experimental Study of the Performance and Emissions Characteristics of Fusel Oil/gasoline Blends in Spark Ignited Engine Using Response Surface Methodology. *Fuel*, 277:118182, 2020.

165. Darryl Ahner and Andrew McCarthy. Response Surface Modeling of Precision-Guided Fragmentation Munitions. *The Journal of Defense Modeling and Simulation*, 17(1):83–97, 2020.

166. Natasha E Sevant, Malcolm IG Bloor, and Michael J Wilson. Aerodynamic Design of a Flying Wing Using Response Surface Methodology. *Journal of Aircraft*, 37(4):562–569, 2000.

167. Swati Sharma and Halis Simsek. Sugar Beet Industry Process Wastewater Treatment Using Electrochemical Methods and Optimization of Parameters Using Response Surface Methodology. *Chemosphere*, 238:124669, 2020.

168. Raymond H Myers, Douglas C Montgomery, and Christine M Anderson Cook. *Response Surface Methodology: Process and Product Optimization Using Designed Experiments*. John Wiley & Sons, Hoboken, New Jersey, 2016.

169. Scott Kirkpatrick, C Daniel Gelatt Jr, and Mario P Vecchi. Optimization by Simulated Annealing. *Science*, 220(4598):671–680, 1983.

170. James Kennedy and Russell Eberhart. Particle Swarm Optimization. In *Proceedings of ICNN'95-International Conference on Neural Networks*, volume 4, pages 1942–1948. IEEE, 1995.

171. Susan M Sanchez. Nolhdesigns Spreadsheet Version 6. *Seed Center for Data Farming. https://harvest.nps.edu*, 2011.

172. George EP Box and David R Cox. An Analysis of Transformations. *Journal of the Royal Statistical Society: Series B (Methodological)*, 26(2):211–243, 1964.

173. Matlab Global Optimization Toolbox ™: User's Guide (r2022b), 2022. Retrieved: March 1, 2022 from `https://www.mathworks.com/help/gads/index.html?s_tid=CRUX_lftnav`.

174. JW Tukey. The Problem of Multiple Comparisons, 1953, Princeton University. *New Jersey*, 1953.

175. Douglas C Montgomery. *Design and Analysis of Experiments*. John Wiley & Sons, Hoboken, NJ, 2017.

176. M Aorpimai and PL Palmer. Repeat-Groundtrack Orbit Acquisition and Maintenance for Earth-Observation Satellites. *Journal of Guidance, Control, and Dynamics*, 30(3):654–659, 2007.

177. Xiaofeng Fu, Meiping Wu, and Yi Tang. Design and Maintenance of Low-Earth Repeat-Ground-Track Successive-Coverage Orbits. *Journal of Guidance, Control, and Dynamics*, 35(2):686–691, 2012.

178. Samuel YW Low, Yongjun Moon, Wen Tao Liu, and Chek-Wu Tan. Designing a Reference Trajectory for Frozen Repeat Near-Equatorial Low Earth Orbits. *Journal of Spacecraft and Rockets*, 59(1):84–93, 2022.

179. Mingjun Pu, Donghong Wang, Yuanbo Wu, Jihe Wang, and Xiaowei Shao. Multi-Objective Optimization Method For Repeat Ground-Track Orbit Design Considering the Orbit Injection Error. *Journal of Aerospace Technology and Management*, 10, 2018.

180. Tan Ju, Xiaowei Shao, Dexin Zhang, and Xiaofang Wei. Repeat Ground-Track Orbit Design Using Objective Dimensionality Reduction and Decoupling Optimization. *IEEE Transactions On Aerospace and Electronic Systems*, 2022.

181. Michel Capderou. *Handbook of Satellite Orbits: From Kepler to GPS*. Springer Cham, Heidelberg New York Dordrecht London, 2014.

182. David Szondy. Japanese Satellite Sets Low Altitude Record. https://newatlas.com/space/satellite-low-altitude-record-tsubame-jaxa/, December 2019.

183. Francesco Vatalaro, Giovanni Emanuele Corazza, Carlo Caini, and Carlo Ferrarelli. Analysis of LEO, MEO, and GEO Global Mobile Satellite Systems in the Presence of Interference and Fading. *IEEE Journal on Selected Areas in Communications*, 13(2):291–300, 1995.

184. Inigo Del Portillo, Bruce G Cameron, and Edward F Crawley. A Technical Comparison of Three Low Earth Orbit Satellite Constellation Systems to Provide Global Broadband. *Acta astronautica*, 159:123–135, 2019.

185. Nils Pachler, Inigo del Portillo, Edward F Crawley, and Bruce G Cameron. An Updated Comparison of Four Low Earth Orbit Satellite Constellation Systems to Provide Global Broadband. In *2021 IEEE International Conference on Communications Workshops (ICC Workshops)*, pages 1–7. IEEE, 2021.

186. Wu Tingyong and Wu Shiqi. Comparison Between Several Satellite Constellation Schemes for MEO-TDRSS of China. *Journal of Systems Engineering and Electronics*, 19(5):907–913, 2008.

187. Paul Muri, Janise McNair, Joe Antoon, Ann Gordon-Ross, Kathryn Cason, and Norman Fitz-Coy. Topology Design and Performance Analysis for Networked Earth Observing Small Satellites. In *2011-MILCOM 2011 Military Communications Conference*, pages 1940–1945. IEEE, 2011.

188. Der-Ming Ma, Zuu-Chang Hong, Tzung-Hang Lee, and Bo-Jyun Chang. Design of a Micro-Satellite Constellation for Communication. *Acta Astronautica*, 82(1):54–59, 2013.

189. Thomas Shake, Jun Sun, Thomas Royster, and Aradhana Narula-Tam. Failure Resilience in Proliferated Low Earth Orbit Satellite Network Topologies. In *MILCOM 2022-2022 IEEE Military Communications Conference*, pages 828–834. IEEE, 2022.

190. Arun Shankar. Optimal Jammer Placement to Interdict Wireless Network Services. Technical report, Naval Postgraduate School Monterey CA, 2008.

191. David Schweitzer and Hugh Medal. Wireless LAN Transmitter Location Under the Threat of Jamming Attacks. *Computers & Operations Research*, 106:14–27, 2019.

192. Brian J Lunday and Hanif D Sherali. Network Interdiction to Minimize the Maximum Probability of Evasion with Synergy Between Applied Resources. *Annals of Operations Research*, 196:411–442, 2012.

193. Aaron M Lessin, Brian J Lunday, and Raymond R Hill. A Bilevel Exposure-Oriented Sensor Location Problem for Border Security. *Computers & Operations Research*, 98:56–68, 2018.

194. Lina Perelman and Saurabh Amin. A Network Interdiction Model for Analyzing the Vulnerability of Water Distribution Systems. In *Proceedings of the 3rd International Conference on High Confidence Networked Systems*, pages 135–144, 2014.

195. Hoese Michel Tornyeviadzi, Emmanuel Owusu-Ansah, Hadi Mohammed, and Razak Seidu. A Systematic Framework for Dynamic Nodal Vulnerability Assessment of Water Distribution Networks Based on Multilayer Networks. *Reliability Engineering & System Safety*, 219:108217, 2022.

196. Jianan Zhang, Hyang-Won Lee, and Eytan Modiano. On the Robustness of Distributed Computing Networks. In *2019 15th International Conference on the Design of Reliable Communication Networks (DRCN)*, pages 122–129. IEEE, 2019.

197. Ziba Jabarzare, Hossein Zolfagharinia, and Mehdi Najafi. Dynamic Interdiction Networks with Applications in Illicit Supply Chains. *Omega*, 96:102069, 2020.

198. Xiaodan Xie and Felipe Aros-Vera. An Interdependent Network Interdiction Model for Disrupting Sex Trafficking Networks. *Production and Operations Management*, 31(6):2695–2713, 2022.

199. J Cole Smith and Yongjia Song. A Survey of Network Interdiction Models and Algorithms. *European Journal of Operational Research*, 283(3):797–811, 2020.

200. Nathaniel Choo, Darryl Ahner, Brian Lunday, and Nathan Gaw. Orbital Parameter Determination of Single Satellite Circular Orbits for Regional Coverage Using a Response Surface Methodology. Technical report, Air Force Institute of Technology, 2023.

201. Nathaniel Choo, Darryl Ahner, Nathan Gaw, and Brian Lunday. Optimal Repeat Parameter Selection for Modifying Orbits from Non-Repeating into Repeating Ground Track Orbits. Technical report, Air Force Institute of Technology, 2023.

202. IBM ILOG CPLEX. V12. 1: User's Manual for CPLEX. *International Business Machines Corporation*, 46(53):157, 2009.

203. R Kevin Wood. Deterministic Network Interdiction. *Mathematical and Computer Modelling*, 17(2):1–18, 1993.

204. Kevin T Kennedy, Richard F Deckro, James T Moore, and Kenneth M Hopkinson. Nodal Interdiction. *Mathematical and Computer Modelling*, 54(11-12):3116–3125, 2011.

REPORT DOCUMENTATION PAGE

Form Approved
OMB No. 0704–0188

1. REPORT DATE *(DD–MM–YYYY)*	2. REPORT TYPE	3. DATES COVERED *(From — To)*
16–05–2023	PhD Dissertation	January 2021 — May 2023

4. TITLE AND SUBTITLE

Design and Analysis of Asymmetric "String-of-Pearls" Common Repeating-Ground-Track Satellite Constellations for Missions Requiring Regional Coverage

5a. CONTRACT NUMBER

5b. GRANT NUMBER

5c. PROGRAM ELEMENT NUMBER

6. AUTHOR(S)

Choo, Nathaniel

5d. PROJECT NUMBER

5e. TASK NUMBER

5f. WORK UNIT NUMBER

7. PERFORMING ORGANIZATION NAME(S) AND ADDRESS(ES)

Air Force Institute of Technology
Graduate School of Engineering and Management (AFIT/ENS)
2950 Hobson Way
WPAFB OH 45433-7765

8. PERFORMING ORGANIZATION REPORT NUMBER

AFIT-ENS-DS-23-J-073

9. SPONSORING / MONITORING AGENCY NAME(S) AND ADDRESS(ES)

Intentionally Left Blank

10. SPONSOR/MONITOR'S ACRONYM(S)

11. SPONSOR/MONITOR'S REPORT NUMBER(S)

12. DISTRIBUTION / AVAILABILITY STATEMENT

DISTRIBUTION STATEMENT A:
APPROVED FOR PUBLIC RELEASE; DISTRIBUTION UNLIMITED.

13. SUPPLEMENTARY NOTES

14. ABSTRACT

Satellite constellation design must balance many factors that emerge from multiple sources, including environmental hazards and competing mission objectives. Restricting satellite constellation designs to predefined geometric frameworks can alleviate many challenges associated with the design problem; however, it raises an important question: which geometric framework performs best for each mission set? To address this question, this research presents a novel topology approach to capture the current state of satellite constellation design literature. It develops metaheuristics for the selection of orbits and design of constellations. It proposes a procedure to transform non-repeating ground tracks into repeating ground tracks via geometric adjustment minimization. It develops a dynamic satellite network interdiction model to identify the worst-case degradation of satellite constellation performance resulting from a fixed number of satellite failures. Lastly, it compares two satellite constellation design frameworks according to their mission performance, robustness, and access to energy.

15. SUBJECT TERMS

Satellite constellation design, String-of-Pearls, Asymmetric String-of-Pearls, Repeating ground tracks, Circular orbits, Earth-observation Coverage, Response surface methodology, Satellite network interdiction, Communications robustness

16. SECURITY CLASSIFICATION OF:			17. LIMITATION OF ABSTRACT	18. NUMBER OF PAGES	19a. NAME OF RESPONSIBLE PERSON
a. REPORT	b. ABSTRACT	c. THIS PAGE			Dr. Darryl Ahner, AFIT/Dean for Research
U	U	U	UU	191	19b. TELEPHONE NUMBER *(include area code)* (937) 255-6565 x4708; darryl.ahner@afit.edu